

Aim and Scope

The Journal of Multifunctional Composites provides an international platform to showcase original, novel, and the latest research into multifunctional composite materials and structures. Analytical, experimental, and computational studies that deal with topics such as design and manufacturing; processing and transport; characterization of physical, mechanical, electrical, chemical, magnetic, and acoustic properties; interface and damage mechanics; microstructural characterization; modeling and simulation; non-destructive testing; durability and performance; and commercial applications are welcomed.

Of particular interest is the behavior of multifunctional composites through studies that bridge the length scales from the molecular to the macro scales, and under extreme environments that span quasistatic to ballistic strain rates and below-freezing to above-melting temperatures. Composite materials include synthetic, natural, and biological sources of fiber and particle reinforcements within polymeric, metallic, and ceramic matrices, and hybrid variants thereof. Biomimetic, self-healing, self-cooling, active-morphing, functionally-graded, nano, green, and smart composite structures are also of interest. Full-length research articles, review articles, and short letters of the highest quality will be accepted for publication after a rigorous peer review. It is the intent of the Editor to complete all reviews in a very timely manner. It is the aim of Multifunctional Composites to provide a globally unified platform to rapidly disseminate the latest and most significant research findings in next-generation multifunctional composites to the international research community.

Editor-in-Chief

Gaurav Nilakantan, Ph.D.
Senior Research Associate
Mork Family Dept. of Chemical Engineering and Materials Science
University of Southern California
3651 Watt Way, VHE 602
Los Angeles, CA 90089

Editorial Advisory Board

Jandro L. Abot, Ph.D., *Catholic University of America, USA*
Brandon J. Arritt, *Air Force Research Laboratory (AFRL), USA*
K. Chandrashekhara, Ph.D., *Missouri University of Science and Technology, USA*
Weinong Chen, Ph.D., *Purdue University, USA*
Paolo Feraboli, Ph.D., *University of Washington, USA*
Geoff Gibson, *Newcastle University, UK*
Carlos Gonzalez, Ph.D., *IMDEA, Spain*
Igor Guz, Ph.D., *University of Aberdeen, UK*
Richard Haber, Ph.D., *Rutgers University, USA*
Pascal Hubert, Ph.D., *McGill University, Canada*
David Hui, Ph.D., *University of New Orleans, USA*
Arthur Jones, Ph.D., *University of Nottingham, UK*
Ryan Karkkainen, *University of Miami, USA*
Michael Kessler, Ph.D., *Iowa State University, USA*
Antonios Kotsos, Ph.D., *Drexel University, USA*
Bruce LaMattina, Ph.D., *Rutgers University, USA*
Michael Maher, *Defense Advanced Research Projects Agency (DARPA), USA*
Steven Nutt, Ph.D., *University of Southern California, USA*
Glaucio Paulino, Ph.D., *University of Illinois-Urbana, USA*
Ton Peijs, Ph.D., *Queen Mary University of London, UK*
Siddiq Qidwai, Ph.D., *Naval Research Laboratory (NRL), USA*
Kenneth Reifsnider, Ph.D., *University of South Carolina, USA*
Jag Sankar, Ph.D., *North Carolina A&T State University, USA*
Michael Sinapius, Ph.D., *University of Braunschweig, Germany*
Henry A Sodano, Ph.D., *University of Florida, USA*
Jonghwan Suhr, Ph.D., *University of Delaware, USA*
James P. Thomas, Ph.D., *Navy Research Laboratory (NRL), USA*
Erik Thostenson, Ph.D., *University of Delaware, USA*
Vikas Tomar, Ph.D., *Purdue University, USA*
Jerome T. Tzeng, Ph.D., *Army Research Laboratory (ARL), USA*
Reza Vaziri, Ph.D., *The University of British Columbia, Canada*
Bingqing Wei, Ph.D., *University of Delaware, USA*
Eric D. Wetzel, Ph.D., *Army Research Laboratory (ARL), USA*
Xinran Xiao, Ph.D., *Michigan State University, USA*
Jenn-Ming Yang, Ph.D., *University of California Los Angeles, USA*
Qingda Yang, Ph.D., *University of Miami, USA*
Fuh-Gwo Yuan, Ph.D., *North Carolina State University, USA*
Zhong Zhang, Ph.D., *National Center for Nanoscience and Technology, China*
James Q. Zheng, Ph.D., *US Army, USA*

JOURNAL OF MULTIFUNCTIONAL COMPOSITES is published by DEStech Publications, Inc., 439 North Duke Street, Lancaster, PA 17602, U.S.A., 717-290-1660; <http://www.destechpub.com>.

Publication frequency: Inaugural year - April and October, then published quarterly - January, April, July and October.
Subscriptions: Annual Online only - \$450.00; Print only - \$470.00; Combined Print and Online - \$480.00 Single copy price - \$130.00
Non U.S. print or combined subscriptions add \$45.00 for postage

ISSN: 2168-4286 doi: 10.12783/issn.2168-4286

 DEStech Publications, Inc.

©2014 DEStech Publications, Inc. All rights reserved.

Journal of Multifunctional Composites

July 2014

Volume 2, Number 3

ISSN 2168-4278

Manufacture and Characterisation of Piezoelectric Broadband Energy Harvesters Based on Asymmetric Bistable Laminates	113
PETER HARRIS, CHRIS R. BOWEN and H. ALICIA KIM	
Simulating Multiphysics of Discrete Fracture Path Development in Fibrous Composites	125
VAMSEE VADLAMUDI, KENNETH REIFSNIDER and PRASUN MAJUMDAR	
A Review on Stability and Vibration Control of Piezolaminated Composite/FGM Plate Structures	139
PRIYANKA A. JADHAV and KAMAL M. BAJORIA	
Aligned Discontinuous Fiber Composites: A Short History	155
MATTHEW SUCH, CARWYN WARD and KEVIN POTTER	



Manufacture and Characterisation of Piezoelectric Broadband Energy Harvesters Based on Asymmetric Bistable Laminates

PETER HARRIS, CHRIS R. BOWEN and H. ALICIA KIM*

Department of Mechanical Engineering, University of Bath, Bath, BA2 7AY, UK

KEYWORDS

bistable
harvesting
scavenging
power
piezoelectric

ABSTRACT

Piezoelectric energy harvesters that convert mechanical vibration into electrical energy are potential power sources for systems such as autonomous wireless sensor networks or safety monitoring devices. However, ambient vibrations generally exhibit multiple time-dependent frequencies, which can include components at relatively low frequencies. This can make typical linear systems inefficient or unsuitable; particularly if the resonant frequency of the device differs from the frequency range of the vibrations it is attempting to harvest. To broaden the frequency response of energy harvesters researchers have introduced elastic non-linearities; for example by designing bistable harvesters with two energy wells. Methods employed to induce bistability include magnetic interactions, axial loading, and buckling of hinge-like components. An alternative method has been recently considered where a piezoelectric element is attached to bistable laminate plates with an asymmetric stacking sequence to induce large amplitude oscillations. Such harvesting composite structures have been shown to exhibit high levels of power extraction over a wide range of frequencies. In this paper we manufacture and characterise the energy harvesting capability of bistable asymmetric laminates coupled to piezoelectric materials. Cantilever configurations are explored and harvested power levels as a function of load impedance, vibration frequency and amplitude assessed. Harvested power levels, natural frequencies and mode shapes are compared with linear cantilevers of similar geometry with a symmetrical stacking sequence to assess the benefits of using bistable laminate configurations.

© 2014 DEStech Publications, Inc. All rights reserved.

1. INTRODUCTION

Devices for the conversion of vibrational energy to electrical power have received increasing interest in the past decade, with a particular application of autonomous low power devices such as wireless sensor nodes. A variety of methods have been considered including electrostatic generation [1], electromagnetic induction [2] and the piezoelectric effect [3].

The piezoelectric effect has a number of advantages including ease of integration within a system, higher strain energy densities compared to electrostatic and electromagnetic systems and a purely solid-state conversion between electrical and mechanical energy [4]. In many cases piezoelectric

energy harvesting devices have been designed to operate close to a resonant frequency to optimise the power generation, for example simple linear cantilevered beam configurations [5]. An alternative approach is to exploit non-linear dynamics, such as bistability, to improve the power harvesting capability. As an example, the dynamic modes of non-linear systems have been observed to produce power across a broadband range of frequencies [6].

A common nonlinear piezoelectric energy harvesting device is a bistable cantilever system where the bistability is induced using an external arrangements of magnets. An alternative method presented by Erturk, *et al.* employs a piezoelectric element attached to the surface of a composite laminate with an asymmetric stacking sequence [3]. Such an approach is aimed at exploiting the inherent bista-

*Corresponding Author: H.A.Kim@bath.ac.uk, Tel: +44 (0) 1225 383375

bility arising from anisotropic thermal properties of laminate composites. Figures 1(a) and 1(b) shows the two stable equilibrium states of a square bistable $[0/90]_T$ carbon fibre reinforced polymer (CFRP) laminate with a Macro Fibre Composite (MFC) piezoelectric element attached to its centre. Figure 1(c) shows the double-well strain energy profile for the range of curvatures of a bistable composite obtained via an analytical model, where the two minima represent the two stable equilibria, State 1 and State 2 [inset of Figure 1(c)] and the saddle point in the centre shows the unstable equilibrium, [7]. The energy hill that needs to be traversed to ‘snap-through’ from one state to the other is also apparent in Figure 1(c).

Bistable laminates have been extensively studied for morphing or adaptive structure concepts [8–10] since snap-through between stable states can result in a large deflection. For harvesting applications, a conformable piezoelectric element is attached to the laminate surface to generate electrical energy by the direct piezoelectric effect as the structure is repeatedly deformed as a result of mechanical vibrations. The onset of snap-through events is thought to lead to large and rapid variation in strain leading to high power outputs achieved over a broad frequency range [3]. Experimentally, such harvesting devices have been shown to exhibit high levels of power extraction over a wide range of frequencies; for example, approximately 30 mW was achieved for an accel-

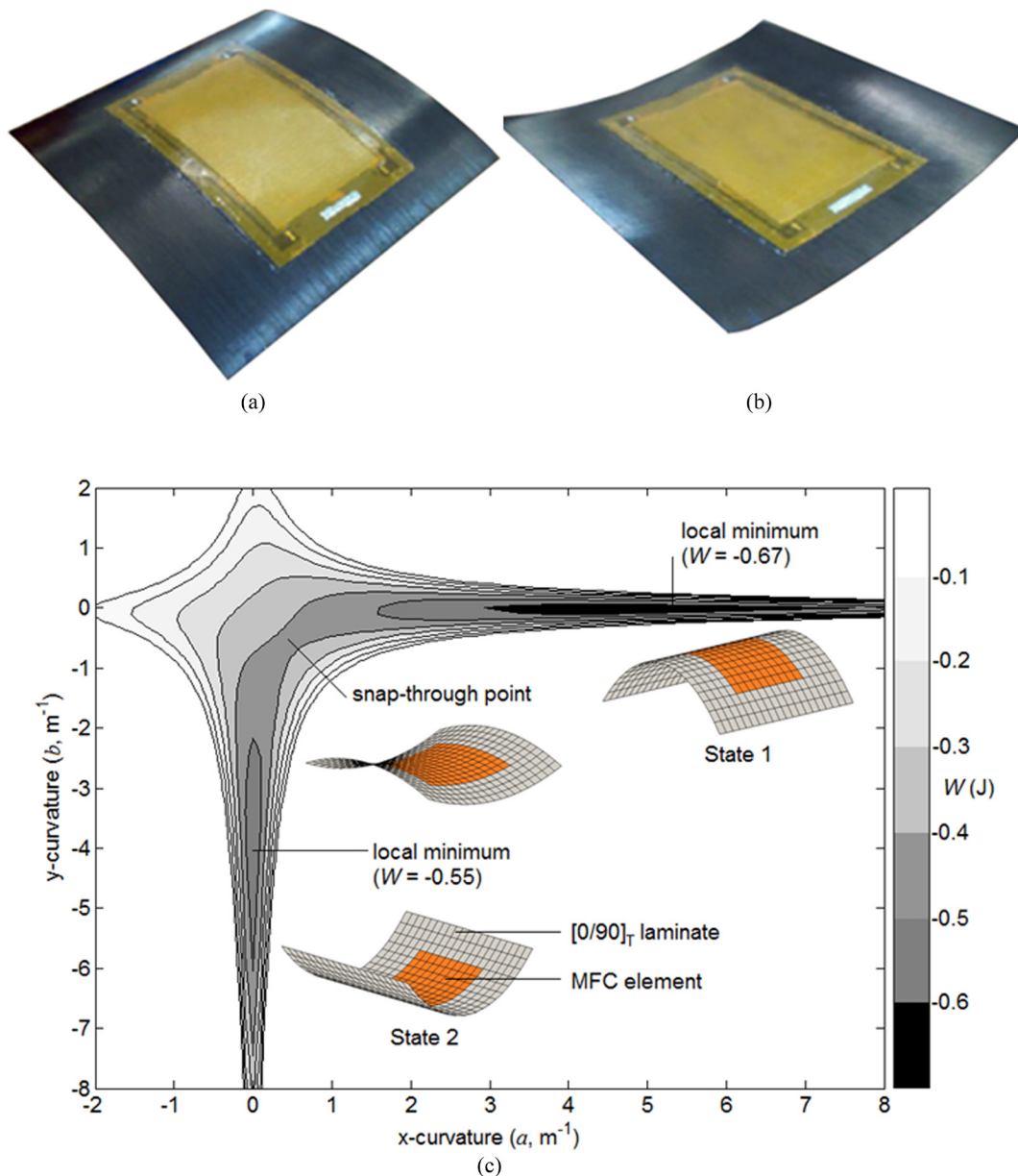


Figure 1. (a) First stable state of $[0/90]_T$ laminate with Macro Fibre Composite (MFC) piezoelectric patch; (b) second state; and (c) corresponding strain energy profile.

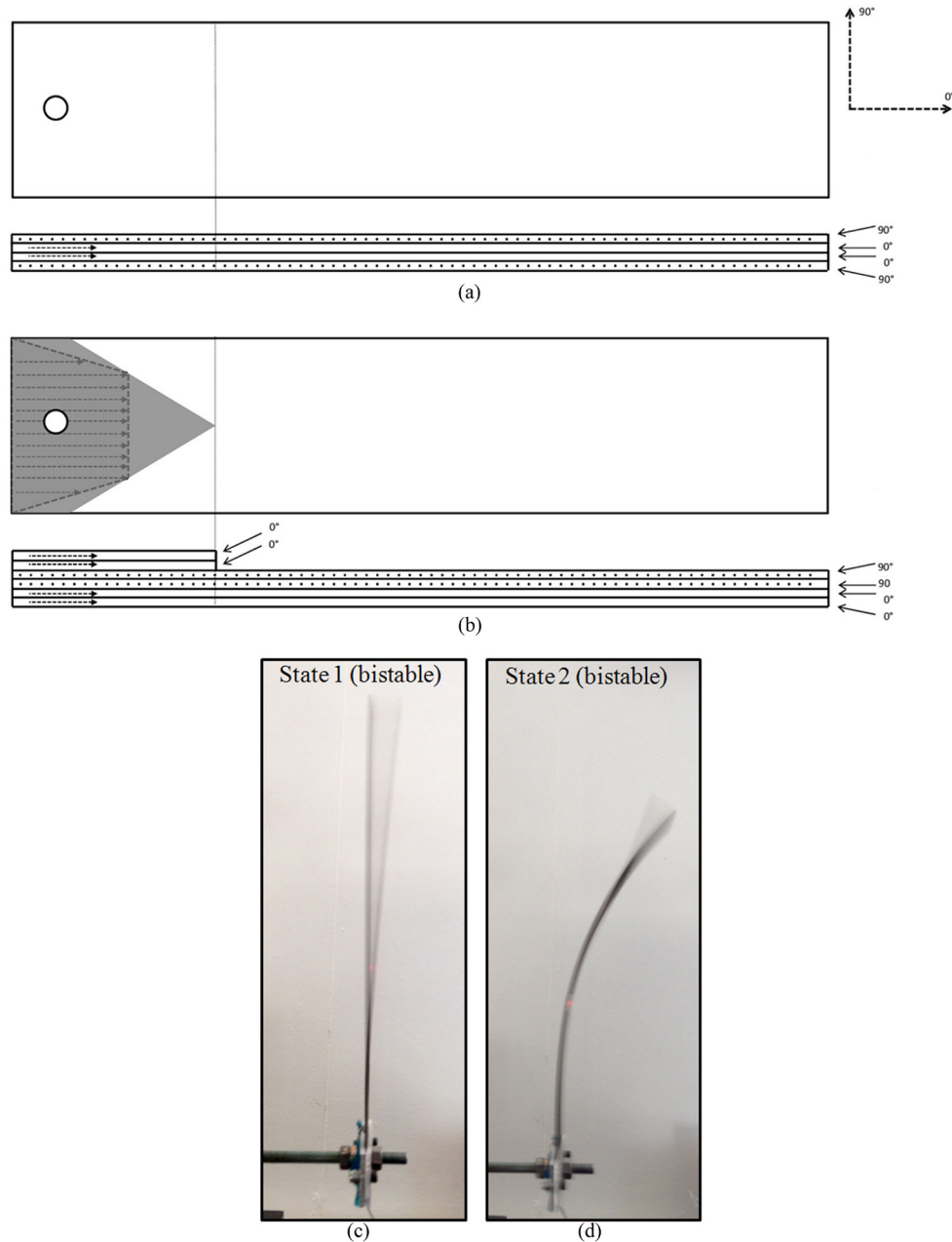


Figure 2. Laminate lay-ups: (a) linear and symmetric $[90/0/0/90]_T$; and (b) bistable and asymmetric $[0/0/90/90]_T$. The cantilevers were clamped at the left hand side. Bistable states: (c) State I; and (d) State II.

eration forcing level of 2.0 g [3], and there are opportunities for further optimisation to increase the power output [11] by tuning the laminate lay-up and geometry. However, what is less clear is how the power output compares quantitatively between linear and bistable energy harvesting devices.

The aim of this paper is to present the comparative investigation of linear and bistable energy harvesters. A cantilevered beam configuration is selected of the same dimensions made from carbon fibre-reinforced polymer (CFRP) laminates. The linear beam has a symmetrical stacking sequence and the bistable beam has an asymmetrical stacking se-

quence of the same plies. The following sections will outline the further details of the experimental set up and discuss the modal characteristics and the power harvesting capability of the two beam configurations.

2. EXPERIMENTAL

2.1. Composite Manufacture

Two cantilevered beams were made using unidirectional CFRP, HexPly M21 (Hexcel) with a Young's modulus (E_{11})

of 178 GPa and shear modulus (G_{12}) of 5.2 GPa [12]. The ply layup for the linear beam was $[90/0/0/90]_T$, as shown in Figure 2(a), and the bistable beam was $[0/0/90/90]_T$, as shown in Figure 2(b) where 0° is along the span of the beams. The beam dimensions were 280 mm long and 60 mm wide and the ply thickness was between 0.185 and 0.195 mm after curing. To ensure the clamped end of the bistable cantilever remained flat in its two stable states, two additional plies were added at one end to make the clamped region symmetric $[0/0/90/90/0/0]_T$, Figure 2(b). Figures 2(c) and 2(d) shows the two states of the bistable beam.

In order to convert mechanical vibrations of the laminate beams into electrical energy a MFC piezoelectric element (M8528-P2, Smart Materials) of dimensions 105 mm \times 34 mm was bonded to the surface of the laminate at 35 mm from the root. The MFC is based on a lead zirconate titanate (PZT) ferroelectric ceramic which is polarised through its thickness with a manufacturer's specified capacitance of

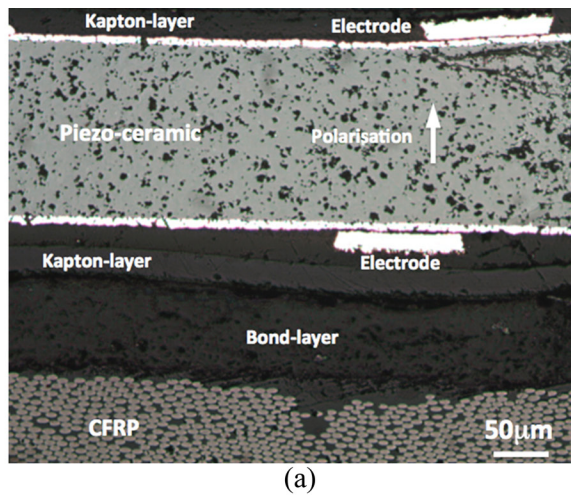
172 nF [13]. Figure 3(a) shows a cross section of the MFC bonded onto the CFRP showing the piezoelectric fibre in the MFC, the upper and lower electrodes to collect the harvested charge and the bond layer. Figure 3(b) shows a top-down view of the MFC attached to the CFRP where the piezoelectric fibres and the upper mesh electrode can be observed.

2.2. Composite Characterisation

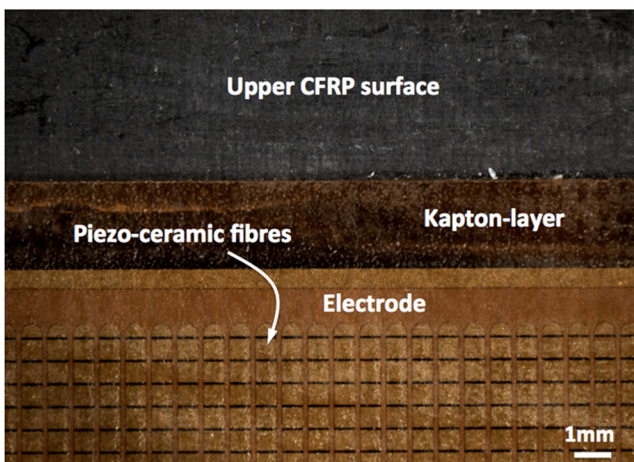
The first 30 mm of the beams were bolted between two aluminum plates to induce the clamped boundary condition, as shown in Figure 4(a), which also shows the overall dimensions. The energy harvester (i.e. the laminate-MFC combination) was mounted to an electrodynamic shaker (LDS V455) as in Figure 4(b). When undertaking frequency sweeps at constant peak acceleration for power generation, the shaker signal was generated in LabVIEW (National Instruments NI-USB-6211 DAQ) which determines the signal amplitude to achieve a desired g-level at a particular frequency. This is achieved by initially measuring the velocity, and then calculating the acceleration of the central shaker attachment for range of drive frequencies (15–200Hz) and shaker input voltages (0.05–5.0V) and generating a calibration table for any chosen g-level. The shaker input in terms of drive frequency and input voltage is achieved via a power amplifier (Europower EP1500).

In order to characterize the frequency response function of the energy harvester, a mechanical input signal was generated using Polytech's 'PSV Acquisition' software (Ver. 8.82). The structural response of the harvester was monitored by a laser vibrometer (Polytec PSV-400-M4 with VD-09 decoder) to measure the displacement and velocity of one point of the harvester 130 mm from the clamped end. Reflective tape was adhered to the harvester to improve the signal return of the scanning laser, as in Figures 4(a) and 4(b). Figure 4(c) shows a schematic of the experimental arrangement to characterize the frequency response.

In order to characterise harvested power it is necessary to attach a resistive load to the piezoelectric element as it is under vibration. A load resistor is attached across the MFC and the potential difference across it measured using an oscilloscope (Agilent 54835A). The optimal load resistance (R_L) for maximum power at a particular frequency (f) is achieved by matching the load impedance to the capacitive load of the piezoelectric ($C_p = 172$ nF); this is achieved at to the condition $2\pi \cdot f \cdot R_L \cdot C_p = 1$. For the initial phase of testing a single load resistance was used which for the linear harvester $R_L = 21$ k Ω (2nd bending mode at 43 Hz) and for the bistable $R_L = 36$ k Ω (1st bending mode at 26 Hz). Figure 4(d) shows a schematic of the experimental arrangement for power characterization and Figure 4(e) shows the harvester electrical circuit diagram. Additional test procedures are also detailed where relevant throughout the paper.



(a)



(b)

Figure 3. (a) Cross-section of MFC-carbon epoxy laminate; and (b) top-down view of piezoelectric showing piezoelectric fibres and electrode structure.

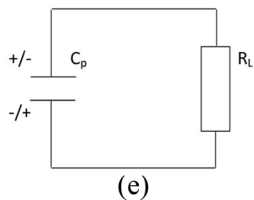
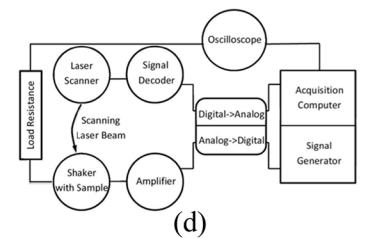
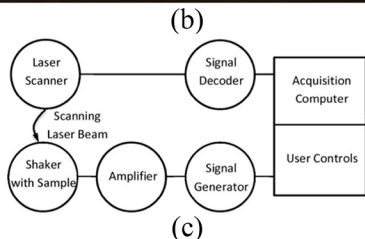
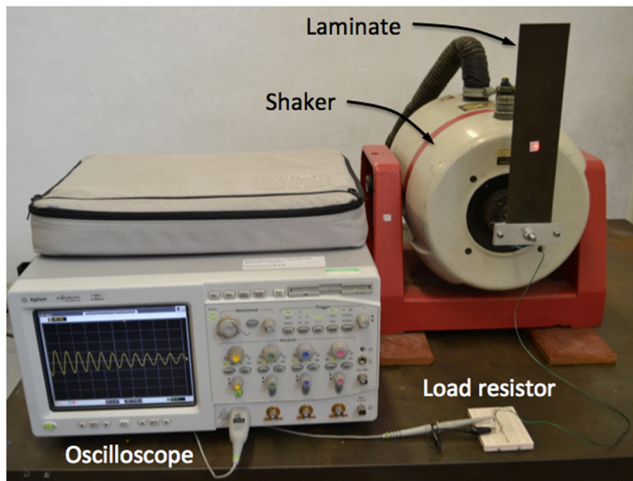
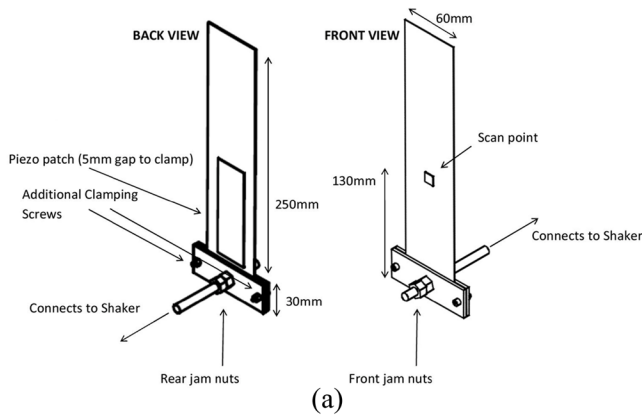


Figure 4. Experimental setup: (a) clamped cantilever beam; (b) cantilever energy harvester on the shaker and reflective tape and a load resistor; (c) schematic of the experimental setup for frequency response function; (d) experimental schematic for power versus frequency, g-level and load resistance; (e) energy harvesting circuit.

3. RESULTS

3.1. Dynamic Modes of Linear and Bistable Cantilever Beams

The frequency response function of the energy harvesters were initially characterized to examine the resonant frequencies of the beams. A frequency range from 1–200 Hz which covers a typical frequency range of a bridge with traffic and ground transport was analyzed [14]. To characterise the response of the linear and bistable beams, they were both subjected to the same perturbation input, and their free vibration response recorded in the time domain and then transformed into the frequency domain using a fast Fourier transform. The perturbation was a burst ‘chirp’ signal which swept through frequencies of 310–340 Hz in approximately 0.32s. From the start of the chirp, the scanner was set to delay measurement for 0.55s, giving the laminate 0.23s to transition into a free response and the shaker’s shank to come to a complete stop. From the time measurement began, velocity data was collected for 6.4 seconds with a sampling frequency of 1.28 kHz. The shaker was driven with a constant voltage of 3.5V resulting in an RMS acceleration of 47g and a maximal value of over 70g. Snap-through of the bistable beam during chirp characterisation was not observed this testing phase.

Figure 5 shows the fast Fourier transform (FFT) of the velocity measurements at the scan point of Figures 4(a) and 4(b) of the linear and bistable cantilevered beams from 1–200 Hz. As the velocity measurement is taken in the centre of the width, torsional or rolling modes around the axis along the span of the beam are not identified. Table 1 summarises the resonant modes and Figures 6(a) and 6(b) shows

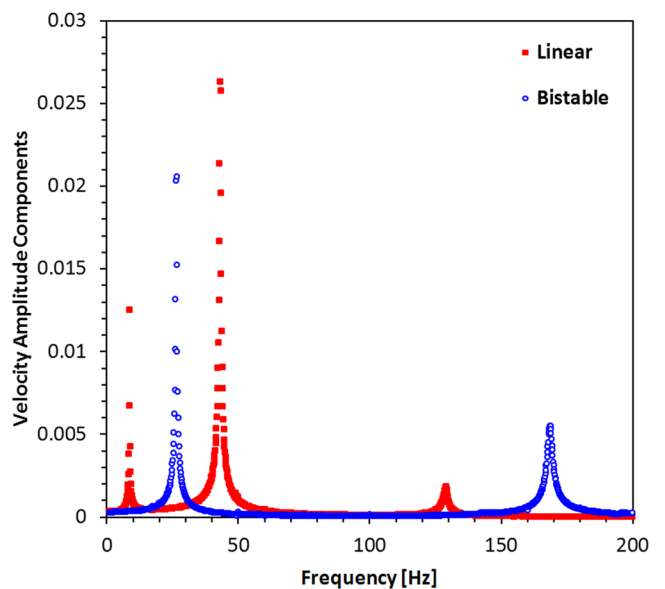
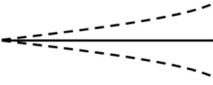
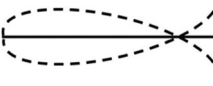
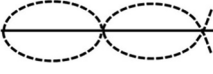


Figure 5. Fast Fourier transform (FFT) of the velocity of the linear and bistable cantilevered beams.

Table 1. Mode Shapes and Associated Frequencies for Linear and Bistable Harvester.

Mode	Mode Shape	Linear Beam	Bistable Beam
1st bending		9 Hz	26 Hz
2nd bending		43 Hz	176 Hz
3rd bending		129 Hz	> 200 Hz (not observed)

the first and second bending modes; the displacement of the third mode was too small to be observed visually. Within the experimental range of 1–200 Hz, three resonant modes were observed for the linear beam while two modes were observed for the bistable beam. Noting that we measured the velocity at the location just off the centre of the beam, the amplitudes of the modes are consistent with the corresponding mode shapes.

As shown in Figure 5, the frequency at which the bistable encounters the different bending mode orders is consistently higher than those of the linear harvester. This is due to higher

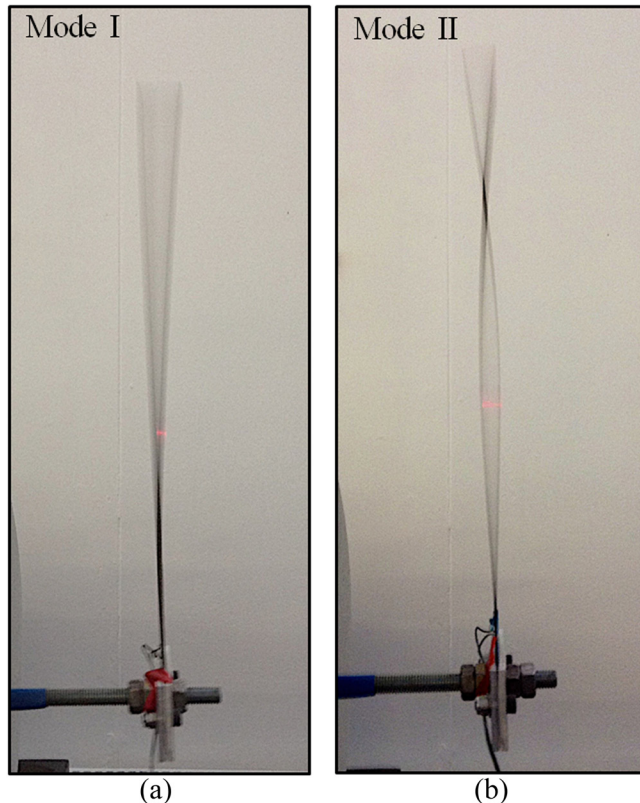


Figure 6. Mode shapes: (a) First bending mode; (b) Second bending mode.

stiffness of the bistable cantilever which is attributable to the fact that the bistable harvester has an extra two layers in the clamping region and the asymmetric nature of the bistable layup leads to a curvature of the cantilever about the longitudinal axis, further increasing the bending stiffness.

3.2. Investigation of Harvested Power with Frequency

To demonstrate the differences between high and low excitation for both of the harvesters, sweeps from 15 Hz to 200 Hz were carried out at 1g and 6g acceleration for both the linear and bistable energy harvester. To highlight in detail the regions of maximal power output, near the natural frequencies, more detailed frequency sweeps with an increment 0.2 Hz were undertaken as shown in Figures 7(b), (c) and Figure 8(b), (c) for the linear and bistable system respectively at 1g, 2g, 4g and 6g. The lower bound of frequencies when performing sweeps such as these is 15 Hz due to the electric current limitations of amplifier powering the shaker system. This limits the investigation for the power harvesting characteristics of the linear first mode which is at 9 Hz. We, therefore, focus our power characteristic investigations on the second and third modes of the linear harvester. Measurements were undertaken by both increasing frequency (‘up-sweep’) and decreasing frequency (‘down-sweep’) to further characterise any non-linear behaviour. Upon changing to each frequency, 0.2s was allowed for the harvester to attain a steady-state response before the velocity data was recorded for 4.8 seconds. From the set of data at each frequency, the peak velocity value and a root mean squared (RMS) voltage were measured. The harvesting power for a specific frequency and g-level was calculated using Equation (1).

$$P = \frac{V_{rms}^2}{R} \quad (1)$$

We see that for the linear harvester, there is a small decrease in the the natural frequency, less than 2 Hz, for the 2nd and 3rd bending modes when the excitation is gradually increased from 1g to 6g [see Figures 7(b) and 7(c)]. The small decrease in natural frequency with increasing excitation is likely due to some softening (non-linearities) inherent to the CFRP material [15,16]. The stiffness of the piezoelectric (PZT ceramic) is also non-linear [17].

For the bistable beam, there is a difference in power output between the upward and downward frequency sweeps at higher g-level (see Figure 8). This is particularly apparent for the 1st bending mode at 6g in Figure 8(b), where the curve becomes asymmetric and leans towards lower frequencies (‘horning’) due to softening at higher excitation levels and is a characteristic of non-linear systems [18]. Snap-through events are shown in Figure 8 by highlighted data points.

Figures 9(a), and 9(b) show the increase of peak power for

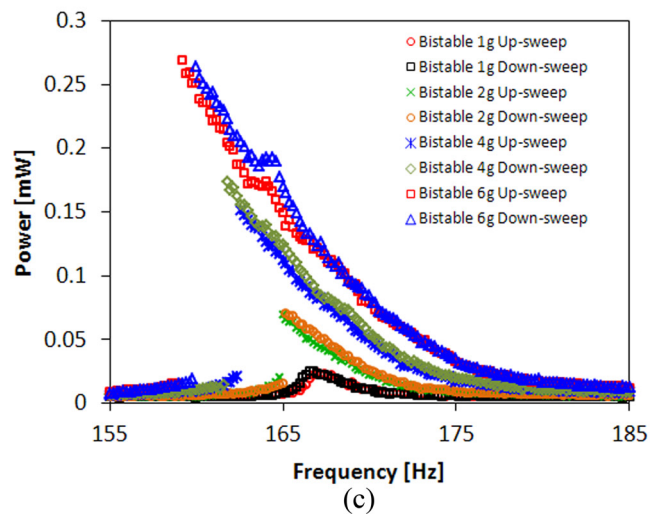
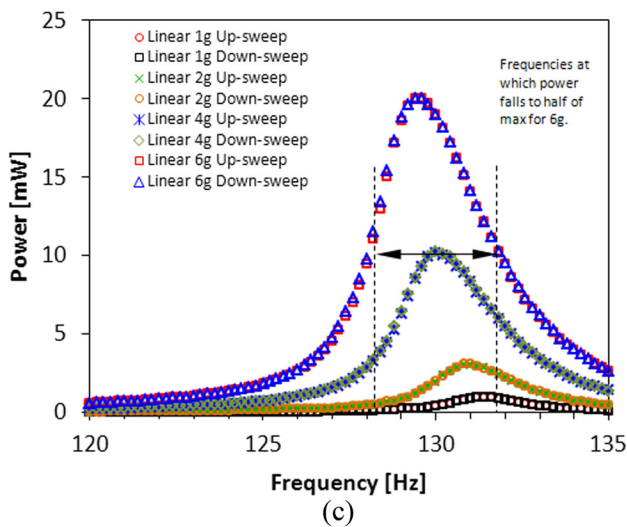
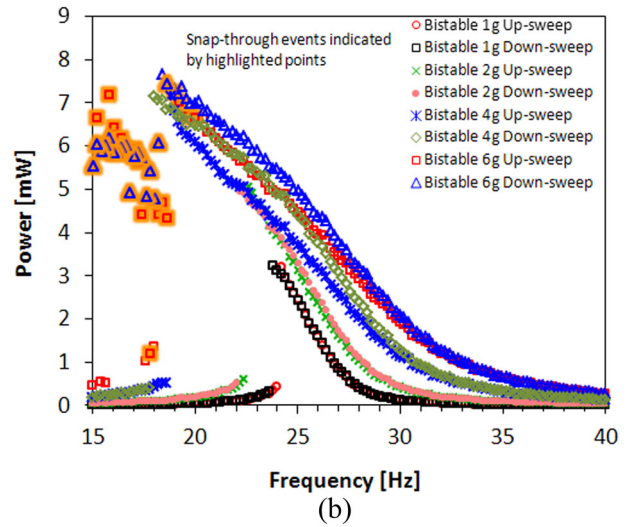
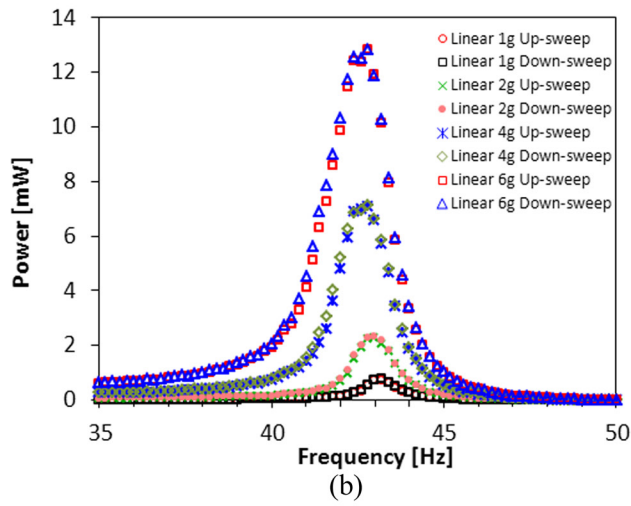
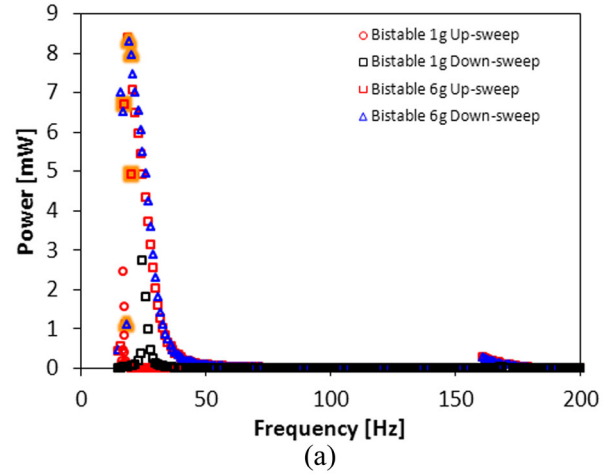
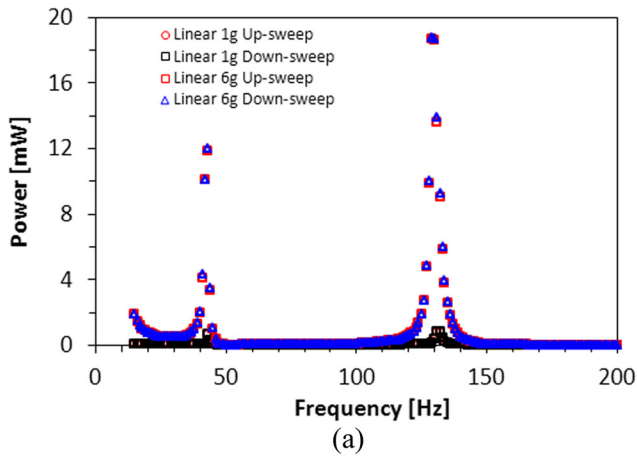


Figure 7. Power versus frequency for 1g, 2g, 4g and 6g for linear beam: (a) frequency range 15–200 Hz; (b) detailed view of 2nd mode; and (c) detailed view of 3rd mode.

Figure 8. Power versus frequency and 1g, 2g, 4g and 6g for bistable beam: (a) frequency range 15–200 Hz; (b) detailed view of 1st mode; and (c) detailed view of 2nd mode.

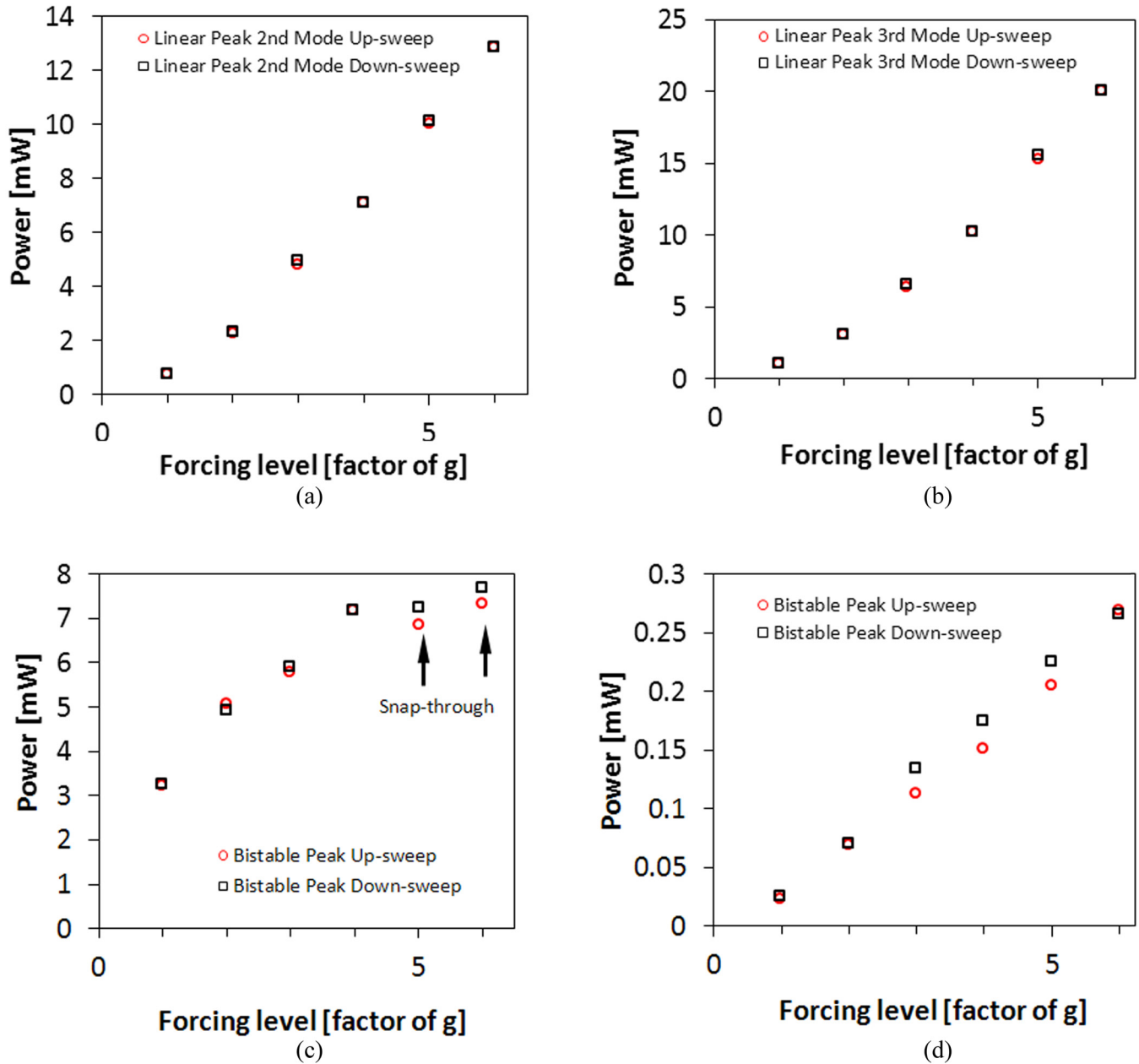


Figure 9. Maximum power output at modes over a range of input acceleration for linear beam: (a) second mode; and (b) third mode. Maximum power output at modes over a range of input acceleration for bistable beam: (c) first mode; and (d) second mode.

the 2nd and 3rd modes of the linear harvesting beam respectively. The relationship between peak power and excitation level is approximately linear. A small degree of nonlinear behavior in the power versus excitation level is observed; this may be due to the fact that both CFRP and PZT exhibits a small degree of non-linear behavior [15–17]. Based on a linear relationship of peak power against the excitation level for the data in Figures 9(a) and 9(b), the R^2 is 0.992 and 0.981 for the second and third bending modes respectively. However, a quadratic relationship leads to R^2 values of 0.999 for both cases. Thus, the power increase over the range is

slightly greater than expected by a linear approximation and any softening of the harvester leads to higher strain in the MFC, resulting in higher power output.

Figures 9(c) and 9(d) show the increase of peak power for the 1st and 2nd modes of the bistable harvester respectively at increasing excitation (g-level). The relationship between the excitation level, the degree of softening and the hysteric behaviour of the power output of the harvester is more complex than the linear system. With reference to the first bending mode, at 1g the ‘up-sweep’ and ‘down-sweep’ power levels are almost coincident since at low excitation levels

the bistable harvester exhibits almost linear behaviour. At increasing excitation level the structure exhibits non-linear behaviour ('softening'), as seen in Figure 8(b). In this case there is an area of instability underneath the 'overhang' in Figure 8(b) where limited power data are recorded. This is due to the fact that on the up-sweep, the state of the system tends to stay on the lower fold until sufficient energy is achieved for the system to switch to the upper fold. During the down-sweep the system tends to stay on the higher of the two folds and stays at a higher state of excitation for a greater duration until energy dissipation causes a jump down to the lower fold. The increase of the degree of softening at higher excitation explains why the peak power outputs diverge for both the up-sweep and down-sweep. At high levels of excitation, especially when there are 'snap-through' events as in Figure 8(b), the position and tendency of the system to jump from one fold to another is highly sensitive which combine to bring the peak powers closer together; see for example data for 5g and above in Figure 9(a).

3.3. Investigation of Harvested Power and Load Resistance

The measurements in the previous sections were undertaken for a fixed load resistance corresponding to impedance matching of the capacitive impedance of the piezoelectric MFC to the load resistance. In this section the load resistance is varied to examine the change in optimal resistance with excitation level due to the shift of peak power frequency [e.g. as in Figure 8(b)]. For measurement of the harvested power both harvesters were connected to an electrical circuit with a range of load resistors as in Figure 4(e).

Since ferroelectric ceramics are highly insulating the piezoelectric patch behaves approximately as a capacitor (C_p) and has a capacitance of 172 nF. During vibration of the harvester the resulting deformation in alternating directions leads to charges of alternating polarity accumulating on the electrodes with each reversal of curvature of the beam. This accumulation of alternate charges translates to an AC voltage signal, dissipating the energy across the resistor (R_L). This resistor represents the load of the electrical system which could be a sensor, or other such electrical component receiving the harvested energy. To maximise the power output, the value of the resistor is chosen to accommodate the harvester's natural frequency, and the value of the capacitance within the circuit. The power output is at a maximum when:

$$R_L = \frac{1}{2\pi \cdot f \cdot C_p} \quad (2)$$

Thus, for the linear harvester a value of 21 k Ω was chosen in the previous section to coincide with the 2nd bending mode at 43 Hz, and for the bistable, and 36 k Ω to coincide

with the first bending mode at 26 Hz. To demonstrate the influence of load resistance on harvested power, additional power characterisation was undertaken at a range of load resistance (1 k Ω to 1000 k Ω).

Figure 10 shows the dependence of the peak power output of the bistable harvester with respect to the load resistance at 1g and 6g. Data for the linear harvester are not shown since it is the bistable system that exhibits the largest degree of softening. The resistances were varied from 1 k Ω , approaching short circuit conditions where the piezoelectric discharges rapidly, to 1 M Ω , approaching open circuit conditions where the piezoelectric discharges slowly. It can be clearly observed that the power generation is highly dependent on load resistance.

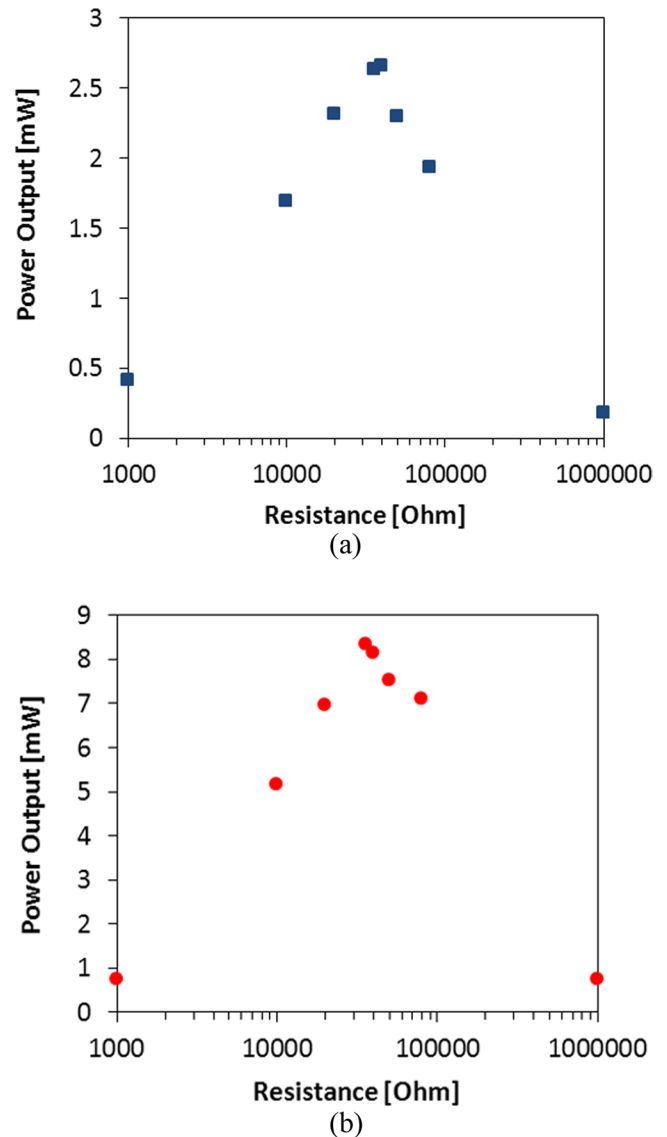


Figure 10. Bistable harvester peak power output over range of load impedance at: (a) 1g peak acceleration; and (b) 6g peak acceleration.

With increasing excitation, there is a softening of the bi-stable, [Figure 8(b)] causing the natural frequency to shift lower, in accordance to $\omega_n = \sqrt{k/m}$, where k relates to the stiffness of the mechanical system, m to its mass, and ω_n to the natural frequency. Figure 10(a) shows that at 1g, the optimal resistance is 40 k Ω . At 6g excitation input, Figure 10(b) shows that the optimal resistance value has changed to 36 k Ω . Thus, it is seen that ideally, the resistance of the harvesting system would be changed actively depending on the input characteristics. For a purely linear harvester a strong dependence of the peak power with respect to load resistance, as in Figure 10, would also be expected since it originates from an impedance mismatch between the piezoelectric element and the load resistance. Compared to a bi-stable system, the main difference would be that the natural frequency of a linear harvester is not dependent on vibration level, as in Figure 7, and the load resistance would not have to be changed with vibration to achieve peak power.

4. COMPARISON OF BROAD-BAND RESPONSE

In practical applications the frequency of the excitation can change significantly with respect to time, meaning that a meaningful comparison requires more than just a comparison of peak power outputs and that the broadness of the power generation capability must be quantified. The frequencies on either side of the maximum at which the power output level reduces to half the maximum value, Full Width Half Maximum (FWHM) is often used to evaluate the broadband nature of harvesters [19,20], an example is indicated in Figure 7(c). Table 2 summarises these three measures for the different modes at excitation levels of 1g and 6g.

Table 2 shows that at an excitation level of 1g, the bistable harvester in Mode 1 generates higher power, at greater bandwidth than the linear harvester. While the power of Mode 2 of the bistable is small, it is a relatively broad response; also shown in Figure 8(c). At a 6g excitation level, the peak power for the Mode 2 and Mode 3 of the linear harvester is

highest and exceeds the power for the Mode 1 and Mode 2 of the bistable harvester, but only over a narrow frequency range [see FWHM bandwidth in Table 2 and Figure 7(a)]. As the excitation level increases the FWHM increases and at a 6g excitation, Mode 1 of the bistable produces the widest FWHM [see Table 2 and figure 8(a)] indicating the potential for such an approach for increase the broadband response.

5. CONCLUSIONS

This paper has examined both linear and bistable cantilever CFRP beams coupled to piezoelectric materials for energy harvesting applications. In comparing the energy harvesting performance of a linear harvester against that of a bistable nonlinear harvester, it has been seen that at low frequency and low excitation, the bistable has higher power output over a broader range of frequencies. The linear harvester has the potential to produce a higher peak power, but at a comparatively narrow bandwidth with respect to the bi-stable system. The similarity of the harvesters was imposed by matching the physical characteristics of dimension and piezoelectric patch placement as closely as possible, but further testing where the dynamic responses are matched could prove useful. The load resistance should be matched with the capacitive load of the piezoelectric element to produce peak power levels. With increasing excitation levels, softening of the bistable system leads to the peak power being produced at lower levels of frequency, necessitating some form of active tuning of the load resistance. It was also observed that the maximum power output of the linear harvesters increased quadratically with the excitation amplitude in the range we tested. The trend for the bistable harvesters was not as clear due to complex interaction of nonlinearity and difference between up- and down-sweeps at high excitation levels.

In this paper the change from a linear to a bistable harvester has been achieved by simply changing from a symmetric layup of $[90/0/0/90]_T$ to an unsymmetric layup $[0/0/90/90]_T$ to enable a comparison between the two cases. Tailoring of the laminate lay-up, cantilever geometry and materials employed (CFRP and piezoelectric) provides a variety of routes to tailor the non-linear characteristics to harvest specific vibration energies.

6. ACKNOWLEDGEMENT

The research leading to these results has received funding from the European Research Council under the European Union's Seventh Framework Programme (FP/2007-2013) / ERC Grant Agreement no. 320963 on Novel Energy Materials, Engineering Science and Integrated Systems (NEMESIS). Dr. H. Alicia Kim acknowledges support from the Engineering and Physical Science Research Council (EPSRC) for Project Reference: EP/J014389/1.

Table 2. Figures of Merit for the Modal Orders and Harvester Types.

	Linear		Bistable		g-level
	Mode 2	Mode 3	Mode 1	Mode 2	
Peak power [mW]	0.738	0.930	3.19	0.023	1
FWHM [Hz]	1.1	2.7	1.9	3.3	
Peak power [mW]	2.29	3.04	5.06	0.069	2
FWHM [Hz]	1.4	3.0	3.3	3.5	
Peak power [mW]	7.07	10.15	7.14	0.15	4
FWHM [Hz]	1.8	3.4	6.6	5.1	
Peak power [mW]	12.83	20.07	7.3	0.268	6
FWHM [Hz]	2.1	3.8	8.4	6.6	

7. REFERENCES

- [1] Mitcheson, P. D., P. Miao, B. H. Stark, E. M. Yeatman, A. S. Holmes, and T. C. Green. 2004. "MEMS Electrostatic Micro-Power Generator for Low Frequency Operation," *Sensors and Actuators A: Physical*, 2(115):523–529. <http://dx.doi.org/10.1016/j.sna.2004.04.026>
- [2] Glynn-Jones, P., M. J. Tudor, S. P. Beeby, and N. M. White. 2004. "An electromagnetic, vibration-powered generator for intelligent sensor systems," *Sensors and Actuators A*, 110(1):344–349. <http://dx.doi.org/10.1016/j.sna.2003.09.045>
- [3] Arrieta A. F., P. Hagedorn, A. Erturk, and D. J. Inman. 2010. "A piezoelectric bistable plate for nonlinear broadband energy harvesting," *Appl. Phys. Lett.*, 97(10), 104102-1-3.
- [4] Betts, D. N., C. R. Bowen, H.A. Kim, R. A. Guyer and P-Y Le Bas 2014. "Modelling the Dynamic Response of Bistable Composite Plates for Piezoelectric Energy Harvesting," *ALAA SciTech*. January 13–17.
- [5] Priya, S. 2007. "Advances in energy harvesting using low profile piezoelectric transducers," *J. of Electroceramics*, 19:167–184. <http://dx.doi.org/10.1007/s10832-007-9043-4>
- [6] Erturk, A., and D. J. Inman. 2009. "An experimentally validated bi-morph cantilever model for piezoelectric energy harvesting from base excitations," *Smart Mater. Struct.*, 18(2):1–18.
- [7] Betts, D. N., C. R. Bowen, H.A. Kim, R. A. Guyer and P-Y Le Bas 2014. "Modelling the Dynamic Response of Bistable Composite Plates for Piezoelectric Energy Harvesting," *ALAA SciTech*. January 13–17.
- [8] Erturk, A., J. Hoffmann, and D. J. Inman. 2009 "A piezomagnetoelastic structure for broadband vibration energy harvesting," *Appl. Phys. Lett.*, 25(94):254102-1-3.
- [9] Hyer, M. W. 1981. "Calculations of the Room-Temperature Shape of Unsymmetric Laminates," *J. Compos. Mater*, 15(4):296–310.
- [10] Bowen, C. R., D. N. Betts, P. F. Giddings, A. I. T. Salo, and H. A. Kim. 2012. "A Study of Bistable Laminates of Generic Lay-Up for Adaptive Structures," *Strain*, 3(48):235–240. <http://dx.doi.org/10.1111/j.1475-1305.2011.00817.x>
- [11] Dano, M. -L., and M. W. Hyer. 1998. "Thermally-induced deformation behavior of unsymmetric laminates," *Int. J. Solids Struct.*, 17(35):2101–2120. [http://dx.doi.org/10.1016/S0020-7683\(97\)00167-4](http://dx.doi.org/10.1016/S0020-7683(97)00167-4)
- [12] Betts, D. N., H. A. Kim, C. R. Bowen, and D. J. Inman. 2012. "Optimal configurations of bistable piezo-composites for energy harvesting," *Appl. Phys. Lett.*, 11(100):114104-1-4.
- [13] Hexcel, 2010 "HexPly® M21 180°C (350°F) curing epoxy matrix Product Data" Accessed April 2014. www.hexcel.com
- [14] Smart Materials, Manufacturer's website, Accessed May 2014. www.smart-material.com
- [15] Neri, I., F. Travasso, R. Mincigrucci, H. Vocca, F. Orfei, and L. Gammaitoni. 2012. "A real vibration database for kinetic energy harvesting application," *J. of Intell. Material Sys.*, 23(18):2095–2101. <http://dx.doi.org/10.1177/1045389X12444488>
- [16] Hou, J. P., and C. Ruiz. 2000. "Measurement of the properties of woven CFRP T300/914 at different strain rates," *Composites. Sci. & Tech.* 15(60):2829–2834. [http://dx.doi.org/10.1016/S0266-3538\(00\)00151-2](http://dx.doi.org/10.1016/S0266-3538(00)00151-2)
- [17] Wolfe, H. F., and C. A. Shroyer. 1994. *Large Amplitude Nonlinear Response of Flat Aluminum, and Carbon Fiber Beams*. Wright Laboratory Flight Dynamics Directorate, pp. 3–4. Report no. WL-TM-94-3077.
- [18] Hall, A. D. 2001. "Nonlinearity in piezoelectric ceramics," *J. Mat. Sci.* 19(36):4575–4601. <http://dx.doi.org/10.1023/A:1017959111402>
- [19] Wagg, D., and S. Neild. 2010. *Nonlinear Vibration with Control*. Springer, 73–75, 162–163.
- [20] Betts, D. N., C. R. Bowen, H. A. Kim, R. A. Guyer, P-Y Le Bas., and D.J. Inman. 2014. "Modelling the Dynamic Response of Bistable Composite Plates for Piezoelectric Energy Harvesting," presented at the 55th American Institute of Aeronautics and Astronautics, Conference, 13–17 January, 2014.
- [21] Lei, A., R. Xu, A. Thyssen, A. C. Stoot, T. L. Christiansen, K. Hansen, R. Lou-Møller, E. V. Thomsen, and K. Birkelund. 2011. "MEMS-based thick film PZT vibrational energy harvester," presented at 24th IEEE International Conference on Micro Electro Mechanical Systems, January 23–27, 2011.



Simulating Multiphysics of Discrete Fracture Path Development in Fibrous Composites

VAMSEE VADLAMUDI, KENNETH REIFSNIDER* and PRASUN MAJUMDAR

Department of Mechanical Engineering, University of South Carolina, Columbia, SC 29209 USA

KEYWORDS

fracture
matrix cracking
non-linear behavior
mechanical properties
crack plane

ABSTRACT

The long-term properties of continuous fiber reinforced composite materials are increasingly important as applications in airplanes, cars, and other safety critical structures are growing rapidly. The mechanical, electrical, and thermal properties of composite materials are altered by the initiation and accumulation of discrete fracture events whose distribution and eventual interaction defines the limits of design, such as strength and life. While a strong foundation of understanding has been established for damage initiation and accumulation during the life, an understanding of the nature and details that define fracture path development at the end of life has not been established. The present paper reports a multiphysics study of that progression, which is focused on measured and predicted changes in through-thickness electric/dielectric response of polymer based composites. Experimental data are compared to simulations of micro-defect interactions and changes in electrical and mechanical properties. Applications of the concepts to prognosis of behavior are discussed.

© 2014 DEStech Publications, Inc. All rights reserved.

1. INTRODUCTION

Unlike metallic materials, engineered materials (e.g. composites) are designed to develop distributed damage consisting of various types of defects and even multiple breaks in the same reinforcing fiber. Generally, creation of a single microscopic crack does not individually affect the strength or life of composite materials. Therefore, the primary interest is not in single local events but in the evolution process of multiple events that have a collective global effect. A recent review article has emphasized the need for understanding such nonlinearity due to damage accumulation, stating that “any analysis of fatigue damage evolution that accounts for the irreversibility driving the damage progression has the potential to predict fatigue life with minimum resort to empiricism” [1].

In the present work, we use the calculated response of an analogue material to a vector electric field that passes through the thickness of the composite to study defect devel-

opment, growth, coalescence, and fracture path development in a heterogeneous material to represent material degradation (progressive damage and fracture path development) under repeated or long-term continuous loading during the life of that material. We simulate the dielectric response to an alternating current (AC) excitation of a test element of the material, for the undamaged and fracture-path case, which are then compared to laboratory experiments. As shown in Figure 1, for the undamaged case, for a material such as a glass-reinforced epoxy composite, the AC response is purely capacitive (no DC conduction), and (for linear materials, over a wide range of the response) the absolute value of the impedance (the square root of the sum of the squares of the real and imaginary components) is an essentially linear function of frequency with downward slope, i.e., inversely proportional to the AC frequency (like a parallel plate capacitor). When a fracture path has developed in the element, by definition, there will be a continuous voided path from one physical face to the other. Let us postulate that air with some hydration or simply diffused moisture (or other gas or fluid with some ionic content) enters that voided space. If that

*Corresponding Author: reifsnid@cec.sc.edu

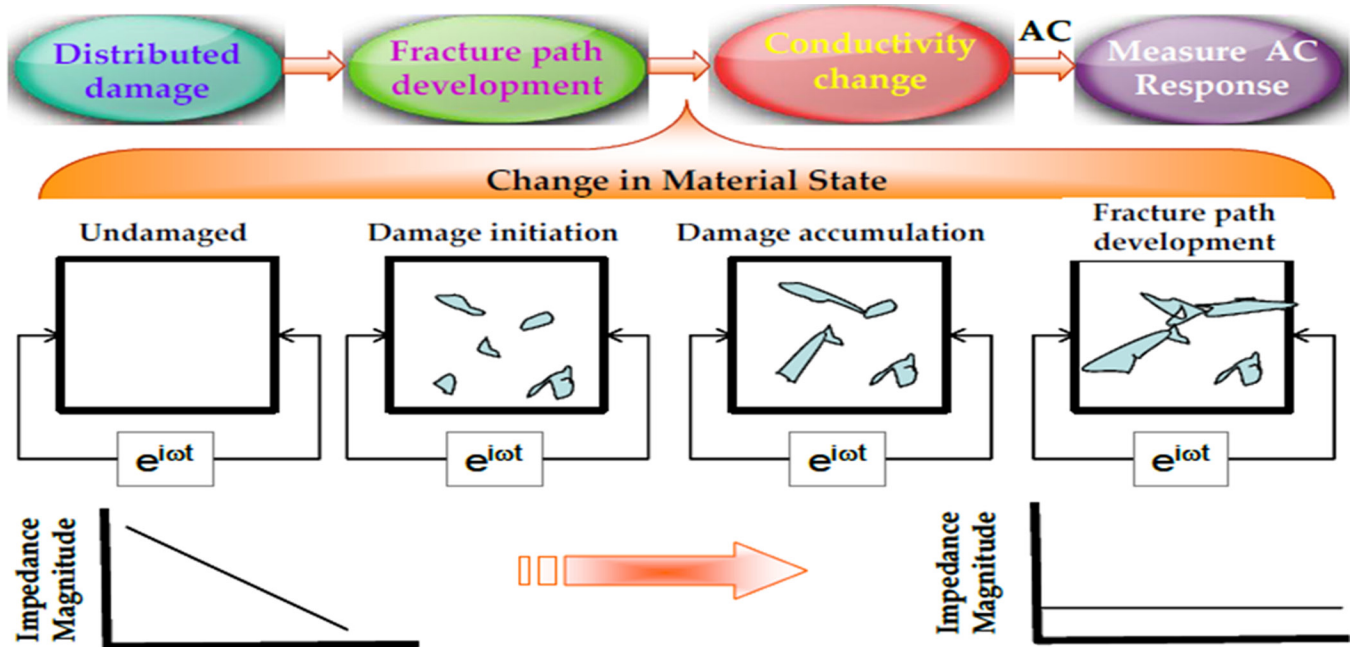


Figure 1. Framework created in previous work [1] that connects material state change to dielectric response.

diffused material is conductive, and the path is continuous, then the idealized response (magnitude of the impedance) will not depend on the frequency of excitation (at least to first order) as shown in Figure 1.

Our physical observations will focus on continuous fiber reinforced structural composite materials, typically laminated with multi-axial ply orientations or with woven fiber architectures, subjected to quasi-static or cyclic loading until fracture. The literature is replete with discussions of the micro-cracking, debonding, delamination, and fiber fracture events that develop during such loadings [2–4]. Examples

of the damage patterns that are observed are shown in Figures 2(a) and 2(b) which show matrix cracks and some fiber fractures, transverse to the principal load axis, through the laminate thickness.

The literature says that “if a group of physical concepts or quantities are related to each other in a certain matter, as by equations of a certain form, and another group of concepts or quantities are interrelated in a similar manner, then an analogy may be said to exist between the concepts of the one group and those of other group” [5]. In the present work, we focus on developing an understanding of fracture path development

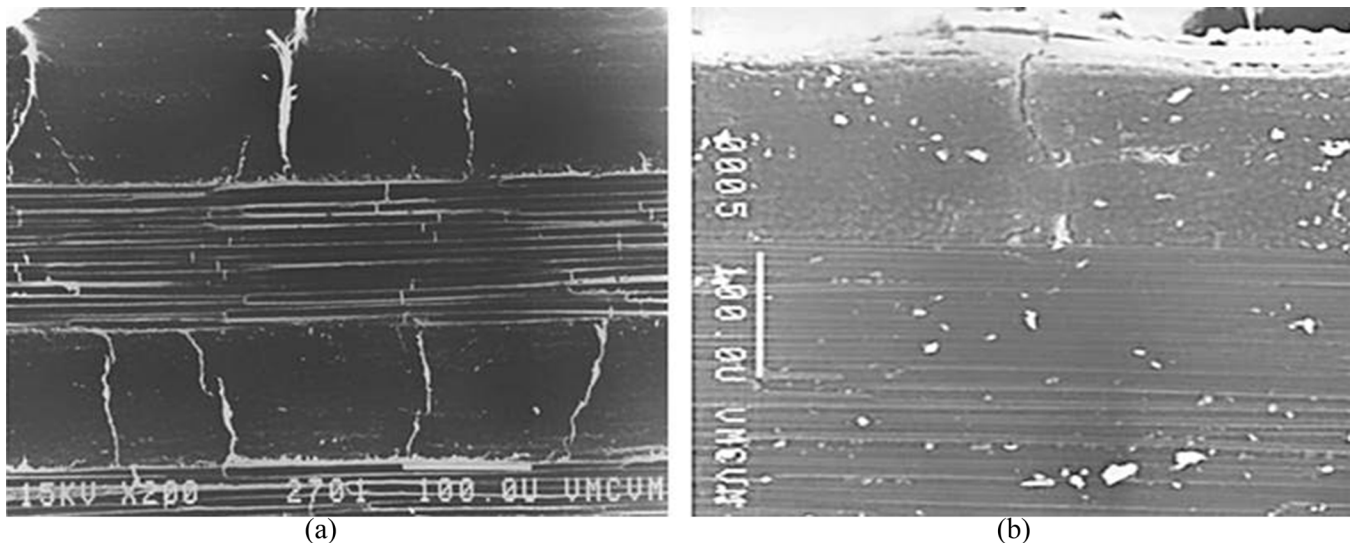


Figure 2. (a) Through-thickness crack pattern development (white lines) in a multi-axial laminate subjected to fatigue loading and (b) surface crack initiation (top center) in such a laminate under quasi-static tensile loading.

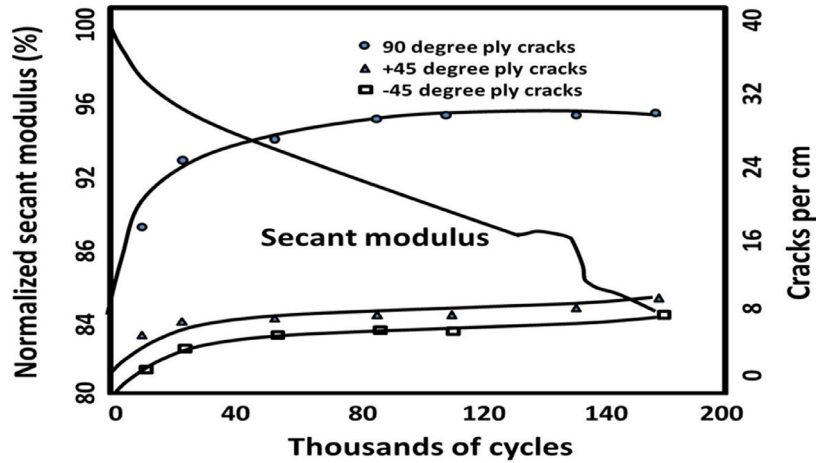


Figure 3. Crack development in off-axis plies and corresponding change in secant stiffness as a function of cyclic load cycles.

in continuous fiber reinforced composites using an analogue problem. Specifically, we construct an electrical analogue which represents the spatial complexity, variation of local material properties (including anisotropy), local field interactions associated with non-dilute damage events, and energy or compliance change-driven fracture path formation and growth to

construct a better understanding of the controlling physics and extrinsic features for such emergent behavior. The model is validated by comparing simulation predictions to actual measurements of the dielectric response of composite materials during damage and fracture path development, also resulting in the establishment of a foundation of understanding for a

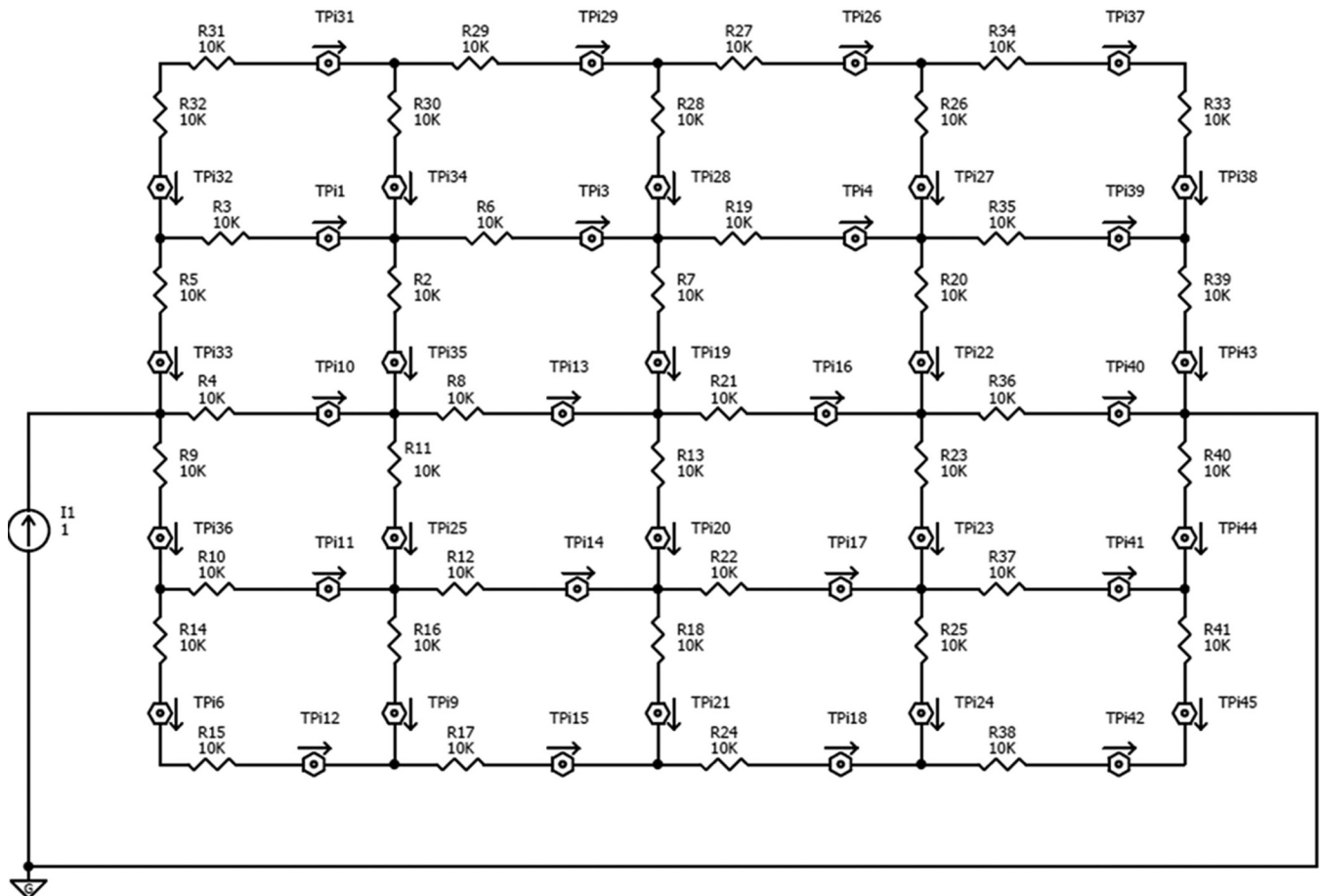


Figure 4. Model comprising of constituent elements (Matrix and Fiber) for Simplicity.

non-invasive method of interrogating the internal details of damage accumulation and incipient fracture in a composite structure during or after loading by the interpretation of its changing dielectric response.

2. FRACTURE PATH DEVELOPMENT

Damage initiation in plies with different orientations occurs at different load levels for quasi-static loading and at different rates for cyclic loading, according to well-understood ply-level strength concepts [6]. A defining feature of this early degradation is a decelerating damage rate; in the case of fatigue loading at a constant load level, the micro-cracking of the individual plies that develop damage reaches a steady state with a characteristic crack spacing. A sample of such behavior is shown in Figure 3. Matrix cracks develop early in the plies that form cracks at the given load level, and reach a stable number and spacing that depends on their relative stiffness in the laminate and on their position through the thickness. The registration of those cracks along the length of the specimen is nominally random, but in the later stages of life (or highest load levels in a tensile

test), the cracks in different plies “seek each other” to try to complete their path through the thickness [as shown in Figure 2(a)]. Fiber fractures align with matrix cracks in some cases, as is shown in the center of Figure 2(a). When this coupling creates a continuous crack through the thickness, a potential “fracture plane” is formed, although it should be remembered that since the matrix cracks run parallel to the fiber directions in each ply, a coincident plane of cracking (through the thickness) in one position [like the edge of the specimen shown in Figure 2(a)] will not be coincident (in the same way) at some other position across the section width.

When a fracture plane forms through the thickness and across the width of the specimen, specimen rupture occurs at the global level. That is a crack coupling process, not represented by the data in Figure 3.

We know remarkably little about that end-of-life coupling process or how it forms the fracture plane. The first question is how to measure something that is sensitive to the damage details in that phase of the life, and how to interpret such measurements in such a way that we can use those interpretive models to extract a “warning” of impending failure.

Fazzino *et al.* have suggested that dielectric response

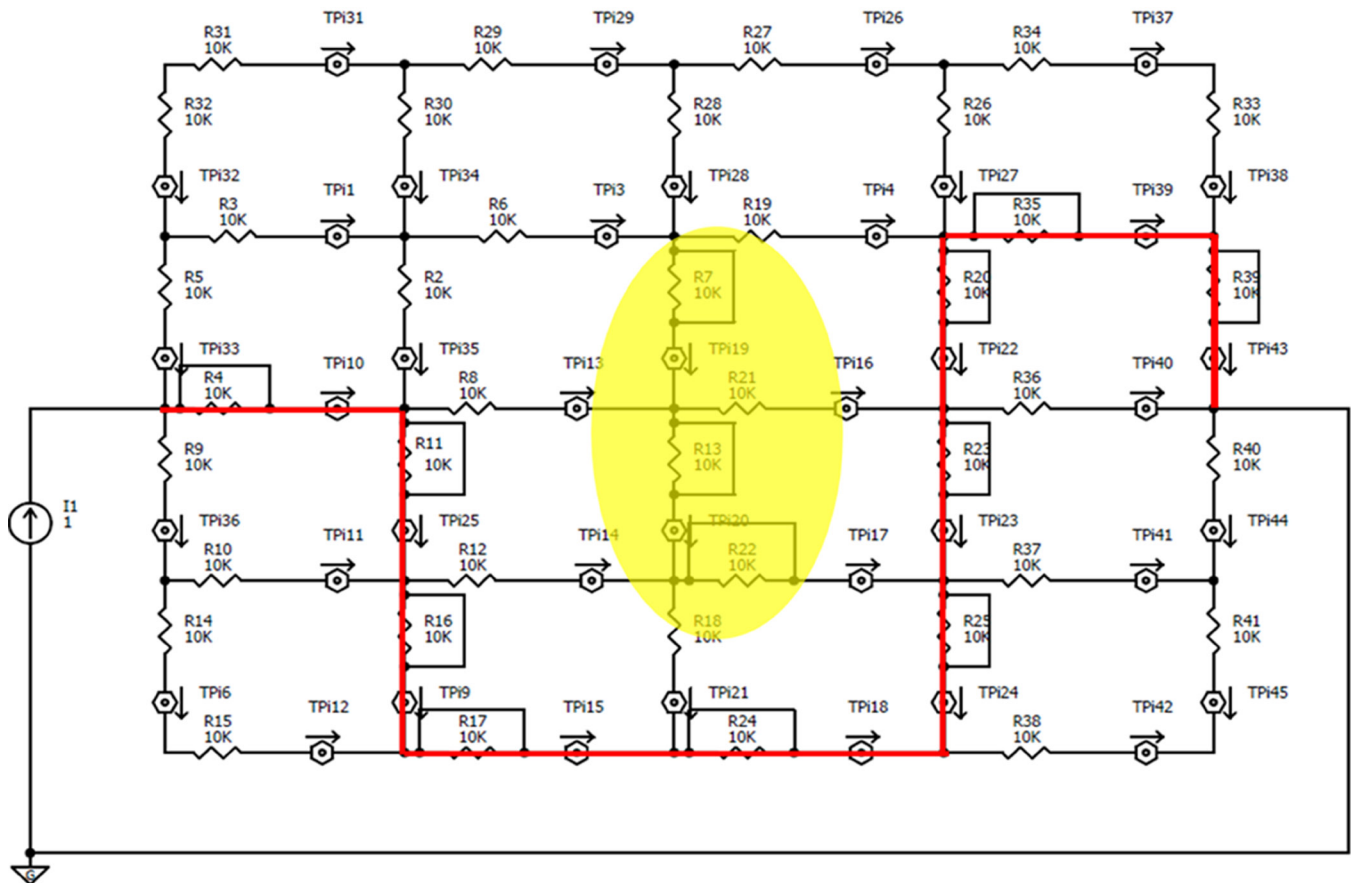


Figure 5. Model with highlighted fracture path and showing the presence of damage accumulation.

Table 1. Values of Current at Different Elements in the Circuit Before and After Shorting.

Element	Ammeter Associated	Value(I amps)		
		Before Shorting	After Shorting	Difference (amps)
R2	TPi35	0.06818	0.05532	-0.01286
R3	TPi1	0.18182	0.17755	-0.00427
R4	TPi10	0.40909	0.40857	-0.00052
R5	TPi33	0.29545	0.28634	-0.00911
R6	TPi3	0.20454	0.19284	-0.0117
R7	TPi19	0	0.016608	0.016608
R8	TPi13	0.27272	0.26477	-0.00795
R9	TPi36	0.29545	0.30508	0.00963
R10	TPi11	0.18182	0.19197	0.01015
R11	TPi25	0.068181	0.08848	0.020299
R12	TPi14	0.20454	0.24618	0.04164
R13	TPi20	0	0.069892	0.069892
R14	TPi6	0.11363	0.11312	-0.00051
R15	TPi12	0.11363	0.11312	-0.00051
R16	TPi9	0.045454	0.034267	-0.01119
R17	TPi15	0.15909	0.14738	-0.01171
R18	TPi21	0	0.064529	0.064529
R19	TPi4	0.20454	0.18021	-0.02433
R20	TPi22	0.068181	0.047882	-0.0203
R21	TPi16	0.27272	0.21148	-0.06124
R22	TPi17	0.20454	0.3806	0.17606
R23	TPi23	0.06818	0.14159	0.073409
R24	TPi18	0.15909	0.082854	-0.07624
R25	TPi24	0.04545	0.18325	-0.02713
R26	TPi27	0.04545	0.039341	0.00611
R27	TPi26	0.15909	0.14485	-0.01424
R28	TPi28	0	0.003979	0.003979
R29	TPi29	0.15909	0.14882	-0.01027
R30	TPi34	0.04545	0.04003	-0.00542
R31	TPi31	0.11363	0.10879	-0.00484
R32	TPi32	0.11363	0.10879	-0.00484
R33	TPi38	0.11363	0.1055	-0.00813
R34	TPi37	0.11363	0.1055	-0.00813
R35	TPi39	0.18182	0.17167	-0.01015
R36	TPi40	0.40909	0.40095	-0.00814
R37	TPi41	0.18182	0.22068	0.003886
R38	TPi42	0.11363	0.10118	-0.01245
R39	TPi43	0.29545	0.27717	-0.01828
R40	TPi44	0.29545	0.32186	0.02641
R41	TPi45	0.11363	0.10118	-0.01245

Table 2. Tabulated Values of Current Readings Through Elements that are a Path of Least Resistance.

Element	Ammeter Associated	Value(I amps)
R2	TPi35	0
R3	TPi1	0
R4	TPi10	1
R5	TPi33	0
R6	TPi3	0
R7	TPi19	0
R8	TPi13	0
R9	TPi36	0
R10	TPi11	0
R11	TPi25	1
R12	TPi14	0
R13	TPi20	0
R14	TPi6	0
R15	TPi12	0
R16	TPi9	1
R17	TPi15	1
R18	TPi21	0
R19	TPi4	0
R20	TPi22	1
R21	TPi16	0
R22	TPi17	0
R23	TPi23	1
R24	TPi18	1
R25	TPi24	1
R26	TPi27	0
R27	TPi26	0
R28	TPi28	0
R29	TPi29	0
R30	TPi34	0
R31	TPi31	0
R32	TPi32	0
R33	TPi38	0
R34	TPi37	0
R35	TPi39	1
R36	TPi40	0
R37	TPi41	0
R38	TPi42	0
R39	TPi43	1
R40	TPi44	0
R41	TPi45	0

(measured through the thickness of a laminate, and interpreted with standard dielectric spectroscopy methods) can provide a multi-physics method of relating the changes in material state (reflected in changes in AC impedance) to the microdetails of damage development, and further, found that such a method was particularly sensitive to the coupling

events at the end of life (reference [7] and Figure 1). However, how the specific changes they observed were related to the details of the coupling of microcracks and the formation of a fracture plane were not determined. The present paper is an attempt to contribute to that interpretation.

Various models have been established to simulate dielectric response such as effective medium theories, bounding

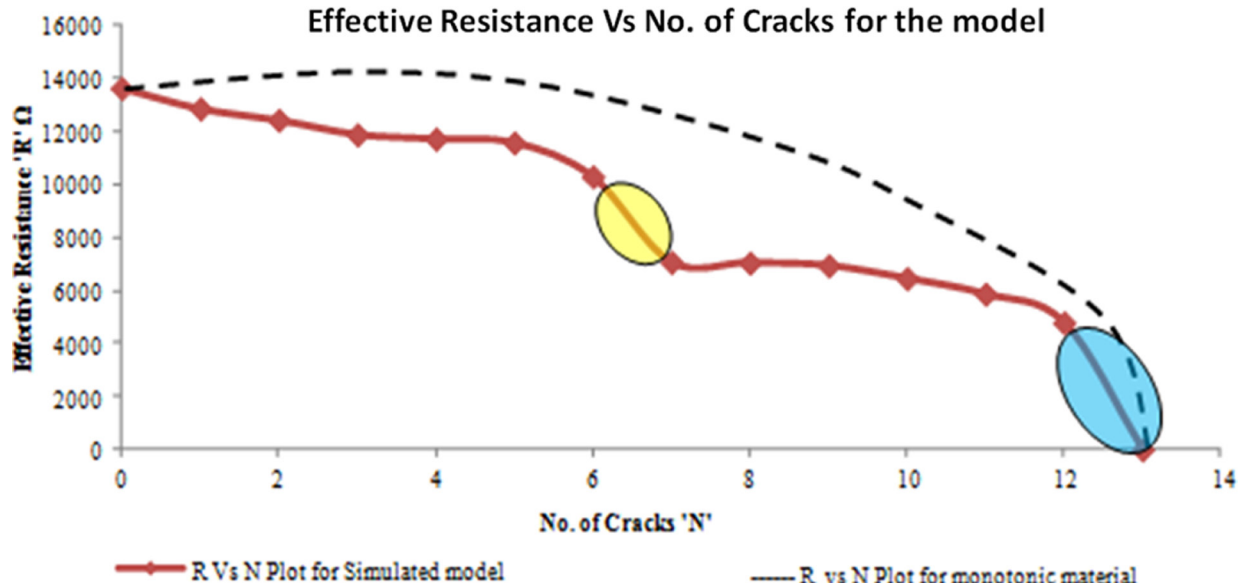


Figure 6. Plot to show the variation of Eff. Resistance 'R' with No. of Cracks 'N' for Simulated and Monotonic model.

methods, percolation theory, random walks, hopping model, Fourier expansion, finite difference time domain methods (FDTD), Monte Carlo techniques, RC network methods, and so on [8]. In the present work we use an RC network model as an approximation to a composite material (e.g. Matrix capacitive nature modeled as capacitors, fibers as conductors or insulators modeled as resistors).

3. DETERMINING THE FRACTURE PATH

3.1. Methodology

In the present case we draw an analogy between how a fracture pattern is generated because of a series of local stress interactions that result in a global fracture path, and local electric current changes when resistive elements are shorted in the analogue network shown below. We consider a Representative Volume Element (RVE) of a laminate section (through the thickness) in which we assume that vertical elements represent constituent material of one type (e.g., fibers) and the horizontal elements represent a second constituent type (e.g. the matrix) as shown in Figure 4.

For simplicity in the current discussion, we initially start with equal electrical resistance values for fiber and matrix segments. The scope of this methodology is not limited to constituents of the laminate; the elements in the circuit could represent different layers of a laminate, or combinations of different materials (ex. metal and composite), or different orientations in a laminate, etc. By varying the magnitude of the electrical properties of the elements in the circuit we can simulate similar local mechanical or electrical property variations.

A current equal to 1 Ampere is chosen as the power source, applied across two opposing surface points. Distribution of that current source was selected as an analog of how a composite material behaves locally, i.e., during loading when matrix cracking starts and local material elements are no longer able to bear the load, the local material micro-damage will redistribute the load to the adjacent elements. Similar behavior can be observed in the case of a current source circuit; when we short any element (to simulate the local failure of a matrix or fiber element), in order to maintain equilibrium the current is redistributed in a manner that is similar to the mechanical phenomenon of local stress re-

Table 3. Table Showing Variation of Effective Resistance 'R' with No of Cracks 'N'.

No. of Cracks 'N'	Effective Resistance 'R' Ohms (Homogeneous)	Effective Resistance 'R' Ohms (Heterogeneous)
0	13636	15578
1	12858	14883
2	12430	14303
3	11885	13543
4	11723	11125
5	11580	5607.7
6	10299	5510.5
7	7071.1	5315.8
8	7049.1	4745.5
9	6941.3	0
10	6457.5	NA
11	5862.6	NA
12	4792.1	NA
13	0.01	NA

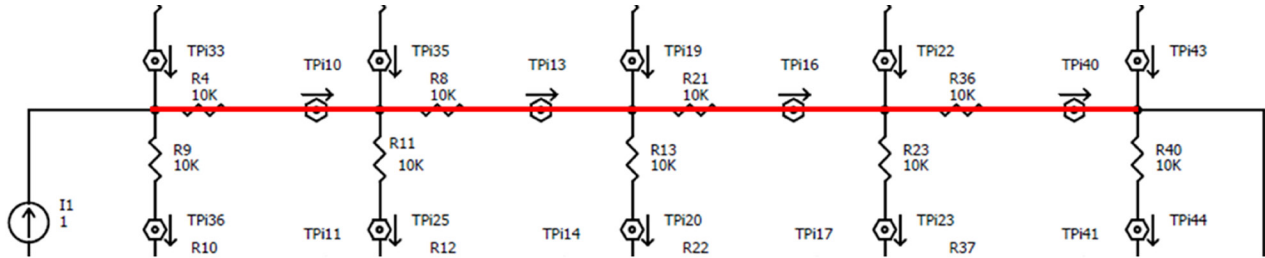


Figure 7. Expected Path of Fracture.

distribution in composites. It also suggests the subsequent direction of “micro-crack” formation.

After shorting an element to simulate local crack formation, we re-analyze the circuit and determine the current at each element in the circuit; we then consider the element that has the highest subsequent difference in current to be the next micro-crack location, which is an analogy to a local stress increase in a composite. The subsequent crack may or may not be adjacent to the last crack location. This cycle is repeated until fracture occurs i.e., to the condition where all the fractured/shorted elements create a continuous path of least resistance through which current flows. That path simulates the

fracture path in the mechanical specimen, and changes in material state variables such as compliance to the global applied field can be predicted and observed during the process.

3.2. Demonstration of the Method

We start with an initial random shorting of an element and then carry on, determining how the circuit behaves as discussed above. Ideally in a “real” composite under mechanical loading, first ply failure (or an equivalent statistical concept) can be applied to determine which element fails first. The initial current readings of all the elements in the

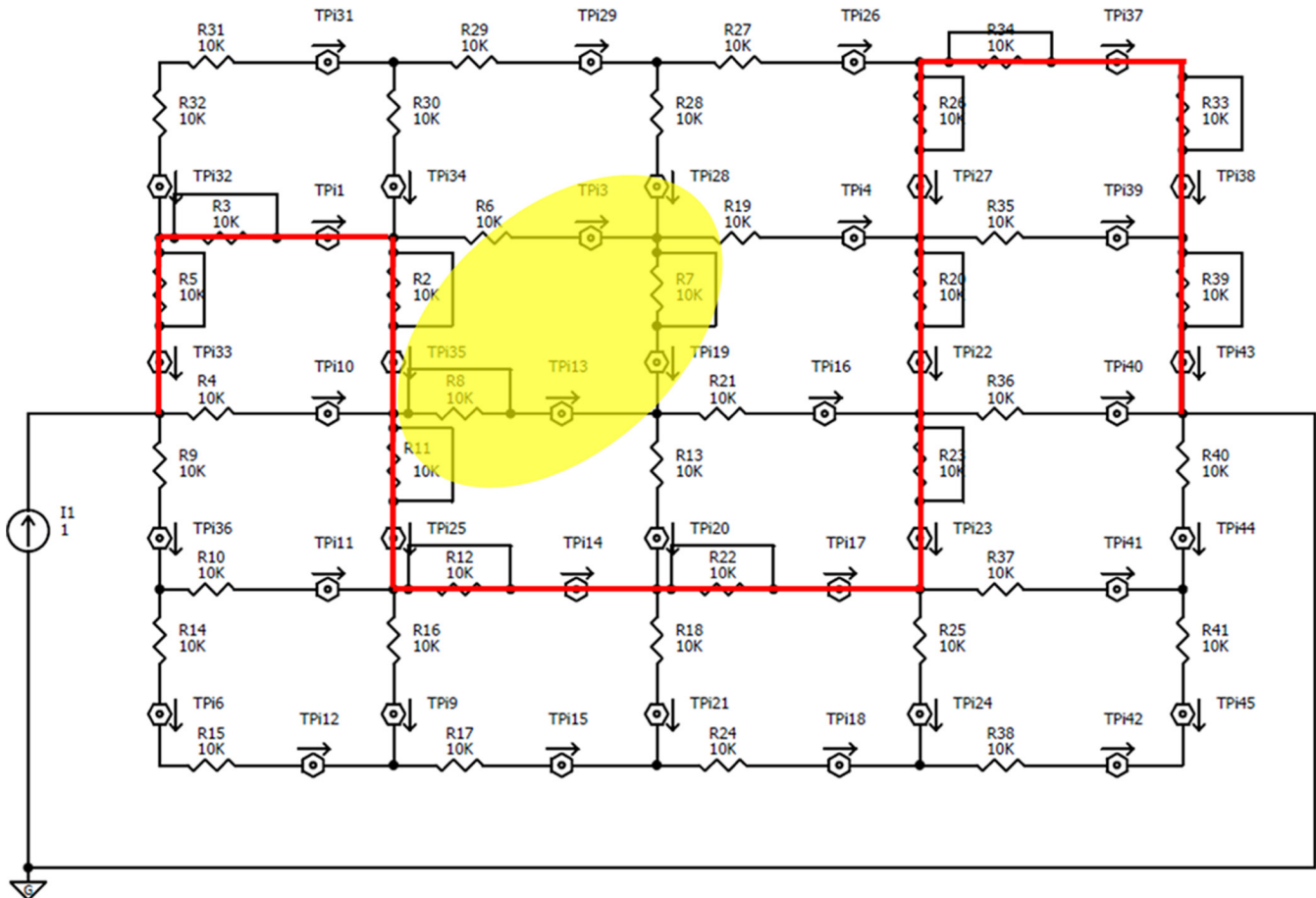


Figure 8. Predicted fracture path.

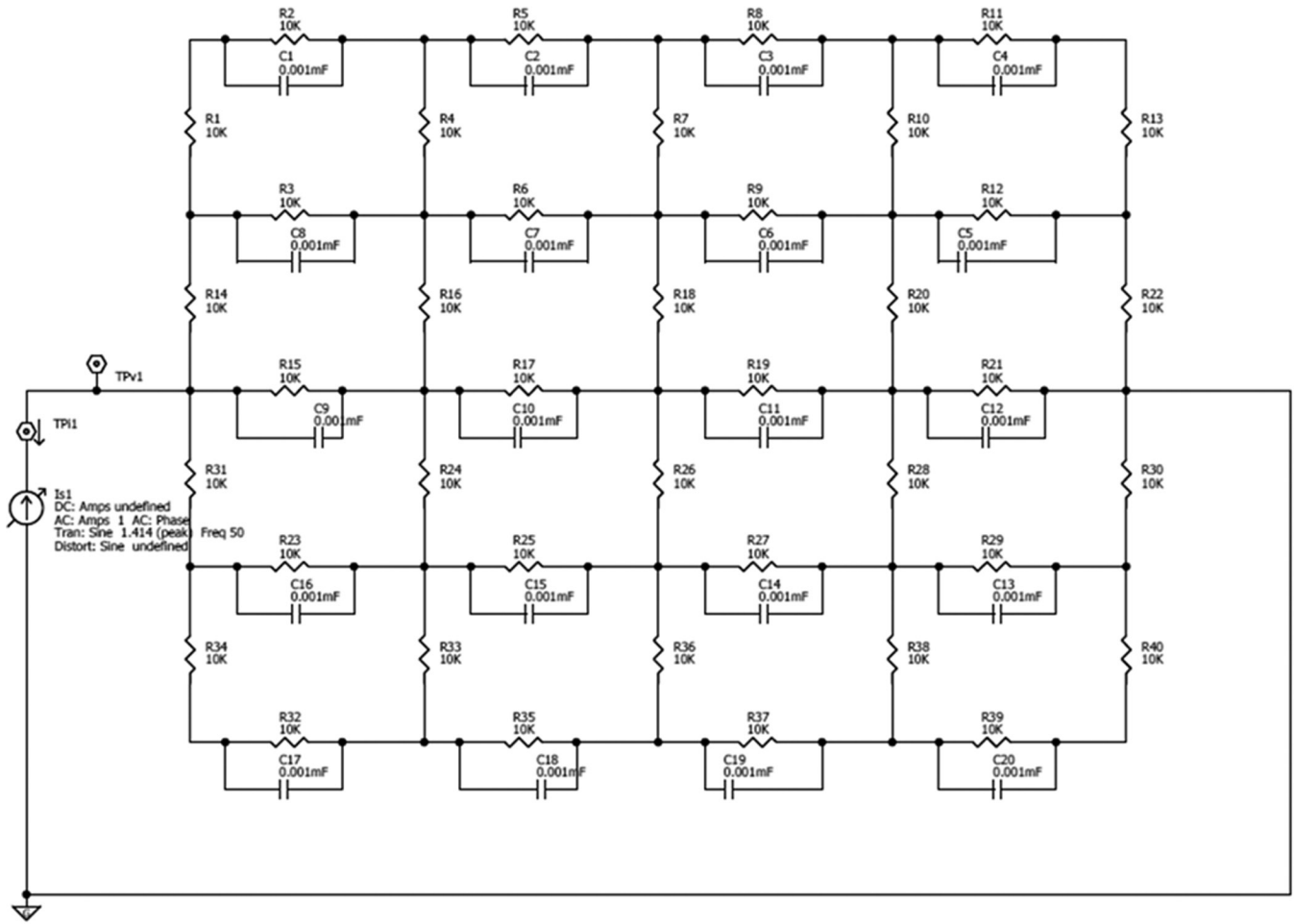


Figure 9. Anisotropic model in initial state with all of the elements intact.

present model have been tabulated under the “Before shorting” column in Table 1. In this case R22 is randomly selected and initially shorted. After shorting R22, the analysis is repeated and the current readings in all remaining elements are noted and tabulated in the “After shorting” column in Table 1. Then the difference in the current at each local ‘ammeter’ is noted and the element with the highest increase in current during the last step is identified for shorting next. That particular element is highlighted in Table 1. The Value highlighted in red had the greatest increase in current, which illustrates that the current flows through the path of least resistance, and since R22 has already been shorted, R23 is the element that has the next highest increase in current (R23 has been highlighted in green in Table 1). This cycle of local shorting to simulate sequential microcracking is repeated until a fracture path is formed, i.e., current passes only through the continuous shorted path of least resistance, as shown in Table 2.

The predicted fracture path is highlighted in Figure 5. It was observed that some elements although shorted at some step of the path development, are not a part of the final con-

tiguous ‘fracture path.’ Those elements are highlighted in Figure 5. This is an analogue of the physical behavior in composites in which a local failure is due to local crack interaction and accumulation, and not due to individual crack

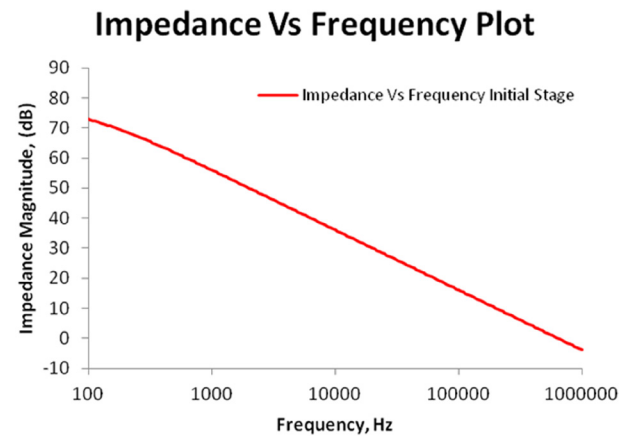


Figure 10. Dielectric Response of the model in the initial state similar to an Insulator.

initiation, propagation, or growth. The staggered final fracture path in Figure 5 has a similar character to the through-thickness patterns in Figure 2.

4. COMPLIANCE CONCEPTS

During the simulation analysis, after shorting of each element, the effective resistance of the circuit is calculated and a comparison between Effective Resistance ‘R’ and No. of Cracks ‘N’ is obtained; values for one set of simulations are tabulated in Table 3.

From the plot of such data shown in Figure 6, it is observed that as the circuit/material accumulation proceeds towards failure its effective resistance reduces (compliance increases) and at the fracture point it reaches 0 (or infinite compliance). In the above plot the highlighted parts of the curve mark a significantly larger change in the effective resistance of the model. This change is brought about when two local ‘cracks’ interact and a tertiary bridging crack or a ‘fracture plane growth’ has occurred. In terms of the physical phenomenon, this change could be attributed to fiber failure, or crack open-

ing, or delamination as observed in Chou’s work [9]. We have observed similar behavior in a COMSOL model, (constructed by one of our PHD Students, Russel Raihan, to be discussed in a subsequent paper) and have published earlier data that support this general compliance concept [10].

5. NON-LINEARITY (DAMAGE ACCUMULATION vs. DAMAGE GROWTH)

Damage accumulation is fundamentally different from crack propagation. If the present analysis is representative of that accumulation process, ‘simple’ crack propagation should not be a preferred result.

To test that premise, we shorted an element along the plane of symmetry between our two contact points and started the analysis. If the model were to exhibit only linear crack growth behavior, than the current would take the horizontal path of least resistance, i.e., the fracture path should be a straight line as shown in Figure 7, but the predicted path with the present analysis method was completely different as shown in Figure 8, which gives evidence that this model can

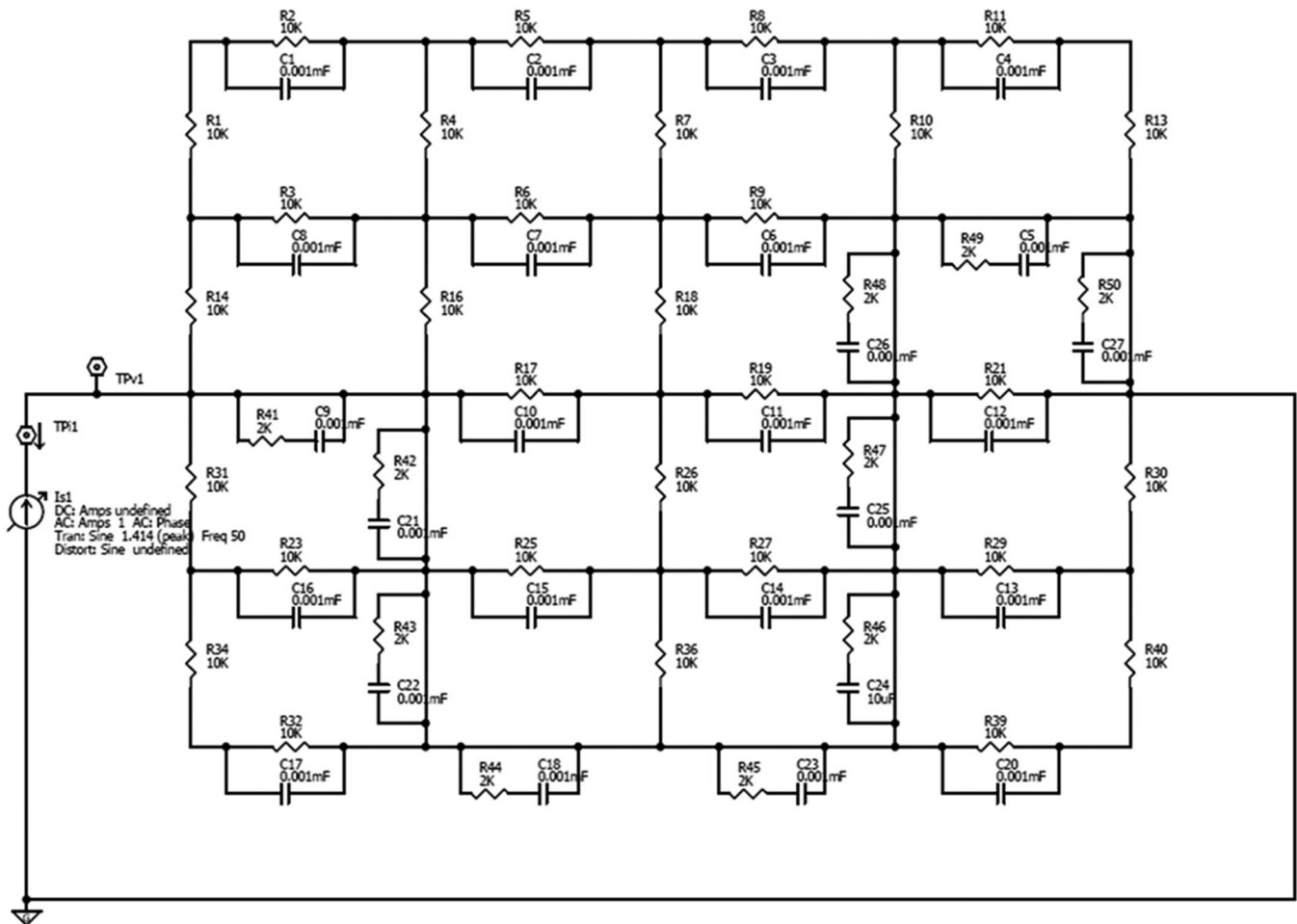


Figure 11. Model with randle’s circuit elements along fractured path.

Table 4. Table Showing Variation of Reactance Peak Frequency with % of Life.

% of Life	Reactance Peak Frequency, Hz
Initial	20.7
25%	20.7
50%	20.7
75%	24.9
Fractured	NA

exhibit the non-linear phenomenon of damage accumulation and fracture path formation observed in fibrous composites (e.g., Figure 2).

6. DIELECTRIC RESPONSE

6.1. Introduction of Anisotropy into the Model

Up to this point the present model was constituted with horizontal and vertical elements with equal initial magnitudes of resistance. In order to introduce anisotropy, a capacitance in parallel with the resistive element is added to the horizontal elements (in this case, the “matrix”) since a polymer matrix, for example, is known to exhibit a capacitive response. Figure 9 shows the resulting circuit.

6.2. Randle’s Circuit

In Electro-Chemical Impedance Spectroscopy (EIS) analysis, a Randle’s circuit is widely used to represent the

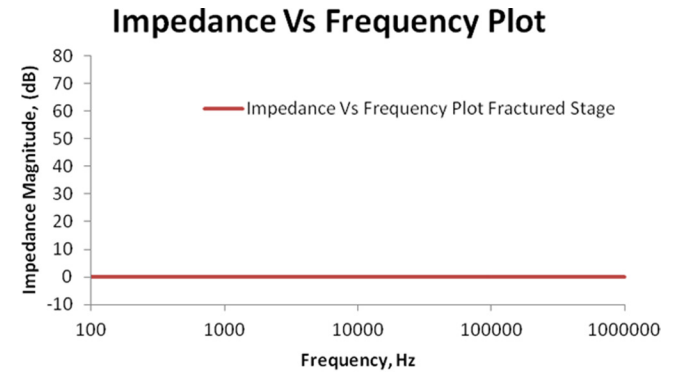
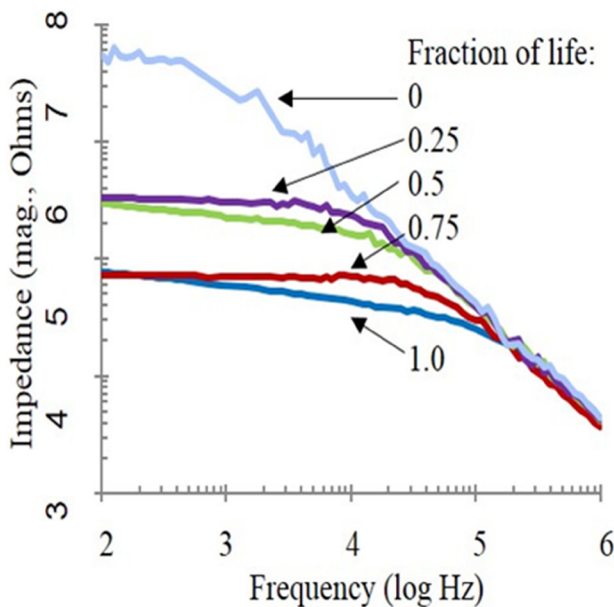


Figure 12. Response of the fractured model similar to a conductor.

dielectric Impedance of material elements. Impedance is the magnitude of the total complex resistance encountered when a current flows through a system, which is most often interpreted as a circuit made of resistors, capacitors, or inductors, or any combination of these [8]. In our AC analysis, when we short a particular element, an additional resistance has been added in series to the capacitance and the value of the main resistance is reduced in order to simulate the damage that has occurred because of the applied “load” and local “micro-fracture.”

6.3. Initial Stage

In the initial stage under a no-load condition in the composite, i.e., without shorting any elements as shown in Figure 9, the dielectric response of the anisotropic model to an AC current was analyzed and the response was found to be

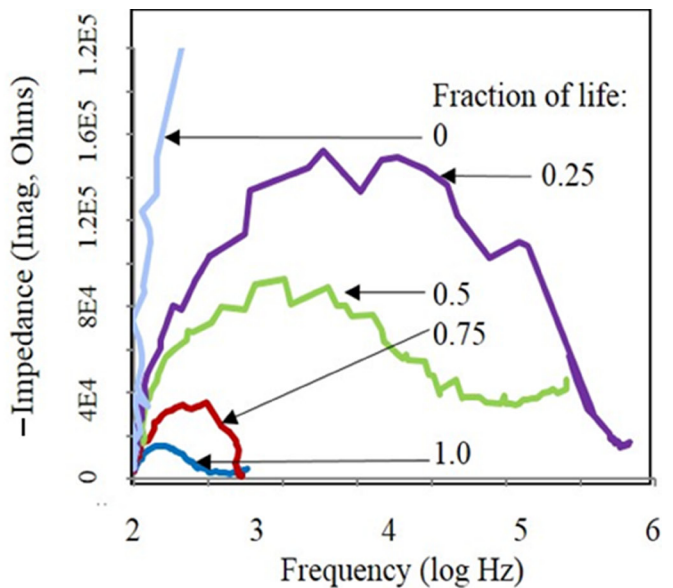


Figure 13. Observed Variation of Impedance with Frequency (left) and Nyquist Plots (right) showing variation of impedance with life in Fazzino’s work [2].

Impedance Vs Frequency Plots @ different stages of life

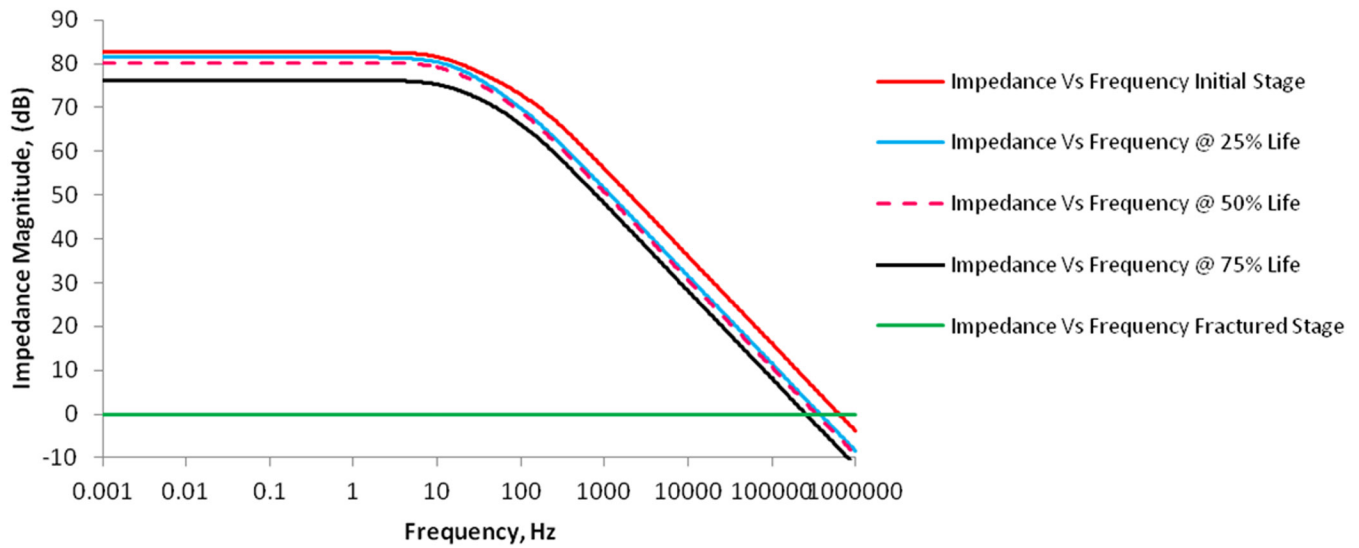


Figure 14. Variation of Di electric response with frequency at different stages of life.

equivalent to an insulator between two plates, as shown in Figure 10 and observed in Figure 1.

6.4. Fracture Path Development

During analysis of the fracture path development, the fractured elements were replaced by a Randle’s circuit as shown in Figure 11 and the dielectric response was analyzed. It was observed that the response becomes more similar to a conductor as shown in Figure 12, and observed in Figure 1.

6.5. Dielectric Response at Different Stages of Life

Based on Previous work, to validate the results obtained at different life fractions of bend-fatigue life, as shown in Figure 13, the results of our model were divided into four different stages. Response at each stage is shown in Figure 14. The predicted behavior closely approximates the observations in Figure 1 that motivated this work.

7. NYQUIST PLOT

By tabulating the real part of impedance, and imaginary part of impedance at different stages of life as shown in Table 5, one can create a new representation of the change in electrical properties with increasing damage in the material. Creating a plot of tabulated values, one can observe that as damage increases the plot shifts to the left which indicates decreasing resistance as seen in Figure 15. Closely observing the plot at each stage of life the reactance increases at

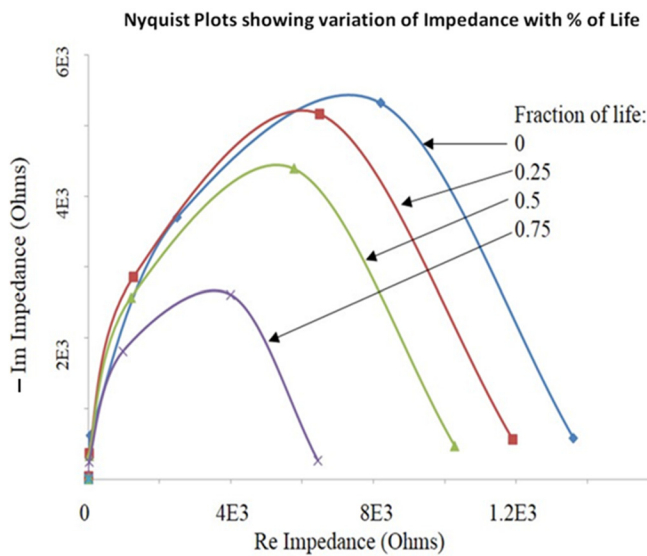


Figure 15. Nyquist plot showing the variation of impedance with % of life.

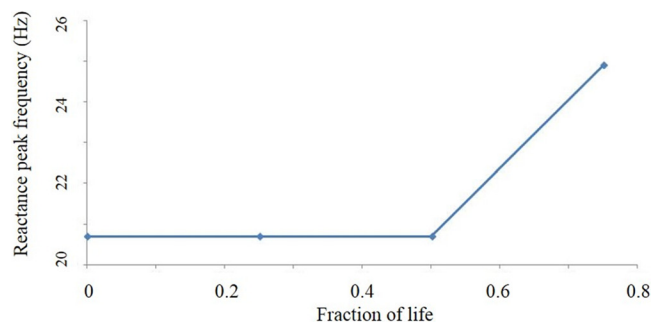


Figure 16. Variation of Reactance peak frequency with % of life.

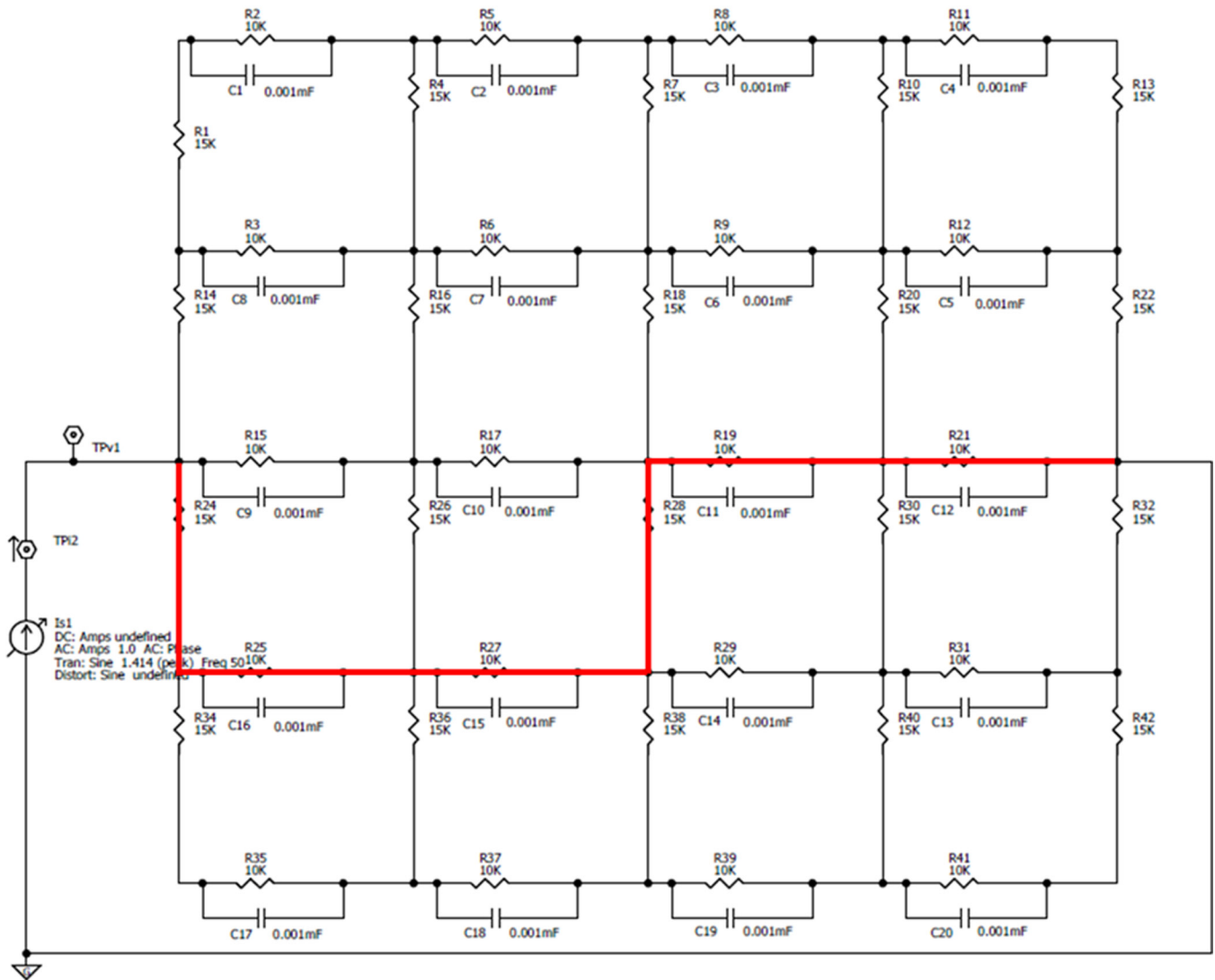


Figure 17. Model with heterogeneous elements with fracture path highlighted.

low frequency values, but as the frequency increases towards 1 MHz the reactance approaches zero. These simulations are consistent with the previous observations of Fazzino, *et al.*[7] We will see that changes in the shape of these curves and the location of the intercepts are strong indicators of material state and sensitive to the final formation of a conductive (“fracture”) path.

8. END OF LIFE PREDICTION

Composite Materials, unlike metals, are capable of significant damage accumulation without loss of strength or stiffness, so it is difficult to measure something unique that can predict the end of life based on standard Non Destructive Testing (NDT) methodologies. However, using the methods of impedance spectroscopy based on the response from the material, as discussed above, one can determine end of life

Impedance Vs Frequency Plot for Heterogeneous Model

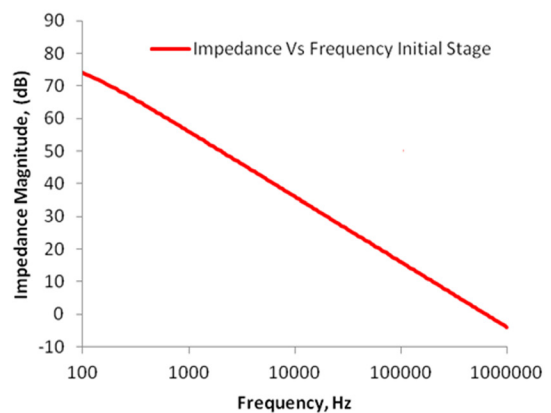


Figure 18. Frequency response of the heterogeneous model at Initial stage.

We have also observed that the global compliance to applied AC electrical fields is closely related to the material compliance to mechanical stress fields during fracture path development. A key feature of that response was the observation of abrupt changes in multiphysics compliance (mechanical and electrical) that were identified with the onset of discrete fracture path instability and rupture. We also identified an inflection point in the frequency dependence of AC impedance that was an indicator of the ‘beginning of the end of life.’

We have provided only a few first steps in simulating the multiphysics response associated with the development of discrete fracture paths in fibrous composites; much is yet to be done. However, on the basis of the present work, it would appear that the dielectric response of continuous fiber reinforced composite materials seems to be uniquely sensitive to the details of microdamage accumulation and especially to “end of life” events such as the formation of contiguous incipient fracture paths.

11. ACKNOWLEDGEMENTS

The authors gratefully acknowledge the support of the computer simulations by NASA/EPSCoR Grant #NNX13A-D43A-USC and support of the broadband dielectric spectroscopy and related work from the Energy Frontier Research Center for Heterogeneous Functional Materials, the HeteroFoam Center, under DoE Grant no.DE-SC0001061 from the Office of Basic Energy Sciences.

12. REFERENCES

- [1] Majumdar, P., Reifsnider, K., “Study of Fracture Path Development and Remaining Life Utilizing Low-Frequency Electrical Response,” Grant #NNX13AD43A-USC.
- [2] Gudmundson, P., and Zhang, W., Thermoelastic properties of micro-cracked composite laminates, *Mechanics of Composite Materials*, 29 #2, (1993) 107–114. <http://dx.doi.org/10.1007/BF00696439>
- [3] *Damage in Composite Materials*, ASTM STP 775, K. L. Reifsnider, Ed., American Society for Testing and Materials (1982) DOI: 10.1520/STP775-EB <http://dx.doi.org/10.1520/STP775-EB>
- [4] Jamison, R.D., Schulte, K., Reifsnider, K., Stinchcomb, W., Characterization and Analysis of Damage Mechanisms in Tension-Tension Fatigue of Graphite/Epoxy Laminates, in Effects of Defects in Composite Materials, ASTM STP 836, ASTM (1984) 21–55. <http://dx.doi.org/10.1520/STP30196S>
- [5] F.A. Firestone, A New analogy between Mechanical and Electrical Systems, *Journal of the Acoustical Society*, (Jan 1933) 250–267.
- [6] Reifsnider, K., and Case, S.W., *Durability and Damage Tolerance of Material Systems*, John Wiley & Sons (2002)
- [7] Fazzino, P., Reifsnider, K., Majumdar, P., “Impedance spectroscopy for progressive damage analysis in woven composites,” *Composites Science and Technology* 169 (2009) 2008–2014. <http://dx.doi.org/10.1016/j.compscitech.2009.05.007>
- [8] Huang, M., Yang, J., Xiao, Z., Sun, J., and Peng, J., “Modeling the Dielectric Response in Heterogeneous Materials using 3D RC Networks,” *Modern Physics Letters B*, 23, No. 25 (2009) 3023–3033. <http://dx.doi.org/10.1142/S0217984909021090>
- [9] Chou, T-W., “Multifunctional Carbon Nanotube-Based Sensors for Damage Detection and Self Healing in Structural Composites,” contractors report, Grant No: FA9550-09-1-0218 (2009).
- [10] Reifsnider, K., Raihan, R. and Liu, Q., “Rational Durability Design of Heterogeneous Functional Materials: Some First Principles,” *Mechanics of Composite Materials*, 49#1 (2013) 31–54. <http://dx.doi.org/10.1007/s11029-013-9317-7>



A Review on Stability and Vibration Control of Piezolaminated Composite/FGM Plate Structures

PRIYANKA A. JADHAV^{1,*} and KAMAL M. BAJORIA²

¹Post-Doctoral Fellow, Department of Aerospace Engineering, Indian Institute of Science Bangalore, India-560 012,
Email: priyankajadhavIITB@gmail.com

²Professor, Department of Civil Engineering, Indian Institute of Technology Bombay, India-400076,
Email: kmb@iitb.ac.in, Tel.: +91-22-2572-7332; fax: +91-22-2572-7302.

KEYWORDS

piezoelectric material
composite plate
functionally graded plate
piezolaminates
vibration control
stability analysis

ABSTRACT

Piezoelectric materials have gained substantial attention due to their potential applications as sensors and actuators for controlling the response of structures. Using the direct and converse piezoelectric effects, surface bonded piezoelectric sensor and actuator layers may be employed to adequately control the deflection, vibrations, shape and buckling of the structures. In response to remarkable increase in research activities in stability and vibration control of composite/functionally graded material (FGM) plates using piezolaminates in last few years, this review paper summarizes the research progress in following categories: stability analysis of piezolaminated composite plates and piezolaminated FGM plates, vibration control of piezolaminated composite plates and piezolaminated FGM plates.

© 2014 DEStech Publications, Inc. All rights reserved.

1. INTRODUCTION

During the past decade, smart materials and structures or intelligent material systems have captured the attention of many engineering professionals and academics because of their potential application as sensors and actuators for controlling the response of structures. Smart structure consists of multifunctional components which activates on sensing and carry out an appropriate response in a controlled and timely manner. It has the capability to respond to a varying external environment as well as internal environmental conditions. Smart structural components are used in aerospace structures, high speed aircrafts and structures where high thermal environment induces buckling instability and vibrations in the structures. The detailed information about piezo history, piezo sensors, actuators and terminology related to piezo analysis is given by [1,2,3]. For various purposes smart materials are used in the realization of smart structures

and focused on the analysis of smart composite structures to improve their performance. The constitutive behavior of these material couples their mechanical response i.e. stress and strain with other physical fields, this way a mechanical stimulus can be transformed into a non-mechanical effect and conversely, a non-mechanical stimulus can be converted into a mechanical effect. This is what happens in piezoelectric materials, where the electric behavior is coupled with the mechanical one due to the direct and converse piezoelectric effect. This effect enables the material to behave as an actuator or a sensor. The smart composite structures are made up of composition of different type of material laminates such as metal, ceramic, fiber reinforcement etc. but such types of composite structures are undergoing delamination because of abrupt changes in material properties, extreme environmental conditions and weakness of interfaces of layers placed between two adjacent laminates of composite structures. In the manufacturing process of composites, interlaminar bonding may be weaker due to the introduction of small flaws or micro cracks under various loading conditions

*Corresponding Author: priyankajadhavIITB@gmail.com

during the service time and this may lead to inter-laminar instability, but FGM can be used to overcome this problem. Koizumi [4] highlighted the FGM activities in Japan. The concept of FGMs was proposed in 1984 by materials scientists in the Sendai area as a means of preparing thermal barrier materials. Continuous changes in the composition, microstructure, porosity, etc. of these materials result in gradients in such properties as mechanical strength and thermal conductivity.

The main objective of the paper is to carry out the review on stability analysis and vibration control of piezolaminated composite and FGM plates and provide the current research activities. It is intended to help readers and researchers to appraise current progress in stability as well as vibration control analysis of piezolaminated composite plates/FGM plates.

2. REVIEW ON STABILITY ANALYSIS OF PIEZOLAMINATED COMPOSITE PLATES/FGM PLATES

Thin and light weight structures and material suffers by buckling and dynamic instability and the research is focused to improve their performance using smart materials. The following section highlights the review on buckling and post-buckling analysis of piezolaminated composite plate and piezolaminated FGM plate.

2.1. Stability Analysis of Piezolaminated Composite Plates

Chandrashekhara and Bhatia [5] developed a finite element model to study the dynamic buckling behavior for composite plates with integrated sensors and actuators. The finite element model is based on the first order shear deformation plate theory (FSDT) in conjunction with linear piezoelectric theory. Icardi and Di Sciuva [6] investigation is carried out to study the 3D stress field of multilayered intelligent plates based on the von Karman strain-displacement relations and developed a third order zigzag layerwise plate theory for multilayered, intelligent, anisotropic plates with a surface-bonded piezoelectric actuator layer. The numerical study has been carried out on simply supported cross ply plates with top and bottom actuators in cylindrical bending under distributed transverse loading. Oh *et al.* [7] formulated non-linear finite element equations based on the layerwise plate theory for a piezolaminated plate subject to thermal and piezoelectric loads and carried out postbuckling analysis as well as vibration analysis considering large thermo-piezoelectric deflections for a square composite plate with fully and partially bonded piezoelectric actuators. Shen [8] presented postbuckling analysis for a simply supported shear deformable laminated plates with piezoelectric actuator subjected to the combined action of mechanical, electrical and

thermal loading. The governing equations of the laminated plate theory based on Reddy's higher order shear deformation theory which includes thermo-piezoelectric effect and a perturbation technique is used to determine postbuckling loads and equilibrium path. Shen [9] presented thermal postbuckling analysis for a simply supported shear deformable laminated plates with piezoelectric actuator subjected to the combined action of thermal and electrical loading. A parabolic distribution of temperature field is assumed over the plate surface and a uniform distribution in the thickness direction. A mixed Galerkin-perturbation technique is employed to determine thermal buckling loads and postbuckling equilibrium paths.

Varelis and Saravanos [10] developed a finite-element formulation to predict the initial buckling of smart piezoelectric plate structures with piezoelectric actuators and sensors. The buckling analysis is carried out on piezoelectric plates subjected to various combinations of applied electric potentials and in-plane forces. Varelis *et al.* [11] presented the theoretical framework for coupled buckling and post buckling analysis of piezoelectric adaptive plate structures. The formulation is based on coupled mixed field piezoelectric laminated theory with consideration of stress stiffening and geometric effect due to large rotations to study the different cases such as plate with different positioned actuator patches, hinged plate with asymmetric actuator, electromechanical buckling and active buckling of plate. Wang *et al.* [12] studied the dynamic stability analysis of active vibration control of piezoelectric composite plates using the negative velocity feedback control law. The analysis is carried out by using Lyapunov's energy functional which is based on derived general governing equations of motion by assuming active damping. The dynamic stability of plate embedded with piezoelectric layers on the top and the bottom surface as actuator and the sensor layers respectively is investigated by Kim and Kim [13] with the active damping layer under a thrust using FSDT and finite element method.

Kapurja and Achary [15] presented an exact 3D piezothermoelasticity solution for buckling of simply-supported symmetrically laminated hybrid cross-ply plates with surface bonded or embedded piezoelectric layers using state space approach. The buckling is considered under uniform temperature with the piezoelectric layers under charge free open circuit condition as well as closed circuit condition with zero and non-zero actuation potentials. Kapurja and Achary [16] extended previous work of Kapurja [14] to present an efficient coupled geometrically nonlinear zigzag theory for hybrid plates including geometric nonlinearity due to deflection only in the sense of Von Karman. Kapurja and Achary [17] developed efficient coupled geometrically nonlinear zigzag theory for hybrid plates under electro-thermo-mechanical load and used to obtain the thermal buckling response of symmetrically laminated hybrid plates. Akhras and Li [18] proposed a new finite layer method for three-

dimensional static, vibration and stability analysis of piezoelectric composite plates. Numerical studies presented to verify the performance of the proposed method and effects of electrical conditions, side-to-thickness ratio and number of plies. Giannopoulos *et al.* [19] presented buckling of smart beams and plates under complex loading in combination with discrete layer kinematic assumptions for through the thickness behavior of the structure. The thermal, electrical and mechanical coupling formulation is presented and incorporated in a finite element solver using discrete layer kinematics and quadratic finite element. In above scenario, there is thermal, mechanical, electrical buckling and postbuckling analysis is presented with different parametric studies. But in composite structures, interlaminar bonding imperfection has received some attention because in the manufacturing process, interlaminar bonding may be weaker due to the introduction of small flaws or micro-cracks are induced under various conditions during the service time.

Kim and Lee [20] investigated the buckling of orthotropic rectangular laminates with weak interface. The state-space formulation is directly established from three dimensional theory of elasticity and spring layer model is evaluated. Akhras and Li [21] studied the three-dimensional thermal buckling analysis of symmetrical cross-ply piezoelectric composite plates with full coupling between the thermal, electrical and mechanical fields using finite layer method proposed by Akhras and Li [18]. Investigation is carried out to show the effects of side-to-thickness ratio, number of plies, electrical conditions, thermal-electrical coupling and heat conduction during the buckling process on the thermal buckling behaviors of piezoelectric laminates. Kim and Lee [22] extended previous work of Kim and Lee [20] to investigate the buckling of an orthotropic piezoelectric rectangular laminate with weak interfaces. The numerical results investigate the interfacial damage as well as it shows that the sensitivities of buckling stress parameter to the interfacial damage depend on various factors. Yang and Huang [23] presented the dynamic stability analysis of a simply supported 3D braided composite laminated plate with surface bonded piezoelectric layers, under the influence of electrical and periodic in-plane mechanical loads. Shariyat [24] presented the dynamic buckling analysis by considering the coupling of mechanical, thermal and electrical field. Here investigation is carried out to show the effect of thermo piezoelectricity on the dynamic buckling for suddenly applied thermal and mechanical loads for piezolaminated composite plates. Formulation is based on higher order shear deformation theory (HSDT) by considering initial geometric imperfection and temperature dependency of the material. Akhras and Li [25] extended previous work of Akhras and Li [21] to the 3D thermal buckling analysis of simply supported rectangular piezoelectric antisymmetric angle-ply laminates and investigated to show the effect of number of layer on thermal buckling of square laminates and adiabatic thermal buckling

of square (p/45°/–45°/45°/–45°/p) laminates, square antisymmetric angle ply laminates, square (p/0°/90°/90°/0°/p), (p/45°/–45°/45°/–45°/p), and rectangular (p/45°/–45°/45°/–45°/p) piezoelectric laminates. Akhras and Li [26] extended the finite layer method to study a 3D stability analysis of simply supported rectangular piezoelectric antisymmetric angle-ply laminates. The Lagrangian polynomials are employed for interpolations of all the generalized displacement components in the thickness direction.

Pradyumna and Gupta [27] studied the dynamic stability behavior of laminated composite plates with piezoelectric layers subjected to periodic in-plane load. The analysis is based on finite element method and earlier developed modified first order shear deformation theory (MFSDT) by Tanov and Tabiei [28]. The formulation includes the effects of transverse shear, in-plane, and rotary inertia and Bolotin's approach is used to obtain the boundaries of dynamic instability regions. Shen and Zhu [29] studied compressive postbuckling and thermal postbuckling under thermal environments and uniform temperature rise for a shear deformable laminated plate with piezoelectric fiber reinforced composite actuators based on a HSDT including thermo-piezoelectric effects. The compressive and thermal postbuckling behaviors of perfect, imperfect, symmetric cross-ply and antisymmetric angle-ply laminated plates with fully covered actuators under the influence of different sets of thermal and electric loading conditions. Moghadam *et al.* [30] developed an analytical model for bending analysis of rectangular hybrid general cross-ply piezolaminated plates with any arbitrary clamped/ simply supported boundary conditions under thermo-electro-mechanical loading. Jabbari *et al.* [31] evaluated the buckling load of porous circular plates integrated with piezoelectric actuator layers, subjected to uniform in-plane radial compression and applied constant voltage on piezo layers. The effects of piezoelectric layers on the buckling load, piezoelectric layer-to-porous plate thickness ratio and variation of porosity are presented in this paper. The extension of this study made in Khorshidvand [32] by integrating plate with piezoelectric sensor and actuator patches, subjected to uniform in-plane radial compression and studied the effects of piezoelectric layers on feedback gain. Wankhade and Bajoria [33] studied stability of piezolaminated plates subjected to combined action of electrical and mechanical loading. Wankhade and Bajoria [34] studied buckling analysis of piezolaminated plate subjected to combined action of electro-mechanical loading using HSDT and finite element method. Piezolaminated plates consist of cross ply symmetric and antisymmetric orientation of laminates with piezo-layer attached at the top and bottom of the plate.

2.2. Stability Analysis of Piezolaminated FGM Plates

Liew *et al.* [35] investigated the buckling and postbuckling behavior of FGM hybrid plate which is surface bonded

with piezoelectric actuators under combined influence of uniform temperature change, in-plane forces and constant applied control voltage. Hybrid plate is formed by combining ceramics and metals i.e. zirconia and aluminum. Modeling is based on Reddy's higher order shear deformation theory by applying semi analytical one dimensional differential quadrature (DQ) approximation based iterative approach which is used to determine the postbuckling response of FGM plate and Galerkin procedure is used to evaluate non-linear algebraic equation, further which is useful for determining postbuckling path by using iterative approach. Yang *et al.* [36] investigated the non-linear bending response of shear deformable FGM rectangular plate which is mixture of zirconia and aluminum, covered with piezoelectric actuator layers under application of thermo-electro-mechanical loads. Material properties are assumed to be graded in thickness direction according to power-law distribution and also it is independent of temperature and electrical field. Formulation is based on Reddy's higher order shear deformation theory and von Karman assumption for influence of geometric non-linearity. Shen [38] studied the postbuckling analysis for a simply supported, shear deformable functionally graded plate with piezoelectric actuators by extending the previous work of Shen [8,37] to the case of mid-plane symmetric FGM hybrid plates subjected to the combined action of mechanical, electrical and thermal loads. Two sets of material mixture for FGMs are considered i.e. silicon nitride and stainless steel and the other is zirconium oxide and titanium alloy. The temperature field considered is assumed to be of uniform distribution over the plate surface and through the plate thickness and the electric field considered only has non zero valued component E_z . Reddy's higher order shear deformation plate theory is used in the analysis and a two step perturbation technique is employed to determine buckling loads and postbuckling equilibrium paths. Shen H.S. [39] studied the thermal postbuckling analysis for a simply supported, shear deformable functionally graded plate considering the heat conduction and temperature-dependent material properties and extended previous work of Shen [37, 38] to the case of geometrically mid-plane symmetric FGM plates subjected to thermal loads. A two-step perturbation technique is employed to determine buckling temperature and postbuckling equilibrium paths.

Chen *et al.* [40] presented the buckling and postbuckling analysis of piezoelectric FGM plate subjected to non-uniformly distributed loads, heat and voltage by using element free Galerkin method by employing penalty coefficients. First calculation is made for pre-buckling stresses of plates subjected to non-uniformly distributed loads and then calculated the buckling load and temperature of the plate by considering Mindlin plate assumption. For validation of above analysis some numerical studies are carried out such as, analysis of rectangular piezoelectric FGM plate which is subjected to pair of in-plane concentrated loads and square

piezoelectric FGM plate subjected different loading such as, several pairs of partial uniform in-plane edge loads, one axial load and two shear loads. Results based on above study show that if small amount of voltage increases then buckling parameter decreases. Shen [41] extended previous work of Shen [38] to investigate the nonlinear compressive postbuckling under thermal environments and thermal postbuckling due to a uniform temperature rise are presented for a simply supported, shear deformable FG plate which is mixture of silicon nitride and stainless steel with piezoelectric fiber reinforced composite actuators. The analysis is based on a HSDT with von Karman type of kinematic nonlinearity.

Shariyat [42] presented the vibration and dynamic buckling of FGM rectangular plates which is mixture of aluminum oxide and titanium alloy with surface bonded piezoelectric sensors and actuators under the influence of thermo-electro-mechanical loading. Finite element formulation is based on higher order shear deformation theory. Dynamic buckling is evaluated for plate is already subjected to electric potential and thermal and electrical loads under suddenly applied mechanical compression. The minus voltage is applied then thermal and mechanical buckling loads are having slightly higher value in case of thin plate, but same result is not acceptable for thick plates. Ke *et al.* [43] presented the analytical solutions for the flexural vibration and buckling of beams made of FGM containing open edge cracks based on Timoshenko beam theory and the rotational spring model. Mirzavand and Eslami [44] presented the thermal buckling of FG rectangular plates which is mixture of zirconium oxide and titanium alloy integrated with surface-bonded piezoelectric actuators. The third order shear deformation plate theory is employed to account for the transverse shear strains. The temperature dependent of the material properties are considered. The buckling analysis of the plate under thermal loadings is carried out using the Reitz method. They indicate that the buckling temperature difference can be controlled by applying a suitable voltage on the actuator layers.

Jadhav and Bajoria [45] and Bajoria and Jadhav [46] presented the stability analysis of a piezolaminated metal based FG plate subjected to electrical and mechanical loading. The finite element model is derived with the von Karman hypothesis and degenerate shell element using the FSDT and HSDT for thin and thick FGM plate respectively. The analysis is carried out on a newly introduced metal based FGM material which is a mixture of aluminum and stainless steel. Khorshidvand *et al.* [47] studied the thermal buckling of circular plates made of FGMs with surface bonded piezoelectric layers subjected to applied constant voltage, uniform temperature rise, nonlinear and linear temperature variation through the thickness for immovable clamped edge of boundary conditions. The general thermoelastic nonlinear equilibrium and linear stability equations for the piezoelectric FG plate are derived using the variational formulations. Panda and Sopan [48] developed finite element model for geometrically non-

linear analysis of FG annular sector plates integrated with the cylindrically orthotropic piezoelectric fiber reinforced composite (PFRC) annular patches based on the FSDT and the Von Karman nonlinear strain-displacement relations.

3. REVIEW ON VIBRATION CONTROL OF PIEZOLAMINATED COMPOSITE PLATES/FGM PLATES

Vibrations of the piezolaminated structures can be effectively controlled using the direct and converse piezo effects with distributed sensors and actuators. Sensor detects the oscillations and the actuator controls the vibration of the system. The classical control laws are constant gain negative velocity feedback and Lyapunov's feedback which are based on output feedback. In the case of classical control laws, the gains are arbitrarily chosen, whereas in case of optimal control law, an optimal control gain is obtained which minimizes as object functions. Several studies have been carried out for vibration control of piezolaminated plate and piezolaminated FGM plate structures. Review is presented to highlight the vibration control studies of the composite / FGM plate structure using piezoelectric effect in following section.

3.1. Vibration Control of Piezolaminated Composite Plates

Lawson [49] investigated the characteristic frequencies of infinite piezoelectric plates vibrating between the grounded electrodes of a plane parallel condenser. The investigation exhibits that the frequencies depend on the piezoelectric constants as well as the elastic constants of the crystal. Tiersten [50] investigated the thickness vibrations of an infinite anisotropic plate with electrodes coated on both surfaces are investigated using the linear piezoelectric equations. In the general case, the three fundamental solutions of the differential equations were found to couple at the traction free surfaces of the plate. Hruska [51] investigated the similar problem of Lawson [49] to study an infinite piezoelectric plate vibrating between two electrodes of a plane parallel condenser for the case of a small d.c. potential maintained across the condenser electrodes. Chandrashekhara and Agarwal [52] developed a finite element formulation for laminated composite plates with integrated piezoelectric sensors and actuators using FSDT. The developed mathematical model is similar to that of Lee [53] however; the FSDT was used instead of classical laminated plate theory (CLPT). The improved structural behavior is demonstrated using a constant gain feedback control. Hwang *et al.* [54] investigated the combined effects of passive and active control on the vibration control of a composite laminated plate with piezoelectric sensors/actuators using finite element formulation and modal analysis. The equations of motion of the system

were formulated using CLPT with the induced strain actuation and Hamilton's principle. The total charge developed on the sensor layer is calculated from the direct piezoelectric equation.

Tzou and Fu [55] investigated the active vibration controls of the plate with various sizes of sensors/actuators and control algorithm, the proportional feedback and lyapunov control were presented and carried out the free vibration analysis to find out natural frequencies and mode shapes. Chandrashekhara and Tenneti [56] developed a finite element model for the active control of thermally induced vibration of laminated composite plates with piezoelectric sensors and actuators. The direct and converse piezoelectric effects are coupled with a constant gain feedback control algorithm to actively control the dynamic response of the plate in a closed loop. A C^0 continuous nine noded shear flexible element is implemented to model the plate. Baz and Ro [57] presented a finite element analysis of the dynamic control of the flat plates which are partially treated with patches of the active constrained layer damping (ACLD) treatment and demonstrated its ability to control the bending vibration of flexible plates. Batra and Liang [58] studied the steady state vibrations of a simply supported rectangular laminated elastic plate with embedded piezoelectric actuators and sensors by using the three-dimensional elasticity theory. Han *et al.* [59] presented an experimental study for active vibration control of composite beams and plates and developed an analytical model using Ritz method to calculate the sensor output history and control voltage history for the composite beam with piezoelectric sensors and actuators. The results of an analytical model are validated with experimental investigations. Abramovich and Meyer [60] presented an exact elasticity solution for forced induced vibrations of a piezolaminated elastic beam being driven by time harmonic voltages applied to the actuators on top and bottom surfaces. The analysis is based on Fourier series.

Goswami and Kant [61] presented a generalised finite element formulation of a consistent plate model for active vibration control of stiffened laminates integrated with piezoelectric polymer layers acting as distributed sensors and actuators. Total charge developed on the sensor layer is calculated from the direct piezoelectric equations. Kang *et al.* [62] analyzed multi-modal vibration control of the cantilevered laminated composite plate using collocated piezoceramic sensors/actuators and verified experimentally for various fiber orientations. The research highlighted an analytical approach to evaluate the passive and the active vibration control of the plate. Lam and Ng [63] presented the theoretical formulations using CLPT and Navier solutions for the analysis of the laminated composite plates with integrated sensors and actuators subjected to both mechanical and electrical loadings. An active control of the dynamic response of the integrated plate structures through closed loop control is carried out using negative force-cum-moment

feedback control algorithm which is coupling with the direct and converse piezoelectric effects. Lin and Huang [64] investigated the vibration control of beam-plates with bonded piezoelectric sensors and actuators based on finite element method and presented the basic equations for piezoelectric sensors and actuators. The equation of motion is derived for a beam-plate structure bonded with pairs of piezoelectric sensors or actuators by using the Hamilton's principle.

Liu *et al.* [65] developed finite element model for the shape control and active vibration suppression of laminated composite plates with integrated piezoelectric sensors and actuators using CLPT and the principle of virtual displacements. Numerical investigations show the influence of stacking sequence and position of sensors and actuators on the response of the plate. Reddy [66] presented a general formulation for laminated composite plates with piezoelectric actuators and sensors. The formulation is based on CLPT, FSDT and third order shear deformation theories incorporating the thermo-electro-mechanical coupling, von Karman type geometric nonlinearity and time dependency. Saravanos [67] presented a coupled electromechanical theory for composite laminates with multiple piezoelectric layers connected to passive electric circuits and a Ritz solution is used for predicting the modal damping, modal frequencies and damped response of composite piezoelectric plates. The equations of motion for passive laminate systems were solved for the case of simply supported plates and eigenvalues of the damped plate were calculated to obtain the modal frequencies and damping. Balamurugan and Narayanan [68] developed a new piezolaminated quadrilateral composite plate/shell finite element and applied to a composite cantilevered plate and cantilevered semicircular shell with distributed PZT piezoceramic sensor and actuator on the top and bottom surfaces. The classical control methods for different kinds of loading environments are used to control vibration composite laminated plates. Results predicts that the velocity feedbacks like constant gain negative velocity feedback and Lyapunov feedback are more effective in controlling the vibrations when compared to displacement feedback like direct proportional feedback but LQR control methods are more effective in controlling the vibration with lesser peak voltages. Valoor *et al.* [69] developed a neural network based control system for self adapting vibration control of laminated plates with piezoelectric sensors and actuators. The finite element model of the plate with integrated piezoelectric sensor and actuators is used to simulate the vibration of the plate.

Kang *et al.* [70] investigated the interaction between active and passive vibration control characteristics by numerically and verified experimentally. The finite element method is used for the analysis of dynamic characteristics of the laminated composite beams. Experiments on the active vibration control of the laminated composite beams were carried out using velocity feedback control. Mukherjee *et al.* [71]

presented active control of stiffened composite plate using piezoelectric materials. The stiffener had been formulated such that, it could have any shape in plan and need not pass through the nodal lines of the finite element mesh. The established formulation could be effectively employed in the analysis of plates with eccentric stiffener. Gao and Shen [72] developed an incremental finite element equations considering the geometrical non-linearity of structures with piezoelectric patches based on virtual velocity incremental variational principles with the assumption of weak mechanical and electric coupling. The numerical investigation exhibits that piezoelectric actuators can produce significant damping and control transient vibration effectively and the numbers and locations of the piezoelectric actuators have influence on the shape control and the vibration control of the structures.

Kulkarni and Bajoria [73,74] presented a new finite element model for the piezolaminated plates/shells using the HSDT and studied the active control of piezolaminated composite plates/shells. Narayanan and Balamurugan [75] presented finite element formulation for active vibration control of shear deformable piezolaminated beam, plate and shell including the stiffness, mass and electromechanical coupling effects of distributed piezoelectric sensor and actuator layers. For the case of plate/shell elements the thermoelectromechanical coupling is considered and studied the active vibration control using the classical control methods like constant gain negative velocity feedback and Lyapunov feedback. Quek *et al.* [76] investigated the placement of collocated piezoelectric sensor/actuator pairs in a laminated composite plate using the finite element method. Two performance functions based on the modal controllability and system controllability are proposed as indices for damping out the free vibration. Chen *et al.* [77] investigated the bending and free vibration of an imperfectly bonded orthotropic piezoelectric rectangular laminates using a three dimensional state-space approach. The interlaminar bonding of the host elastic laminate was assumed to be imperfect, described by a spring layer model while the bonding between the host elastic laminate and the surface piezoelectric actuator and sensor layers was perfect. A general spring layer was adopted to model the bonding imperfections. Chen *et al.* [78] employed the same three dimensional state-space approach to investigate the static and dynamic problems of simply supported adaptive angle ply laminates in cylindrical bending featuring interlaminar bonding imperfections. Liew *et al.* [79] developed an element free Galerkin method based on the FSDT for the shape control and vibration suppression of the piezolaminated composite plates. Also investigation has been carried out on the free vibration analysis of simply supported square piezolaminated plates by considering different orientations of composite substrates and locations of piezoelectric patches.

Moita *et al.* [80] presented a finite element formulation for active vibration control of thin plate laminated structures

with integrated piezoelectric layers acting as sensors and actuators. The model is based on the Kirchhoff's CLPT and can be applied to plate and shell adaptive structures. Newmark method is considered to calculate the dynamic response of the laminated structures. Raja *et al.* [81] studied the influence of active stiffening on the frequency control of piezo-hydro-thermo-elastic laminated plates and shells for various elastic modes using coupled piezoelectric finite element formulation involving a hygrothermal strain field based on virtual work principles. Vel *et al.* [82] presented an analytical solution for the cylindrical bending vibrations of linear piezoelectric laminated plates which is obtained by extending the Stroh formalism to the generalized plane strain vibrations of piezoelectric materials. Tzou *et al.* [83] presented a thorough review on smart materials including material histories characteristics, material varieties, limitations, sensor/actuator/structure applications of piezoelectrics, shape memory materials, electro and magnetostrictive materials, electro and magnetorheological fluids, polyelectrolyte gels, superconductors, pyroelectrics, photostrictive materials, photoferroelectrics, magneto-optical materials. Duan *et al.* [84] presented the free vibration analysis of piezoelectric coupled annular plates using the Kirchhoff's and Mindlin plate models. Sinusoidal function is used to describe the distribution of electric potential along the thickness direction of thin and thick plate. Maxwell's static electricity equation is included as one of the governing equations. The results are verified against three dimensional finite element analysis using ABAQUS.

Huang and Shen [85] studied the nonlinear vibration and dynamic response of simply supported shear deformable cross ply laminated plates with piezoelectric actuators subjected to mechanical, electrical and thermal loads. The theoretical formulation is based on the HSDT and general von Karman's type strains including thermo-piezoelectric effects. Oh [86] studied the nonlinear dynamics of active piezolaminated plates to investigate thermo-piezoelectric snap-through phenomena. A multi-field layer wise finite element is proposed for high accuracy and nonlinearity of displacement, electric and thermal fields. The thermoelastic postbuckling of the structural models is investigated and the characteristics of piezoelectric active responses are studied for finding snap-through piezoelectric potentials and the load-path tracking map. Peng *et al.* [87] developed a methodology for piezoelectric patches placement optimization and introduces adaptive feedforward control into smart structure vibration control. The optimization methodology is based on modeling using ANSYS. Du *et al.* [88] obtained exact solutions for thickness vibrations of a piezoelectric plate under uniform biasing acceleration with the consideration of the piezoelectric stiffening.

Chen *et al.* [89] extended previous work of Chen *et al.* [77] to investigate bending and free vibrations of simply supported cross ply piezolaminated cylindrical panel featur-

ing with interlaminar bonding imperfections. Qu *et al.* [90] investigated the vibration behavior of a piezoelectric composite plate with cracks and developed the dynamic model based on the principle of minimum energy and analyzed the effects of cracks and piezoelectric materials on mode shapes. Kulkarni and Bajoria [91] extended previous work of Kulkarni and Bajoria [73] to investigate the large deformation analysis of piezolaminated smart structures using finite element analysis based on FSDT and HSDT. Heidary and Eslami [92] studied the piezo-control of forced vibrations of the laminated thermoelastic plate and presented the dynamic response under the rapidly applied mechanical excitation and prescribed thermal loading. The structural vibrations induced in a laminated thermoelastic plate are controlled by appropriate control voltage applied to piezoelectric layers. Ghasemi-Nejhad *et al.* [93] presented study on the use of piezoelectric stack and monolithic patch actuators in finite element analysis and examined the effects of the actuator location on the vibration suppression and the level of optimum voltage. Balamurugan *et al.* [94] studied the active vibration control performance of the piezolaminated smart composite plates using finite element model based on HSDT by applying various control strategies.

Kulkarni and Bajoria [95] presented the geometrically nonlinear finite element analysis of smart structures and presented numerical investigations of piezolaminated composite beams, plates and shell structures using the FSDT and HSDT. Lee and Guo [96] developed a finite element simulation model for the active control of nonlinear composite panel vibration using von Karman nonlinear strain-displacement relations for large deflection responses and linear piezoelectricity constitutive relations under random excitation. Four control methods, velocity feedback, lead, lag and H_∞ are employed and examined for cases of small and large amplitude vibrations. The H_∞ method works better under small excitations with small piezoelectric actuators and the lag compensator performs better under large excitations with large piezoelectric actuators. Della and Shu [97] developed a mathematical model for the vibration of beams with piezoelectric inclusions. The piezoelectric inclusion in a non-piezoelectric matrix is analyzed as two inhomogeneous inclusion problems as elastic and dielectric by using Eshelby's equivalent inclusion method. The Euler-Bernoulli beam theory and Rayleigh-Ritz approximation technique are used for analysis. In addition a parametric study was conducted to investigate the influence of the energies due to piezoelectric coupling on the natural frequency of the beam.

Zhang and Shen [98] presented an analytical formulation for structural vibration control of laminated plates consisting of piezoelectric fiber reinforced composite layers and orthotropic composite layers. The active controlled electric field was applied to the piezocomposite layers equipped with Interdigitated Electrodes (IDE). Based on the thin plate theory the governing differential equations for axial vibra-

tion and transverse vibration are established. The solution is obtained through the separation of variables and Fourier expansion method. Pietrzakowski [99] formulated models of piezoelectric coupled laminated plates based on Kirchhoff's and Mindlin's kinematic assumptions involving the electric potential distribution, which satisfies the Maxwell electrostatics equation. In the first model the displacement field is based on the Kirchhoff hypothesis and in second model the Mindlin plate theory is applied. Dash and Singh [100] studied the nonlinear free vibration of geometrically nonlinear shear deformable laminated plate with embedded and/or surface bonded piezoelectric layers in Green Lagrange sense. The formulation is based on the HSDT. Jayakumar *et al.* [101] studied nonlinear free vibrations of simply supported piezolaminated rectangular plates with immovable edges based on utilizing Kirchhoff's hypothesis and von Karman's strain-displacement relations. Applying the modified Galerkin's method to the governing nonlinear partial differential equations, a modal equation of Duffing's type is obtained and solved by exact integration.

Ray and Shivakumar [102] analyzed active composite layer damping (ACLD) of geometrically nonlinear transient vibrations of laminated thin composite plates using piezoelectric fiber reinforced composite materials. The Golla-Hughes-McTavish (GHM) method had been used to model the constrained viscoelastic layer of the ACLD treatment in the time domain. A finite element model was developed for the cross ply and antisymmetric angle ply plates undergoing geometrically nonlinear vibrations. For deriving coupled electromechanical nonlinear finite element model, von Karman type nonlinear strain displacement relations and the FSDT were used. Singh *et al.* [2009] studied the post buckling load response of laminated composite plates supported on linear elastic foundation with random system properties using HSDT with von-Karman nonlinear strain-displacement relations. A finite element method is used for spatial discretization of the laminate. Tian *et al.* [104] proposed a yield criterion that is related to the spherical stress tensor is proposed to describe the mixed hardening of damaged orthotropic materials based on the elasto-plastic mechanics and continuum damage theory. The finite difference method and the Newmark- β method are adopted to make the undetermined variables discretized in the space and time domains respectively. Trindade and Benjeddou [105] presented a analysis of methodologies to evaluate the effective electromechanical coupling coefficient for structures with piezoelectric elements. Finite element method is used to modeling of the electric boundary conditions and comparisons between numerical, analytical and experimental results for beams with bonded extension and embedded shear piezoelectric materials are carried out. Umesh and Ganguli [106] developed a finite element model for a smart composite plate with matrix cracks and studied the effect of matrix cracks in a cantilevered smart composite plate with different electrical and mechanical

loadings for several different laminate types and ply angles. Balamurugan and Narayanan [107] extended previous work of Balamurugan and Narayanan [68] to developed a general finite element formulation of stiffened shell structures with distributed piezoelectric sensors and actuators.

Chandrashekhar and Ganguli [108] investigated the nonlinear vibration analysis using a C0 assumed strain interpolated finite element plate model based on Reddy's third order theory. The variance of linear and non linear natural frequencies of the plate due to randomness in its material properties is obtained using Monte Carlo Simulation with Latin Hypercube Sampling technique. Yiming *et al.* [109] presented a nonlinear model for active vibration control analysis of cross ply piezoelectric laminated plates containing the damage effect of the intra-layer materials and inter-laminar interfaces by using the Von Karman type of nonlinear strains. The active control of damping is derived to the nonlinear dynamic equations and used to actively control the vibration response of the plate by using the Hamilton variation principle and the simple negative velocity feedback control algorithm. Farhadi and Hashemi [110] investigated the feasibility of using piezoelectric patches for multi-mode vibration control of moderately thick rectangular plates based on a finite element formulation. An active damping controller is designed using modal velocity feedbacks for suppression of plate vibrations. Kerur and Ghosh [111] presented a coupled electro-mechanical finite element formulation for active control of geometrically nonlinear transient response of laminated composite plate is studied using FSDT and von Karman type non-linear strain displacements. The Newton Raphson iterative method in association with Newmark time integration method is used to solve the nonlinear finite element equilibrium equation and negative velocity feedback control algorithm is used to control the dynamic response of the smart laminated composite plate.

Sarangi and Ray [112] investigated the performance of the active constrained layer damping (ACLD) treatment in which the constraining layer is made of the vertically reinforced 1-3 piezoelectric composite in time domain for active damping of nonlinear transient vibrations of laminated composite plates using three dimensional finite element model. Dash and Singh [113] developed a probabilistic procedure especially for highly nonlinear problems to obtain mean and standard deviation of the nonlinear natural frequency of the smart laminated composite plate having random material property. Her and Lin [114] investigated the vibration response of a simply supported composite laminated plate excited by piezoelectric actuators and obtained an analytical solution of the vibration response of a simply supported laminated rectangular plate under time harmonic electrical loading. Phung-Van *et al.* [117] extended formulation based on a cell-based smoothed stabilized discrete shear gap element (CS-FEM-DSG3) presented by Nguyen-Thoi *et al.* [116] and Bletzinger *et al.* [115] to investigate the static and free

vibration analyses and dynamic control of composite plates integrated with piezoelectric sensors and actuators. The electric potential is assumed to be a linear function through the thickness for each piezoelectric sub-layer. In case of active vibration control of the static deflection, a displacement and velocity feedback control algorithm is used and closed loop control is used to evaluate dynamic response of the plates. Shivakumar *et al.* [118] studied the geometrically nonlinear vibration control of smart laminated composite panels using the patches of ACLD treatment, which is made of horizontally reinforced PFRC material using three dimensional finite element model.

3.2. Vibration Control of Piezolaminated FGM Plates

He *et al.* [119] presented a finite element formulation based on the CLPT for the shape and vibration control of the FGM plates with integrated piezoelectric sensors and actuators. The properties of the FGM plates are functionally graded in the thickness direction according to a volume fraction power law distribution. A constant velocity feedback control algorithm is used for the active control of the dynamic response of the FGM plate through closed loop control. The static and dynamic responses are presented for an FGM plate of aluminum oxide/Ti-6Al-4V material composition. Liew *et al.* [120] presented a finite element formulation based on FSDT for static and dynamic piezothermoelastic analysis and active control of FGM plates subjected to a temperature gradient using integrated piezoelectric sensor/actuator layers. A constant displacement-cum-velocity feedback control algorithm is applied to provide an active feedback control of the integrated FGM plate in a self monitoring/controlling system for the bending control and the torsional control. Ootao and Tanigawa [121] developed the theoretical formulation of a control of the transient thermoelastic displacement for a FG rectangular plate bonded to a piezoelectric plate due to nonuniform heat supply. The numerical study is carried out for a FG rectangular plate mixture of zirconium oxide and titanium alloy, bonded to a piezoelectric plate of a cadmium selenide solid.

Liew *et al.* [122] Finite element model based on CLPT is presented for static and dynamic piezothermoelastic analysis and active control of FGM plates under temperature gradient environments using integrated piezoelectric sensor/actuator layers. The properties of FGM plate are in the thickness direction according to a volume fraction power law distribution. FGM plate consists of zirconia and aluminum. Huang and Shen [123] presented the nonlinear free and forced vibration analyses for simply supported, hybrid FGM plate subjected to the combined action of transverse dynamic, electric and thermal loading. The substrate FGM layer consists of zirconia and aluminum. The formulations are based on HSDT and general von Karman type equations

and include thermo-piezoelectric effects. Analytical solutions have been presented by using an improved perturbation technique. Kargarnovin *et al.* [124] analyzed a FGM rectangular plate which is bonded with piezoelectric rectangular patches on the top and/or bottom surface as an actuators/sensors. The governing differential equations of the motion are derived using CLPT and constant electric charge. The solution for the motion equation is obtained using a Fourier series method. Reddy and Ray [125] investigated the optimal control of FG plates using a distributed actuator made of the PFRC material proposed by Mallik and Ray [126] and a distributed monolithic piezoelectric sensor layer. The optimal controller developed by employing the linear quadratic regulator design with output feedback. Ebrahimi and Rastgo [127] investigate the free vibration behavior of circular FG plate integrated with two uniformly distributed actuator layers (PZT4) on the top and bottom surfaces of the circular FG plate based on the CLPT. The material properties of the FG substrate plate are assumed to be graded in the thickness direction according to the power law distribution in terms of the volume fractions of the constituents. The differential equations of the motion are solved analytically for clamped edge boundary condition of the plate. Ebrahimi *et al.* [128] presented a free vibration analysis of moderately thick circular FG plate integrated with two thin piezoelectric (PZT4) layers based on Mindlin plate theory. The investigation is carried to show the effect of varying the gradient index of FG plate on the free vibration characteristics of the structure.

Ohadi and Fakhari [129] investigated the large amplitude vibration control of FGM plates under thermal gradient and mechanical loads using piezoelectric sensor/actuator layers and presented the nonlinear finite element formulations based on the third order shear deformation theory. A proportional derivative (PD) feedback control algorithm is employed in the analysis and studied the effects of controller gains and presence of noise in sensor voltage on the controller performance. Ebrahimi and Rastgoo [130] presented nonlinear vibration analysis of thin circular pre-stressed FG plate integrated with two uniformly distributed piezoelectric actuator layers with an initial nonlinear large deformation. The nonlinear governing equations of motion are derived based on CPT with von-Karman type geometrical large nonlinear deformations. The initial stress state and pre-vibration deformations of the FG plate that is subjected to in-plane forces and applied actuator voltage is first solved then derived the differential equations that govern the nonlinear vibration behavior of pre-stressed piezoelectric coupled FGM plates by adding an incremental dynamic state. Ebrahimi *et al.* [131] presented a theoretical model for geometrically nonlinear vibration analysis of piezoelectrically actuated circular FGM using Kirchhoff's Love hypothesis with von-Karman type geometrical large nonlinear deformations. The FGM plate is the mixture of alumina and aluminum. Panda and Ray [132] presented a geometrically nonlinear dynamic

analysis for FG plates integrated with a patch of active constrained layer damping (ACLD) treatment, which is subjected to a temperature field. The temperature field is assumed to be spatially uniform over the substrate plate surfaces and varied through the thickness of the host FG plates and assumed temperature dependent material properties of the FG substrate plates in the analysis.

Panda and Ray [133] presented the geometrically nonlinear dynamic analysis of FG laminated composite plates integrated with a patch of (ACLD) treatment. The constraining layer of the ACLD treatment is considered to be made of the piezoelectric fiber reinforced composite (PFRC) material. The constrained viscoelastic layer of the ACLD treatment is modeled using the Golla-Hughes-McTavish (GHM) method. Finite element model has been developed to model the open-loop and closed-loop nonlinear dynamics of the overall FG laminated composite plates which are based on the FSDT. Xia and Shen [134] presented the nonlinear free and forced vibration analyses for simply supported, FGM plates with fully covered PFRC actuators subjected to the combined action of transverse dynamic, thermal and electric loads. The material properties of both FGM and PFRC layers are assumed to be temperature dependent. The formulations are based on HSDT and general von Karman-type equation. Hashemi *et al.* [135] presented an analytical method to analyze the vibration of piezoelectric coupled thick annular FG plates subjected to different combinations of soft simply supported, hard simply supported and clamped boundary conditions at the inner and outer edges of the annular plate on the basis of the Reddy's third order shear deformation theory. The properties of host plate are graded in the thickness direction according to a volume fraction power law distribution. The differential equations of motion are solved analytically for various boundary conditions of the plate.

Fakhari and Ohadi [136] developed finite element formulation to investigate geometrically nonlinear vibration behavior of FGM plate with surface bonded piezoelectric layers under thermal, electrical and mechanical loads using HSDT. The von Karman nonlinear strain-displacement relationship is used to account for the large deflection of the plate. The two control algorithms are employed to control large amplitude vibration control of FGM plate as, classical displacement velocity feedback control and robust H2 control. Yiqi and Yiming [137] analyzed the nonlinear dynamic response and active vibration control of the piezoelectric FG plate based on HSDT and elastic piezoelectric theory, the nonlinear geometric and constitutive relations of the piezoelectric FG plate are established, and then the nonlinear motion equations of the piezoelectric FG plate are obtained through Hamilton's variational principle. The nonlinear active vibration control of the structure is carried out with adoption of the negative velocity feedback control algorithm. Fakhari *et al.* [138] developed finite element formulation based on HSDT to analyze nonlinear natural frequencies, time and

frequency responses of FG plate with surface-bonded piezoelectric layers under thermo-electro-mechanical loads. The von Karman nonlinear strain-displacement relationship is used to account for the large deflection of the plate. The material properties of FGM are assumed temperature dependent. Shirazi *et al.* [139] studied active vibration control of a simply supported rectangular plate made from FGMs with fuzzy logic control. Modal analysis was implemented to obtain the first nine natural frequencies and mode shapes of the plate.

Ebrahimi [140] presented a nonlinear dynamics and vibration analysis on pre-stressed FG circular plates that are bonded with piezoelectric actuator layers in a thermal environment. The equations of motion are derived using CLPT based on Kirchhoff's-Love hypothesis with von-Karman type geometrical large nonlinear deformations. The material properties of the FG core plate are assumed to be graded in the thickness direction according to the power law distribution. Jadhav and Bajoria [141] investigated the active vibration control analysis of thick FG plate integrated with piezoelectric layer at top and bottom face using finite element method based on FSDT and HSDT, von-Karman's hypothesis and degenerated shell element. The analysis is carried out on newly introduced metal based FGM material which is mixture of aluminum and stainless steel. Jadhav and Bajoria [142] developed a finite element model for free and forced vibration analysis of a piezoelectric thin FGM plate using HSDT. The natural frequencies are compared with the natural frequencies of a layered composite plate with 21 layers using ANSYS. Jodaei *et al.* [143] studied the free vibration analysis of FG piezoelectric annular plates using state-space based differential quadrature method and comparative behavior modeling by an artificial neural network. Talabi and Saidi [144] developed a novel exact closed-form procedure based on the third order shear deformation plate theory to analyze in-plane and out-of-plane frequency responses of circular/annular FGM plates embedded in piezoelectric layers for both close/open circuit electrical boundary conditions.

4. CONCLUSIONS

This article makes an effort in summarizing recent development in stability as well as vibration control analysis of piezolaminated composite and FGM plates. Piezoelectric materials possesses a property of direct and converse piezoelectric effects which can be adequately employed to control the deflection, vibration, shape and buckling of the structure. The review paper is divided into following sections: stability analysis of piezolaminated composite plates and piezolaminated FGM plates, vibration control of piezolaminated composite plates and piezolaminated FGM plates. This paper is an evidence of contributions from researchers for high quality and tremendous work in the area of stability as well

as vibration control analysis of piezolaminated composite plates and piezolaminated FG plates.

5. REFERENCES

- [1] Schwartz M. 2002 Encyclopedia of smart materials volume 1 and volume 2 John Wiley and Sons, Inc., New York.
- [2] Yang J. 2005 An introduction to the theory of piezoelectricity Springer Science + Business Media, Inc.
- [3] IEEE Standard on Piezoelectricity 1988 The Institute of Electrical and Electronics Engineers, Inc.
- [4] Koizumi M. 1997 FGM activities in Japan. *Composites Part B*, 28B 1–4.
- [5] Chandrashekhara K. and Bhatia K. 1993 Active buckling control of smart composite plates-finite-element analysis. *Smart Materials and Structures* 2, 31–39. <http://dx.doi.org/10.1088/0964-1726/2/1/005>
- [6] Icardi U. and Di Sciuva M. 1996 Large-deflection and stress analysis of multilayered plates with induced-strain actuators. *Smart Materials and Structures* 5, 140–164. <http://dx.doi.org/10.1088/0964-1726/5/2/004>
- [7] Oh I. K. Han J H. and Lee I. 2000 Postbuckling and vibration characteristics of piezolaminated composite plate subject to thermo-piezoelectric loads. *Journal of Sound and Vibration*. 233, 19–40. <http://dx.doi.org/10.1006/jsvi.1999.2788>
- [8] Shen H. S. 2001a Postbuckling of shear deformable laminated plates with piezoelectric actuators under complex loading conditions. *International Journal of Solids and Structures*, 38, 7703–7721. [http://dx.doi.org/10.1016/S0020-7683\(01\)00120-2](http://dx.doi.org/10.1016/S0020-7683(01)00120-2)
- [9] Shen H. S. 2001b Thermal postbuckling of shear-deformable laminated plates with piezoelectric actuators. *Composites Science and Technology* 61, 1931–1943. [http://dx.doi.org/10.1016/S0266-3538\(01\)00099-9](http://dx.doi.org/10.1016/S0266-3538(01)00099-9)
- [10] Varelis D. and Saravanos D. A. 2002 Nonlinear coupled mechanics and initial buckling of composite plates with piezoelectric actuators and sensors. *Smart Materials and Structures*, 11, 330–336. <http://dx.doi.org/10.1088/0964-1726/11/3/302>
- [11] Varelis D. and Saravanos D. A. 2004 Coupled buckling and post-buckling analysis of active laminated piezoelectric composite plates. *International Journal of Solids and Structures*, 41, 1519–1538. <http://dx.doi.org/10.1016/j.ijsolstr.2003.09.034>
- [12] Wang S. Y. Quek S. T. and Ang K. K. 2004. Dynamic stability analysis of finite element modeling of piezoelectric composite plates. *International Journal of Solids and Structures*, 41, 745–764. <http://dx.doi.org/10.1016/j.ijsolstr.2003.09.041>
- [13] Kim H. W. and Kim J. H. 2005. Effect of piezoelectric damping layers on the dynamic stability of plate under a thrust. *Journal of Sound and Vibration*, 284, 597–612. <http://dx.doi.org/10.1016/j.jsv.2004.06.045>
- [14] Kapuria S. A. 2004. Coupled zig-zag third-order theory for piezoelectric hybrid cross-ply plates. *Journal of Applied Mechanics*, 71, 604–614.
- [15] Kapuria S. and Achary G. S. 2005. Exact 3D piezothermoelasticity solution for buckling of hybrid cross-ply plates using state space approach. *Journal of Applied Mathematics and Mechanics*, 85, 189–201.
- [16] Kapuria S. and Achary G. S. 2006a Nonlinear coupled zigzag theory for buckling of hybrid piezoelectric plates. *Composite Structures*, 74, 253–264. <http://dx.doi.org/10.1016/j.compstruct.2005.04.010>
- [17] Kapuria S. and Achary G. S. 2006b Nonlinear zigzag theory for electrothermomechanical buckling of piezoelectric composite and sandwich plates. *Acta Mechanica*, 184, 61–76. <http://dx.doi.org/10.1007/s00707-006-0318-7>
- [18] Akhras G. and Li W. C. 2007 Three-dimensional static, vibration and stability analysis of piezoelectric composite plates using a finite layer method. *Smart Materials and Structures*, 16, 561–569. <http://dx.doi.org/10.1088/0964-1726/16/3/002>
- [19] Giannopoulos G. Santafe F. Monreal J. and Vantomme J. 2007 Thermal, electrical, mechanical coupled mechanics for initial buckling analysis of smart plates and beams using discrete layer kinematics. *International Journal of Solids and Structures*, 44, 4707–4722. <http://dx.doi.org/10.1016/j.ijsolstr.2006.11.048>
- [20] Kim G. W. and Lee K. Y. 2007. Influence of weak interfaces on buckling of orthotropic rectangular laminates. *Composite Structures* 81, 427–431. <http://dx.doi.org/10.1016/j.compstruct.2006.09.002>
- [21] Akhras G. and Li W. C. 2008. Three-dimensional thermal buckling analysis of piezoelectric composite plates using the finite layer method. *Smart Materials and Structures*, 17, 055004. <http://dx.doi.org/10.1088/0964-1726/17/5/055004>
- [22] Kim G. W. and Lee K. Y. 2008. Influence of weak interfaces on buckling of orthotropic piezoelectric rectangular laminates. *Composite Structures*, 82, 290–294. <http://dx.doi.org/10.1016/j.compstruct.2007.01.006>
- [23] Yang J. and Huang X. 2009. Dynamic stability behavior of 3D braided composite plates integrated with piezoelectric layer. *Journal of Composite Materials*, 43, 2223–2238. <http://dx.doi.org/10.1177/0021998309339219>
- [24] Shariyat M. 2009. Dynamic buckling of imperfect laminated plates with piezoelectric sensors and actuators subjected to thermo-electro-mechanical loadings, considering the temperature-dependency of the material properties. *Composite Structures*, 88, 228–239. <http://dx.doi.org/10.1016/j.compstruct.2008.03.044>
- [25] Akhras G. and Li W. C. 2010a. Three-dimensional thermal buckling analysis of piezoelectric antisymmetric angle-ply laminates using finite layer method. *Composite Structures*, 92, 31–38. <http://dx.doi.org/10.1016/j.compstruct.2009.06.010>
- [26] Akhras G. and Li W. C. 2010b. Three-dimensional stability analysis of piezoelectric antisymmetric angle-ply laminates using finite layer method. *Journal of Intelligent Material Systems and Structures*, 21, 719–727. <http://dx.doi.org/10.1177/1045389X10364865>
- [27] Pradyumna S. and Gupta A. 2011. Dynamic stability of laminated composite plates with piezoelectric layers subjected to periodic in-plane load. *International Journal of Structural Stability and Dynamics*, 11, 297–311. <http://dx.doi.org/10.1142/S0219455411004105>
- [28] Tanov R. and Tabiei A. 2000 A simple correction to the first-order shear deformation shell finite element formulations. *Finite Elements in Analysis and Design*, 35, 189–197. [http://dx.doi.org/10.1016/S0168-874X\(99\)00069-4](http://dx.doi.org/10.1016/S0168-874X(99)00069-4)
- [29] Shen and Zhu 2011. Compressive and thermal postbuckling behaviors of laminated plates with piezoelectric fiber reinforced composite actuators. *Applied Mathematical Modelling*, 35, 1829–1845.
- [30] Moghadam P. Y. Tahani M. and Naserian-Nik A. M. 2013. Analytical solution of piezolaminated rectangular plates with arbitrary clamped/simply-supported boundary conditions under thermo-electro-mechanical loadings. *Applied Mathematical Modelling*, 37, 3228–3241. <http://dx.doi.org/10.1016/j.apm.2012.07.034>
- [31] Jabbari M. Joubaneh E. F. Khorshidvand A. R. and Eslami M. R. 2013. Buckling analysis of porous circular plate with piezoelectric actuator layers under uniform radial compression. *International Journal of Mechanical Sciences*, 70, 50–56. <http://dx.doi.org/10.1016/j.ijmecsci.2013.01.031>
- [32] Khorshidvand A. R. Joubaneh E. F. Jabbari M and Eslami M. R. 2013. Buckling analysis of a porous circular plate with piezoelectric sensor-actuator layers under uniform radial compression *Acta Mechanica* DOI 10.1007/s00707-013-0959-2. <http://dx.doi.org/10.1007/s00707-013-0959-2>
- [33] Wankhade R. and Bajoria K. 2013. Stability of simply supported smart piezolaminated composite plates using finite element method. *International Journal of Advancements in Mechanical and Aeronautical Engineering*, 1, 14–19.
- [34] Wankhade R. and Bajoria K. 2013. Buckling analysis of piezolaminated plates using higher order shear deformation theory. *International Journal of Composite Materials*, 3, 92–99.
- [35] Liew K. M. Yang J. and Kitipornchai S. 2003. Postbuckling of piezoelectric FGM plates subject to thermo-electro-mechanical loading. *International Journal of Solids and Structures*, 40, 3869–3892. [http://dx.doi.org/10.1016/S0020-7683\(03\)00096-9](http://dx.doi.org/10.1016/S0020-7683(03)00096-9)

- [36] Yang J. Kitiporncha S. and Liew K. M. 2004. Non-linear analysis of the thermo-electro-mechanical behaviour of shear deformable FGM plates with piezoelectric actuators. *International Journal for Numerical Methods in Engineering*, 59, 1605–1632. <http://dx.doi.org/10.1002/nme.932>
- [37] Shen H. S. 2002. Nonlinear bending response of functionally graded plates subjected to transverse loads and in thermal environments. *International Journal of Mechanical Sciences*, 44, 561–584. [http://dx.doi.org/10.1016/S0020-7403\(01\)00103-5](http://dx.doi.org/10.1016/S0020-7403(01)00103-5)
- [38] Shen H. S. 2005. Postbuckling of FGM plates with piezoelectric actuators under thermo-electro-mechanical loadings. *International Journal of Solids and Structures*, 42, 6101–6121. <http://dx.doi.org/10.1016/j.ijsolstr.2005.03.042>
- [39] Shen H. S. 2007. Thermal postbuckling behavior of shear deformable FGM plates with temperature-dependent properties. *International Journal of Mechanical Sciences*, 49, 466–478. <http://dx.doi.org/10.1016/j.ijmecsci.2006.09.011>
- [40] Chen X. L. Zhao Z. Y. and Liew K. M. 2008. Stability of piezoelectric FGM rectangular plates subjected to non-uniformly distributed load, heat and voltage. *Advances in Engineering Software*, 39, 121–131. <http://dx.doi.org/10.1016/j.advengsoft.2006.12.004>
- [41] Shen H. S. 2009. A comparison of buckling and postbuckling behavior of FGM plates with piezoelectric fiber reinforced composite actuators. *Composite Structures*, 91, 375–84. <http://dx.doi.org/10.1016/j.compstruct.2009.06.005>
- [42] Shariyat M. 2009. Vibration and dynamic buckling control of imperfect hybrid FGM plates with temperature-dependent material properties subjected to thermo-electro-mechanical loading conditions. *Composite Structures*, 88, 240–252. <http://dx.doi.org/10.1016/j.compstruct.2008.04.003>
- [43] Ke L. Yang J. Kitipornchai S. and Xiang Y. 2009. Flexural vibration and elastic buckling of a cracked timoshenko beam made of functionally graded materials. *Mechanics of Advanced Materials and Structures*, 16, 488–502. <http://dx.doi.org/10.1080/15376490902781175>
- [44] Mirzavand B. and Eslami M. R. 2011. A closed-form solution for thermal buckling of piezoelectric FGM rectangular plates with temperature-dependent properties. *Acta Mechanica*, 218, 87–101. <http://dx.doi.org/10.1007/s00707-010-0402-x>
- [45] Jadhav P. and Bajoria K. 2012. Buckling of piezoelectric functionally graded plate subjected to electro-mechanical loading. *Smart Materials and Structures*, 21, 105005. <http://dx.doi.org/10.1088/0964-1726/21/10/105005>
- [46] Bajoria K. M. and Jadhav P. A. 2013. Buckling of simply supported piezoelectric FGM plates subjected to electro-mechanical loading using higher-order shear deformation theory. *Advanced Materials Research*, 622–623, 200–205.
- [47] Khorshidvand A. R. Jabbari M. and Eslami M. R. 2012. Thermoelastic buckling analysis of functionally graded circular plates integrated with piezoelectric layers. *Journal of Thermal Stresses*, 35, 695–717. <http://dx.doi.org/10.1080/01495739.2012.688666>
- [48] Panda S. and Sopan G. G. 2013. Nonlinear analysis of smart functionally graded annular sector plates using cylindrically orthotropic piezoelectric fiber reinforced composite. *International Journal of Mechanics and Materials in Design*, 9, 35–53. <http://dx.doi.org/10.1007/s10999-012-9204-8>
- [49] Lawson A. W. 1942. The vibration of piezoelectric plates. *Physical Review*, 62, 71–76. <http://dx.doi.org/10.1103/PhysRev.62.71>
- [50] Tiersten H. F. 1962. Thickness vibrations of piezoelectric plates. *The Journal of the Acoustical Society of America*, 35, 53–58. <http://dx.doi.org/10.1121/1.1918413>
- [51] Hruska K. 1969. Vibration of piezoelectric plates with a small non-zero potential across their electrodes. *Journal of Physics B*, 9, 1315–1321.
- [52] Chandrashekhara K. and Agarwal A. N. 1993. Active vibration control of laminated composite plates using piezoelectric devices: A finite element approach. *Journal of Intelligent Material Systems and Structures*, 4, 496–508. <http://dx.doi.org/10.1177/1045389X9300400409>
- [53] Lee C. K. 1990. Theory of laminated piezoelectric plates for the design of distributed sensors/actuators. part I: Governing Equations and Reciprocal Relationships. *Journal of Acoustical Society of America*, 87, 1144–1158. <http://dx.doi.org/10.1121/1.398788>
- [54] Hwang W. S. Park H. C. and Hwang W. 1993. Vibration control of a laminated plate with piezoelectric sensor/actuator: finite element formulation and modal analysis. *Journal of Intelligent Material Systems and Structures*, 4, 317–329. <http://dx.doi.org/10.1177/1045389X9300400304>
- [55] Tzou H. S. and Fu H. Q. 1994. A study of segmentation of distributed piezoelectric sensors and actuators, Part II: Parametric study and active vibration controls. *Journal of Sound and Vibration*, 172, 261–275. <http://dx.doi.org/10.1006/jsvi.1994.1173>
- [56] Chandrashekhara K. and Tenneti R. 1995. Thermally induced vibration suppression of laminated plates with piezoelectric sensors and actuators. *Smart Materials and Structures*, 4, 281–290. <http://dx.doi.org/10.1088/0964-1726/4/4/008>
- [57] Baz A. and Ro J. 1996. Vibration control of plates with active constrained layer damping. *Smart Materials and Structures*, 5, 272–280. <http://dx.doi.org/10.1088/0964-1726/5/3/005>
- [58] Batra R. C. and Liang X. Q. 1997. The vibration of a rectangular laminated elastic plate with embedded piezoelectric sensors and actuators. *Computers and Structures*, 63, 203–216. [http://dx.doi.org/10.1016/S0045-7949\(96\)00349-5](http://dx.doi.org/10.1016/S0045-7949(96)00349-5)
- [59] Han J. Rew K. and Lee I. 1997. An experimental study of active vibration control of composite structures with a piezo-ceramic actuator and a piezo-film sensor. *Smart Materials and Structures*, 6, 549–558. <http://dx.doi.org/10.1088/0964-1726/6/5/006>
- [60] Abramovich H. and Meyer-Piening H. R. 1998. Induced vibrations of piezolaminated elastic beams. *Composite Structures*, 43, 47–55. [http://dx.doi.org/10.1016/S0263-8223\(98\)00094-4](http://dx.doi.org/10.1016/S0263-8223(98)00094-4)
- [61] Goswami S. and Kant T. 1998. Active vibration control of intelligent stiffened laminates using smart piezoelectric materials by the finite element method. *Journal of Reinforced Plastics and Composites*, 17, 1472–1493.
- [62] Kang Y. K. Kim M. H. Park H. C. and Agrawal B. 1998. Multi-modal vibration control of laminated composite plates using piezoceramic sensors/actuators. *Journal of Intelligent Material Systems and Structures*, 9, 988–990. <http://dx.doi.org/10.1177/1045389X9800901203>
- [63] Lam K. Y. and Ng T. Y. 1999. Active control of composite plates with integrated piezoelectric sensors and actuators under various dynamic loading conditions. *Smart Materials and Structures*, 8, 223–237. <http://dx.doi.org/10.1088/0964-1726/8/2/008>
- [64] Lin, C. and Huang, H. 1999. Vibration control of beam-plates with bonded piezoelectric sensors and actuators. *Computers and Structures*, 73, 239–248. [http://dx.doi.org/10.1016/S0045-7949\(98\)00280-6](http://dx.doi.org/10.1016/S0045-7949(98)00280-6)
- [65] Liu, G. R. Peng, X. Q. and Lam, K. Y. 1999. Vibration control simulation of laminated composite plates with integrated piezoelectrics. *Journal of Sound and Vibration*, 220, 827–846. <http://dx.doi.org/10.1006/jsvi.1998.1970>
- [66] Reddy, J. N. 1999. On laminated composite plates with integrated sensors and actuators. *Engineering Structures*, 21, 568–593. [http://dx.doi.org/10.1016/S0141-0296\(97\)00212-5](http://dx.doi.org/10.1016/S0141-0296(97)00212-5)
- [67] Saravanas, D. A. 1999. Damped vibration of composite plates with passive piezoelectric-resistor elements. *Journal of Sound and Vibration*, 221, 867–885. <http://dx.doi.org/10.1006/jsvi.1998.2037>
- [68] Balamurugan, V. and Narayanan, S. 2001. Shell finite element for smart piezoelectric composite plate/shell structures and its application to the study of active vibration control. *Finite Elements in Analysis and Design*, 37, 713–738. [http://dx.doi.org/10.1016/S0168-874X\(00\)00070-6](http://dx.doi.org/10.1016/S0168-874X(00)00070-6)
- [69] Valoor, M. T. Chandrashekhara, K. and Agarwal, S. 2000. Active vibration control of smart composite plates using self-adaptive neuro-controller. *Smart Materials and Structures*, 9, 197–204. <http://dx.doi.org/10.1088/0964-1726/9/2/310>
- [70] Kang, Y. Park, H. Kim, J. and Choi, S. 2002. Interaction of active and passive vibration control of laminated composite beams with piezoceramic sensors/actuators. *Materials and Design*, 23, 277–286. [http://dx.doi.org/10.1016/S0261-3069\(01\)00081-4](http://dx.doi.org/10.1016/S0261-3069(01)00081-4)

- [71] Mukherjee, A. Joshi, S. P. and Ganguli, A. 2002. Active vibration control of piezolaminated stiffened plates. *Composite Structures*, 55, 435–443. [http://dx.doi.org/10.1016/S0263-8223\(01\)00171-4](http://dx.doi.org/10.1016/S0263-8223(01)00171-4)
- [72] Gao, J. X. and Shen, Y. P. 2003. Active control of geometrically nonlinear transient vibration of composite plates with piezoelectric actuators. *Journal of Sound and Vibration*, 264, 911–928. [http://dx.doi.org/10.1016/S0022-460X\(02\)01189-6](http://dx.doi.org/10.1016/S0022-460X(02)01189-6)
- [73] Kulkarni, S. A. Bajoria, K. M. 2003. Finite element modeling of smart plates/shells using higher order shear deformation theory. *Composite Structures*, 62, 41–50. [http://dx.doi.org/10.1016/S0263-8223\(03\)00082-5](http://dx.doi.org/10.1016/S0263-8223(03)00082-5)
- [74] Kulkarni, S. A. 2004. Active vibration control and geometrically non linear analysis of piezolaminated plates/shells Ph. D. Thesis IIT Bombay Mumbai India.
- [75] Narayanan, S. and Balamurugan, V. 2003. Finite element modelling of piezolaminated smart structures for active vibration control with distributed sensors and actuators. *Journal of Sound and Vibration*, 262, 529–562. [http://dx.doi.org/10.1016/S0022-460X\(03\)00110-X](http://dx.doi.org/10.1016/S0022-460X(03)00110-X)
- [76] Quek, S. T. Wang, S. Y. and Ang, K. K. 2003. Vibration control of composite plates via optimal placement of piezoelectric patches. *Journal of Intelligent Material Systems and Structures*, 14, 229–245. <http://dx.doi.org/10.1177/1045389X03034686>
- [77] Chen, W. Q. Ying, J. Cai, J. B. and Ye, G. R. 2004a. Benchmark solution of imperfect angle-ply laminated rectangular plates in cylindrical bending with surface piezoelectric layers as actuator and sensor. *Computers and Structures*, 82, 1773–1784. <http://dx.doi.org/10.1016/j.compstruc.2004.05.011>
- [78] Chen, W. Q. Ying, J. Cai, J. B. and Ye, G. R. 2004b. Exact three-dimensional solutions of laminated orthotropic piezoelectric rectangular plates featuring interlaminar bonding imperfections modeled by a general spring layer. *International Journal of Solids and Structures*, 41, 5247–5263. <http://dx.doi.org/10.1016/j.ijsolstr.2004.03.010>
- [79] Liew, K. M. He, X. Q. Tan, M. J. and Lim, H. K. 2004. Dynamic analysis of laminated composite plates with piezoelectric sensor/actuator patches using the FSDT mesh-free method. *International Journal of Mechanical Sciences*, 46, 411–431. <http://dx.doi.org/10.1016/j.ijmecsci.2004.03.011>
- [80] Moita, J. M. S. Correia, I. F. P. Soares, C. M. M. and Soares, C. A. M. 2004. Active control of adaptive laminated structures with bonded piezoelectric sensors and actuators. *Computers and Structures*, 82, 1349–1358. <http://dx.doi.org/10.1016/j.compstruc.2004.03.030>
- [81] Raja, S. Sinha, P. K. Prathap, G. Dwarakanathan, D. 2004. Influence of active stiffening on dynamic behaviour of piezo-hygro-thermo-elastic composite plates and shells. *Journal of Sound and Vibration*, 278, 257–283. <http://dx.doi.org/10.1016/j.jsv.2003.10.002>
- [82] Vel, S. S. Mewer, R. C. and Batra, R. C. 2004. Analytical solution for the cylindrical bending vibration of piezoelectric composite plates. *International Journal of Solids and Structures*, 41, 1625–1643. <http://dx.doi.org/10.1016/j.ijsolstr.2003.10.012>
- [83] Tzou H S Lee H J and Arnold S M 2004 Smart materials, precision sensors/actuators, smart structures, and structronic systems. *Mechanics of Advanced Materials and Structures*, 11, 367–393. <http://dx.doi.org/10.1080/15376490490451552>
- [84] Duan W H Quek S T and Wang Q 2005 Free vibration analysis of piezoelectric coupled thin and thick annular plate. *Journal of Sound and Vibration*, 281, 119–139. <http://dx.doi.org/10.1016/j.jsv.2004.01.009>
- [85] Huang X L and Shen H S 2005 Nonlinear free and forced vibration of simply supported shear deformable laminated plates with piezoelectric actuators. *International Journal of Mechanical Sciences*, 47, 187–208. <http://dx.doi.org/10.1016/j.ijmecsci.2005.01.003>
- [86] Oh I K 2005 Thermopiezoelectric nonlinear dynamics of active piezolaminated plates. *Smart Materials and Structures*, 14, 823–834. <http://dx.doi.org/10.1088/0964-1726/14/4/042>
- [87] Peng F Ng A and Hu Y 2005 Actuator placement optimization and adaptive vibration control of plate smart structures. *Journal of Intelligent Material Systems and Structures*, 16, 263–271. <http://dx.doi.org/10.1177/1045389X05050105>
- [88] Du J K Wang J and Zhou Y Y 2006 Thickness vibrations of a piezoelectric plate under biasing fields. *Ultrasonics*, 44, 853–857. <http://dx.doi.org/10.1016/j.ultras.2006.05.183>
- [89] Chen W Q Jung J P and Lee K Y 2006 Static and dynamic behavior of simply-supported cross-ply laminated piezoelectric cylindrical panels with imperfect bonding. *Composite Structures*, 74, 265–276. <http://dx.doi.org/10.1016/j.compstruct.2005.04.011>
- [90] Qu G M Li Y Y Cheng L and Wang B 2006 Vibration analysis of a piezoelectric composite plate with cracks. *Composite Structures*, 72, 111–118. <http://dx.doi.org/10.1016/j.compstruct.2004.11.001>
- [91] Kulkarni S A Bajoria K M 2006 Geometrically nonlinear analysis of smart thin and sandwich plates. *Journal of Sandwich Structures and Materials*, 8, 321–341. <http://dx.doi.org/10.1177/1099636206063385>
- [92] Heidary F and Eslami M R 2006 Piezo-control of forced vibrations of a thermoelastic composite plate. *Composite Structures*, 74, 99–105. <http://dx.doi.org/10.1016/j.compstruct.2005.03.011>
- [93] Ghasemi-Nejhad M N Pourjalali S Uyema M and Yousefpour A 2006 Finite element method for active vibration suppression of smart composite structures using piezoelectric materials. *Journal of Thermoplastic Composite Materials*, 19, 319–333.
- [94] Balamurugan V Manikandan B and Narayanan S 2007 A higher order finite element modeling of piezolaminated smart composite plates and its application to active vibration control. *International Journal of Computational Methods*, 4, 141–162. <http://dx.doi.org/10.1142/S0219876207001114>
- [95] Kulkarni S A and Bajoria K M 2007 Large deformation analysis of piezolaminated smart structures using higher-order shear deformation theory. *Smart Materials and Structures*, 16, 1506–1516. <http://dx.doi.org/10.1088/0964-1726/16/5/002>
- [96] Lee Y Y and Guo X 2007 Non-linear vibration suppression of a composite panel subject to random acoustic excitation using piezoelectric actuators. *Mechanical Systems and Signal Processing*, 21, 1153–1173. <http://dx.doi.org/10.1016/j.ymsp.2005.12.004>
- [97] Della C N and Shu D 2007 Vibration of beams with piezoelectric inclusions. *International Journal of Solids and Structures*, 44, 2509–2522. <http://dx.doi.org/10.1016/j.ijsolstr.2006.08.002>
- [98] Zhang H Y and Shen Y P 2007 Vibration suppression of laminated plates with 1-3 piezoelectric fiber reinforced composite layers equipped with interdigitated electrodes. *Composite Structures*, 79, 220–228. <http://dx.doi.org/10.1016/j.compstruct.2005.12.003>
- [99] Pietrzakowski M 2008 Piezoelectric control of composite plate vibration: Effect of electric potential distribution. *Computers and Structures*, 86, 948–954. <http://dx.doi.org/10.1016/j.compstruc.2007.04.023>
- [100] Dash P and Singh B N 2009 Nonlinear free vibration of piezoelectric laminated composite plate. *Finite Elements in Analysis and Design*, 45, 686–694. <http://dx.doi.org/10.1016/j.finel.2009.05.004>
- [101] Jayakumar K Yadav D and Nageswara Rao B. 2009 Nonlinear free vibration analysis of simply supported piezo-laminated plates with random actuation electric potential difference and material properties. *Communications in Nonlinear Science and Numerical Simulation*, 14, 1646–1663. <http://dx.doi.org/10.1016/j.cnsns.2008.02.003>
- [102] Ray M C and Shivakumar J 2009 Active constrained layer damping of geometrically nonlinear transient vibrations of composite plates using piezoelectric fiber-reinforced composite. *Thin Walled Structures*, 47, 178–189. <http://dx.doi.org/10.1016/j.tws.2008.05.011>
- [103] Singh B N Lal A and Kumar R 2009 Post buckling response of laminated composite plate on elastic foundation with random system properties. *Communications in Nonlinear Science and Numerical Simulation*, 14, 284–300. <http://dx.doi.org/10.1016/j.cnsns.2007.08.005>
- [104] Tian Y Fu Y and Wang Y 2009 Nonlinear dynamic response and vibration active control of piezoelectric elasto-plastic laminated plates with damage. *Journal of Vibration and Control*, 15, 1463–1492. <http://dx.doi.org/10.1177/1077546309103265>
- [105] Trindade M A and Benjeddou A 2009 Effective electromechanical coupling coefficients of piezoelectric adaptive structures: critical evaluation and optimization. *Mechanics of Advanced Materials and Structures*, 16, 210–223. <http://dx.doi.org/10.1080/15376490902746863>

- [106] Umesh K and Ganguli R 2009 Shape and vibration control of a smart composite plate with matrix cracks. *Smart Materials and Structures*, *18*, 025002. <http://dx.doi.org/10.1088/0964-1726/18/2/025002>
- [107] Balamurugan V and Narayanan S 2010 Finite element modeling of stiffened piezolaminated plates and shells with piezoelectric layers for active vibration control. *Smart Materials and Structures*, *19*, 105003. <http://dx.doi.org/10.1088/0964-1726/19/10/105003>
- [108] Chandrashekhara M and Ganguli R 2010 Nonlinear vibration analysis of composite laminated and sandwich plates with random material properties. *International Journal of Mechanical Sciences*, *52*, 874–891. <http://dx.doi.org/10.1016/j.ijmecsci.2010.03.002>
- [109] Yiming F Sheng L and Yejie J 2010 Nonlinear active vibration control of piezoelectric laminated plates considering interfacial damage effects. *Journal of Vibration and Control*, *16*, 1287–1320. <http://dx.doi.org/10.1177/1077546309339442>
- [110] Farhadi S and Hosseini-Hashemi S H 2011 Active vibration suppression of moderately thick rectangular plates. *Journal of Vibration and Control*, *17*, 2040–2049. <http://dx.doi.org/10.1177/1077546310395962>
- [111] Kerur S B and Ghosh A 2011 Active control of geometrically nonlinear transient response of smart laminated composite plate integrated with AFC actuator and PVDF sensor. *Journal of Intelligent Material Systems and Structures*, *22*, 1149–1160. <http://dx.doi.org/10.1177/1045389X11414222>
- [112] Sarangi S K and Ray M C 2011 Active damping of geometrically nonlinear vibrations of laminated composite plates using vertically reinforced 1-3 piezoelectric composites. *Acta Mechanica*, *222*, 363–380. <http://dx.doi.org/10.1007/s00707-011-0531-x>
- [113] Dash P and Singh B N 2012 Geometrically nonlinear free vibration of laminated composite plate embedded with piezoelectric layers having uncertain material properties. *Journal of Vibration and Acoustics*, *134*/061006 1–13.
- [114] Her S and Lin C 2013 Vibration analysis of composite laminate plate excited by piezoelectric actuators. *Sensors*, *13*, 2997–3013. <http://dx.doi.org/10.3390/s130302997>
- [115] Bletzinger K U Bischoff M and Ramm E 2000 A unified approach for shear-locking free triangular and rectangular shell finite elements. *Computers & Structures*, *75*, 321–334. [http://dx.doi.org/10.1016/S0045-7949\(99\)00140-6](http://dx.doi.org/10.1016/S0045-7949(99)00140-6)
- [116] Nguyen-Thoi T Phung-Van P Nguyen-Xuan H and Thai-Hoang C 2012 A cell-based smoothed discrete shear gap method using triangular elements for static and free vibration analyses of Reissner-Mindlin plates. *International Journal for Numerical Methods in Engineering*, *91*, 705–741.
- [117] Phung-Van P Nguyen-Thoi T Le-Dinh T and Nguyen-Xuan H 2013 Static and free vibration analyses and dynamic control of composite plates integrated with piezoelectric sensors and actuators by the cell-based smoothed discrete shear gap method (CS-FEM-DSG3). *Smart Materials and Structures*, *22*, 095026. <http://dx.doi.org/10.1088/0964-1726/22/9/095026>
- [118] Shivakumar J Ashok M H and Ray M C 2013 Active control of geometrically nonlinear transient vibrations of laminated composite cylindrical panels using piezoelectric fiber reinforced composite. *Acta Mechanica*, *224*, 1–15. <http://dx.doi.org/10.1007/s00707-012-0724-y>
- [119] He X Q Ng T Y Sivashanker S and Liew K M 2001 Active control of FGM plates with integrated piezoelectric sensors and actuators. *International Journal of Solids and Structures*, *38*, 1641–1655. [http://dx.doi.org/10.1016/S0020-7683\(00\)00050-0](http://dx.doi.org/10.1016/S0020-7683(00)00050-0)
- [120] Liew K M He X Q Ng T Y and Sivashanker S 2001 Active control of FGM plates subjected to a temperature gradient: Modelling via finite element method based on FSDT. *International Journal for Numerical Methods in Engineering*, *52*, 1253–1271. <http://dx.doi.org/10.1002/nme.252>
- [121] Ootao Y and Tanigawa Y 2001 Control of the transient thermoelastic displacement of a functionally graded rectangular plate bonded to a piezoelectric plate due to non-uniform heating. *Acta Mechanica*, *148*, 17–33. <http://dx.doi.org/10.1007/BF01183666>
- [122] Liew K M He X Q Ng T Y and Kitipornchai S 2003 Finite element piezothermoelasticity analysis and the active control of FGM plates with integrated piezoelectric sensors and actuators. *Computational Mechanics*, *31*, 350–358.
- [123] Huang X L and Shen H S 2006 Vibration and dynamic response of functionally graded plates with piezoelectric actuators in thermal environments. *Journal of Sound and Vibration*, *289*, 25–53. <http://dx.doi.org/10.1016/j.jsv.2005.01.033>
- [124] Kargarnovin M H Najafizadeh M M and Viliani N S 2007 Vibration control of a functionally graded material plate patched with piezoelectric actuators and sensors under a constant electric charge. *Smart Materials and Structures*, *16*, 1252–1259. <http://dx.doi.org/10.1088/0964-1726/16/4/037>
- [125] Reddy B A and Ray M C 2007 Optimal control of smart functionally graded plates using piezoelectric fiber reinforced composites. *Journal of Vibration and Control*, *13*, 795–814. <http://dx.doi.org/10.1177/1077546307075574>
- [126] Mallik N and Ray M C 2003 Effective coefficients of piezoelectric fiber-reinforced composites. *AIAA Journal*, *41*, 704–710. <http://dx.doi.org/10.2514/2.2001>
- [127] Ebrahimi F and Rastgo A 2008 A free vibration analysis of smart FGM plates. *International Journal of Aerospace and Mechanical Engineering*, *2*, 94–99.
- [128] Ebrahimi F Rastgoo A and Kargarnovin M H 2008 Analytical investigation on axisymmetric free vibrations of moderately thick circular functionally graded plate integrated with piezoelectric layers. *Journal of Mechanical Science and Technology*, *22*, 1058–1072.
- [129] Ohadi A R and Fakhari V 2008 Nonlinear vibration control of FGM plate with piezoelectric sensor/actuator layers under thermal gradient and mechanical load. *15th International Congress on Sound and Vibration*, Daejeon, Korea.
- [130] Ebrahimi F and Rastgoo A 2009 Nonlinear vibration of smart circular functionally graded plates coupled with piezoelectric layers. *International Journal of Mechanics and Materials in Design*, *5*, 157–165. <http://dx.doi.org/10.1007/s10999-008-9091-1>
- [131] Ebrahimi F Naei M H and Rastgoo A 2009 Geometrically nonlinear vibration analysis of piezoelectrically actuated FGM plate with an initial large deformation. *Journal of Mechanical Science and Technology*, *23*, 2107–2124.
- [132] Panda S and Ray M C 2008 Active constrained layer damping of geometrically nonlinear vibrations of functionally graded plates using piezoelectric fiber-reinforced composites. *Smart Materials and Structures*, *17*, 025012. <http://dx.doi.org/10.1088/0964-1726/17/2/025012>
- [133] Panda S and Ray M C 2009 Active control of geometrically nonlinear vibrations of functionally graded laminated composite plates using piezoelectric fiber reinforced composites. *Journal of Sound and Vibration*, *325*, 186–205. <http://dx.doi.org/10.1016/j.jsv.2009.03.016>
- [134] Xia X K and Shen H S 2009 Nonlinear vibration and dynamic response of FGM plates with piezoelectric fiber reinforced composite actuators. *Composite Structures*, *90*, 254–262. <http://dx.doi.org/10.1016/j.compstruct.2009.03.018>
- [135] Hashemi H Eshaghi M and Karimi M 2010 Closed-form vibration analysis of thick annular functionally graded plates with integrated piezoelectric layers. *International Journal of Mechanical Sciences*, *52*, 410–428. <http://dx.doi.org/10.1016/j.ijmecsci.2009.10.016>
- [136] Fakhari V and Ohadi A 2010 Nonlinear vibration control of functionally graded plate with piezoelectric layers in thermal environment. *Journal of Vibration and Control*, *17*, 449–469. <http://dx.doi.org/10.1177/1077546309354970>
- [137] Yiqi M and Yiming F 2010 Nonlinear dynamic response and active vibration control for piezoelectric functionally graded plate. *Journal of Sound and Vibration*, *329*, 2015–2028. <http://dx.doi.org/10.1016/j.jsv.2010.01.005>
- [138] Fakhari V Ohadi A and Yousefian P 2011 Nonlinear free and forced vibration behavior of functionally graded plate with piezoelectric layers in thermal environment. *Composite Structures*, *93*, 2310–2321. <http://dx.doi.org/10.1016/j.compstruct.2011.03.019>

- [139] Shirazi A H N Owji H R and Rafeeyan M 2011 Active vibration control of an FGM rectangular plate using fuzzy logic controllers. *Procedia Engineering*, 14, 3019–3026.
- [140] Ebrahimi F 2013 Analytical investigation on vibrations and dynamic response of functionally graded plate integrated with piezoelectric layers in thermal environment. *Mechanics of Advanced Materials and Structures*, 20, 854–870. <http://dx.doi.org/10.1080/15376494.2012.677098>
- [141] Jadhav P A and Bajoria K M 2013a Active vibration control of piezoelectric metal based fgm plate subjected to electro-mechanical loading using finite element method. *International Journal of Mechanics and Solids*, 8, 1–20.
- [142] Jadhav P A and Bajoria K M 2013b Free and forced vibration control of piezoelectric FGM plate subjected to electro-mechanical loading. *Smart Materials and Structures*, 22, 065021. <http://dx.doi.org/10.1088/0964-1726/22/6/065021>
- [143] Jodaei A Jalal M and Yas M H 2013 Three-dimensional free vibration analysis of functionally graded piezoelectric annular plates via SSDQM and comparative modeling by ANN. *Mathematical and Computer Modelling*, 57, 1408–1425. <http://dx.doi.org/10.1016/j.mcm.2012.12.002>
- [144] Talabi M R and Saidi A R 2013 An explicit exact analytical approach for free vibration of circular/annular functionally graded plates bonded to piezoelectric actuator/sensor layers based on Reddy's plate theory. *Applied Mathematical Modelling*, 37, 7664–7684. <http://dx.doi.org/10.1016/j.apm.2013.03.021>



Aligned Discontinuous Fibre Composites: A Short History

MATTHEW SUCH*, CARWYN WARD and KEVIN POTTER

Advanced Composites Centre for Innovation and Science, Queens Building, University of Bristol, Bristol, BS8 1TR, UK

KEYWORDS

composite materials
discontinuous
short fibre
alignment

ABSTRACT

The most popular methodologies employed to manufacture composite components still lack sufficient rate to meet demand. Furthermore, the state of the art in automated processes imposes restrictions on component geometrical complexity. Many of these restrictions arise directly as a result of the use of continuous fibre reinforcements. Processing and use of highly-aligned discontinuous fibres may avoid many of the manufacturing defects induced in continuous fibre architectures, which are a result of design decisions and manipulations during processing operations, while theoretically allowing for similar mechanical properties if alignment and orientation are tightly controlled. An overview of the history of aligned short fibre composites has been presented, with the focus upon process and application of highly aligned advanced composites with properties near to that of continuous fibre composites. When continuous carbon fibres were first developed, there remained an interest to create aligned discontinuous fibre composites in order to form more complex components. This interest has reappeared in recent years with methods divided into those which align short fibres and those which introduce discontinuities into aligned fibres. It is clear that discontinuous material systems have their uses and applications, but greater development is still required in order to better quantify and categorise the materials and their associated properties and processes.

© 2014 DEStech Publications, Inc. All rights reserved.

1. INTRODUCTION

The mantra of “Bigger, Faster, Cheaper” is an increasingly highlighted requirement for composites manufacturing; bigger size and production volume, faster production rate, and all for a cheaper price [1] without impacting on quality (rather improving on it). Quality in this instance refers to assuring low variability in the manufacturing process. Within the automotive sector the need for vehicle light-weighting may be answered by increased use of composites materials but this requires vastly improved productivity. The generally adopted automated methods do not yet meet demanded lay-up rates, largely hindered by the delays in areas such as quality inspection, and the use of continuous fibre architectures can lead to numerous induced defects. Discontinuous

fibre architectures are currently employed in non-loadbearing structures with random alignment in both thermoset and thermoplastic matrices in order to attempt to meet production volume, but with heavily reduced properties owing to the lack of alignment (such as [2]). There is certainly a great potential for highly aligned short fibre composites to enter production within an automotive basis if they provide the ability to meet productivity targets without significant reductions in material properties [3].

The price of composite materials remains very restrictive for low value, high volume production and the variability of the material as supplied, in terms of mass distribution and fibre waviness [4], translates to designs being more conservative—meaning a greater volume of material is needed. Material supply could soon be an issue as there is a growing demand for carbon fibre in a number of markets with forecasts predicting upwards of 100,000 metric tonnes required for 2020 [5]. It is predicted that while aerospace and

*Corresponding author. E-mail: Matthew.Such@bristol.ac.uk,
Tel : +44-(0)117-331-5769

consumer markets will experience predictable growth, the industrial sector, which includes automotive, will see rapid growth. Analysts predict that the widespread use of composite materials relies on a heavily reduced price for carbon fibre to around \$10/kg or lower [6]. For example the ability of BMW to deliver the i3 body panels at the production rate and cost that it has achieved is due, in part, to securing raw material supply and to increasing rates of automation via novel preforming and stamp/infusion forming. In order to meet the future demand, carbon fibre precursors will need to be found from alternative sources rather than petrochemical, and for automotive needs lignin based precursors may be more suitable, although the derived fibres currently lack desired properties. Materials will also have to have a greater degree of multifunctionality—to do more with less.

The major drivers for employing discontinuous composites thus revolve around the ability to increase productivity by utilising forming methods unavailable to continuous fibre composites, changing design criteria to allow geometrical complexity, increasing fibre hybridisation by intermingling a larger array of fibre types to tailor material properties for greater ductility or stiffness retention, and increased sustainability by aligning recycled and reclaimed fibres in non-loadbearing cases. The application of discontinuous fibre composites could be considered an enabling technology for low value, high volume production, as it will help increase productivity without having too great a shift on the current manufacturing landscape. Conversely, it could be seen as a disruptive technology for high value, low volume production where it will impact design choices but may enable the incorporation of multifunctional materials.

This paper overviews the history of aligned short fibre composites and their applications, the focus being upon highly aligned advanced composites with properties near to that of continuous fibre composites, neglecting those methods which do not provide sufficient alignment. The aim of the paper is to steer the development and use of aligned discontinuous fibre composites, by unifying current work and highlighting required development routes. It concentrates on process development and applications rather than reporting mechanicals by type in detail as this is beyond the scope of the review (evidence within this work suggests further work is needed in this area).

2. DISCONTINUOUS MATERIALS

Much of the early work in advanced composites focused on the development of materials incorporating natural fibres, which by their very nature are discontinuous, within a polymeric matrix. Gordon-Aerolite [7] is an example of this, which utilised flax fibre within phenolic resin. It was realised early on that in order to derive the best performance from a composite, a high degree of fibre alignment was needed. Within the UK, research led by J.E. Gordon at the Explo-

sives Research and Development Establishment (ERDE), developed several alignment processes while working on novel structural materials. A drive for stiffer fibres resulted in the development of ceramic whiskers and filaments, with alignment moving away from random mat. Eventually the production of continuous carbon fibres in the 1960's saw unidirectional and woven fabrics gain popularity. As fibres transitioned to continuous forms, interest was apparently lost in developing alignment mechanisms and using discontinuous material. However, as highlighted by McMullen [8] in 1984, short fibre composites offered improved drapeability and allowed for a greater degree of hybridisation than their continuous fibre rivals. There has been a resurgent interest in discontinuous materials over recent years with a number of processing methods being reported in open literature. Had these methods been available prior to the development of continuous fibre it could be suggested to be a more advanced field than it stands today. The hierarchy of discontinuous fibre composites, as reviewed, is shown in Figure 1. The dashed box highlights those methods which have been reviewed, other discontinuous methods which exist do not impart enough alignment, utilise long fibre lengths (> 200 mm), or both. Both thermoset and thermoplastic matrices are considered.

In order to achieve aligned discontinuous fibres a number of methods and processing methodologies have arisen over time, with a clear divide in approaches between methods which introduce discontinuity into virgin fibres via breaking and slicing, and those which attempt to align short fibres (< 100 mm) through a number of fluid, acoustic, electric, or mechanical mechanisms. The prior has a much more commercial focus with alignment being present from the outset, and introduced discontinuities providing enhanced manufacturing capabilities via faster forming operations. The latter has the potential to utilise short fibres from a variety of sources, and it is thought that future developments will enable recycled materials to be utilised, as well as hold the ability to intermingle fibres for hybridisation. The ability to create hybrid composites may serve to be beneficial and alleviate many of the problems currently encountered with the brittle nature of continuous carbon fibre composites. It may also enable multifunctional capabilities, including those outlined by Gibson [9]. Hybrid composites generated a lot of interest in the 1970's and 1980's in order to further understand the synergistic hybrid effect. Many properties deviate from a simple rule of mixtures and hybridisation can lead to increased ductility, important as composites seek to advance beyond the elastic limits often associated to the material class. Swolfs *et al.* [10] recently review fibre hybridisation and discussed the growing trend of pseudo-ductility. Intermingling of different fibre types may lead to more effective load distribution by introducing a small amount of high modulus carbon fibres alongside high strength carbon fibres. When compared with continuous fibre composites, these dif-

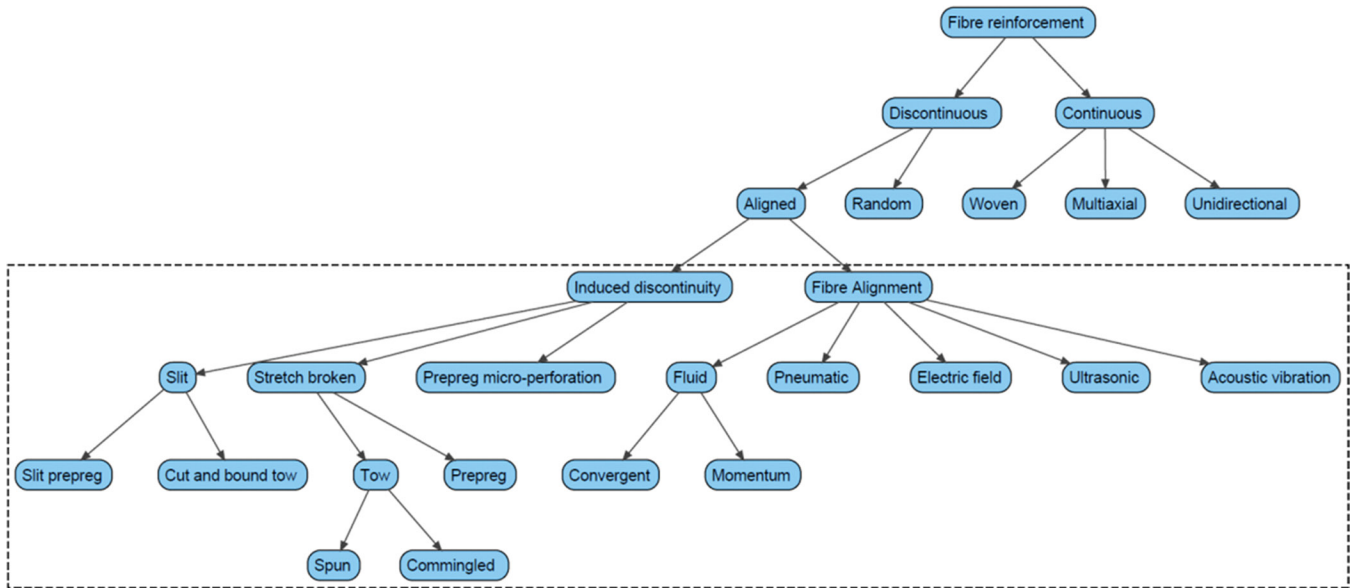


Figure 1. Scope of reviewed methods within the paper.

ferences should lead to a decrease in process costs as well as an increase in flexibility.

2.1. Fiber Alignment Processes

A number of processes exist within the textile industry for the alignment of short fibres. These techniques, such as carding, have limited applicability within an advanced composites environment; suffering from numerous restrictions due to non-homogenous packing and insufficient alignment [11]. The dominant mechanisms of alignment therefore involve utilising a carrier fluid to induce fibre alignment with a converging flow.

One of the earliest reported methods in open literature, was developed in the early 1960’s; it was an alginate process to align whiskers of silicon carbide [12]—a fibre suspension (whiskers mixed within a few percent of ammonium alginate in water) was extruded through a precipitating bath before being wound onto a drum and then washed and dried. This

technique is however somewhat hampered by the slow carrier fluid removal, and a restricted volume fraction. A development of the technique, using similar convergent fluid principles, is the ERDE glycerine technique. Bagg *et al.* [11] investigated the alignment of fibres and whiskers by the use of this process, and an overview of the set-up is shown in Figure 2, similarly within US Patent 3,617,437 [13]. It involved suspending asbestos, and later carbon, fibres within a glycerine solution bath which was deposited onto a flat gauze filter bed with a pump to remove the carrier fluid, via a reciprocating tapered profile nozzle. Excess glycerine was then washed off and a heater used to dry the mat, and matrix infusion was subsequently carried out.

Salariya and Pittman [14] used the technique to prepare aligned discontinuous prepreps, and provided a thorough analysis to assist in the design and operation of the process. In comparison to earlier work by Kacir *et al.* [15-19], a higher degree of alignment was achieved by use of single carbon fibres rather than glass fibre bundles. It was concluded that

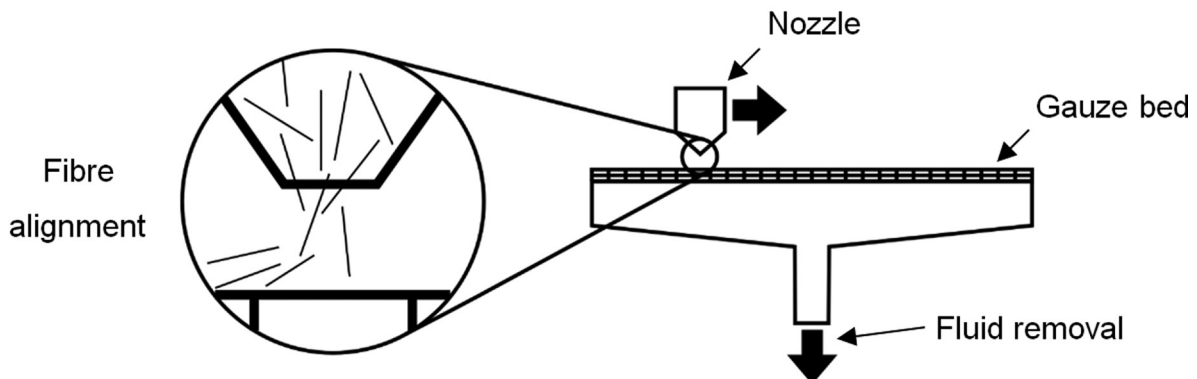


Figure 2. Glycerine process overview.

shorter fibres suffered from less alignment loss on exiting the nozzle. The problem with the work as reported is the low volume fraction of the fibres in the resulting preform. As with many reviewed methods, large reductions were noted in strength with a lesser reduction in stiffness, when compared to continuous fibre composites. One of the biggest difficulties encountered with the glycerine process, which imposes a restriction on the productivity of the process as well as preform thickness, is successful removal of the carrier fluid without causing fibre misalignment. Allan *et al.* [20] utilised shear controlled orientation in order to align short fibres during injection moulding. Building on previous work by Allan and Bevis [21], a quadruple live-feed moulding device was able to control macroscopic shears to induce fibre alignment. This orientation controlled injection moulding allowed greater part quality, with reduced variability in stiffness and strength in comparison to conventional moulding techniques, but the process has somewhat limited application to simple components with strongly anisotropic requirements.

An evolution of the glycerine process, arising in the 1970's, to more efficiently remove carrier fluid is the centrifugal alignment process as presented by Edwards and Evans [22]. An overview of the set-up is shown in Figure 3, similarly within US Patent 4,016,031 [23]. In this process alignment was achieved by spraying a fibre suspension (again utilising glycerine as a carrier fluid) through a tapered nozzle directed at a rotating mesh cylinder, with fluid removed via an outlet, in order to create a fibre mat. The technique was able to produce aligned carbon, glass, and hybrid fibre mats, with improved fibre alignment compared to the glycerine method as evident from material performance testing. A vacuum drum filter technique [24] was also developed at a similar time, and involved depositing the fibre suspension onto a rotating vacuum drum filter in order to again create an aligned fibre mat. As previously, this highlighted the ability to use short fibres for hybrid materials and the potential to utilise recycled material. The drawbacks are the limited production rate of a batch process, and limited production size that was dependent on the centrifuge dimensions.

Friedrich *et al.* [25] investigated the static and fatigue properties of discontinuous fibres reinforcing two thermoplastic matrix systems of polyimide and polyethersulphone, prepared by the vacuum drum filter technique reported previously by Richter [24]. It was observed that the failure mechanisms were similar in nature to continuous fibre composites; however there were far more crack initiation sites owing to an increased number of available fibre ends. The UK's MoD reportedly licensed their alignment technology to both Klinger and Technical Fiber Products Ltd to create 'Highform' and 'Disco' respectively, which suffered from reduced properties alongside improved formability [26–27]. Flemming *et al.* [28] investigated a highly aligned discontinuous carbon fibre thermoplastic prepreg produced by Technical Fiber Products Ltd, most probably the 'Disco' material but this is not confirmed. The process involved mixing carbon and thermoplastic fibres in a fluid before passing them through nozzles onto a sloping rail and then onto a rotating cylindrical mandrel. Unfortunately while the statistics reported fibre alignment of $\pm 4^\circ$ it is evident from the supplied micrograph and histogram that fibre alignment was actually over a greater range. It is noted that both Highform and Disco failed to commercialise successfully and were discontinued in the mid-1990's, somewhat attributed to processing difficulties, though research on available stock clearly continued for a short period afterwards.

A number of alignment processes involving pneumatic alignment have been reported in literature. It originates from techniques used to create random mat composites providing low levels of alignment involving chopping and spraying fibres to create preforms, dating back to circa 1950. Ericson and Berglund [29] oriented discontinuous glass fibres within a thermoplastic matrix to produce oriented glass-mat-reinforced thermoplastics (GMT) components. Glass was fed through a rotating cutter and mixed with thermoplastic powder and then blown onto a perforated steel sheet via orientation plates. The process had the advantage of being net shape, with accompanying low scrap rates, but suffered from a lack of alignment. The P4 process ('Programmable Powder

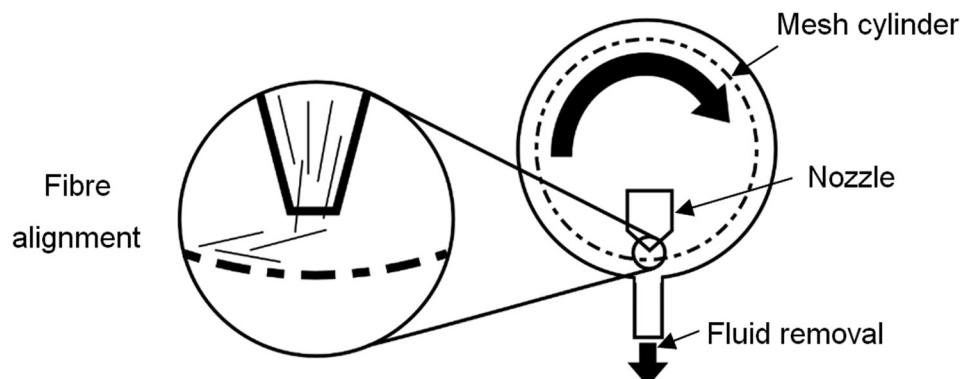


Figure 3. Centrifuge process overview.

Preform Process'), was developed to achieve a greater degree of alignment in fibreglass preforms in the early 1990's by a similar process [30]. It was later developed to create carbon fibre preforms for aerospace (P4-A) as investigated by Rondeau *et al.* [31], with reference to the effect of varying tow size on mechanical properties. It concluded that a better tensile strength was attained by smaller diameter carbon fibre tows which have accompanying lower stress concentrations. During the transition of the process there were a number of difficulties reported, relating to problems with chopping and dispersion of carbon tows, effectively leading to a reduced throughput in comparison to glass (500 g/min instead of 1900 g/min respectively) [32]. Reeve *et al.* [33] investigated the mechanical property translation in the P4-A process, concluding that there is a future potential for use in aerospace structures due to acceptable percentages of stiffness and strength retention.

Harper *et al.* [34] investigated the feasibility for alignment in the Directed Carbon Fiber Preforming (DCFP) process. Chopped carbon fibres and powdered binder are sprayed through a robot mounted convergent nozzle onto a shaped and perforated tool, to create a solid preform, which is later infused to produce the component. The motion of the robot in combination with the nozzle contributes to the alignment of the deposited fibres. This is somewhat analogous to the convergent fluid flow in the glycerine process. The alignment of different fibre lengths (28, 58, and 115 mm) was measured alongside mechanical properties and it was found that fibre length, tow size, and preform thickness have an effect on the level of alignment. It was noted that bundles of fibres were much easier to align, in contrast to the glycerine method, but generally more difficult to impregnate with resin. The dry alignment techniques suffer from restrictions on minimum fibre length and productivity of batch processes, but successful demonstration of applications with recycled carbon fibre has also been made [35].

Shotton-Gale *et al.* [36] reported on two techniques under development to create discontinuous aligned preregs, namely, an acoustic vibration method and a fibre chopper delivery system. The fibre chopper method involved chopping E-glass fibres roughly 7mm in length immediately prior to deposition onto a variable-speed conveyor belt with an adhesive substrate. The acoustic vibration method used a speaker unit to encourage alignment in 4.5 mm E-glass fibres as they passed along two flutes, prior to deposition onto a resin substrate. Neither method achieved the desired level of orientation or property retention. Vyakarnam and Drzal [37–38] experimented with aligning fibres by the use of an electric field to align dry fibres in a continuous process but the achieved orientation is again lacking. Scholz *et al.* [39] used ultrasonic assembly to align milled glass fibres, wherein a standing acoustic wave manipulates reinforcing particles to pressure nodes. It is thought that the development of such a process will lead to a wider range of possible

fibre architectures, but it is currently hampered by volume fraction and alignment issues.

Many of the methods within the literature align tows as opposed to individual fibres. From this a strength reduction is witnessed due to the required increase in critical fibre length, and the greater size of the discontinuity at the tow ends compared to a fibre. That is to say, a short fibre tow has an increased diameter compared to a single fibre, thus requiring a longer critical length to maximise the stress transfer capability. Therefore the methods which align singular fibres, compared to tows, appear to be more beneficial. This may create future process requirements to separate tows reclaimed from reused or recycled materials (in order to maximise the resulting material strength in order to utilise fibres from larger tows while standardising produced ply thickness). Such processes appear to offer the best route to include hybrids/multifunctionality at the fibre level, but depending on the type it may not be cost effective to do so. Hence tow/fabric level incorporation may need to be targeted as a route to incorporation, although this appears largely by spray processes, and this could reduce the available material options.

The problem with most of the fluid methods is the restricted productivity due to batch processing or carrier fluid removal stages, whereas other alignment techniques suffer from lack of alignment and consequently low fibre volume fraction. Yu *et al.* [40–42] have recently reported on a new wet method (HiPerDiF) which aligns fibres via the momentum change of a fibre suspension in water impacting a plate. It is a continuous process which utilises water as a low viscosity carrier fluid, and therefore has the potential for an increased production rate over glycerine based processes, due to the relatively shorter time needed to remove the carrier fluid. It has demonstrated very high alignment and property retention figures in comparison to other reported continuous alignment techniques. A similar water borne technique has been recently reported by [43], which targets recycled materials commingled with cellulose, although producing a more random mat form. Interestingly in this process phenolic resin could be used in the water as a suspension that on drying will act as a tacifier, and which in principle could be used to create core materials amongst others, although early results suggest development of the mechanical properties of the products are required.

2.2. Induced Discontinuity Processes

A number of different methods have been utilised in order to introduce discontinuities into unidirectional prepreg or fabric. Stretch breaking is a process normally used in the textile industry to shorten natural fibres prior to spinning. An overview of the set-up is shown in Figure 4, similarly within European Patent 0,272,088 [44]. The process involves tensioning a tow between rollers and randomly breaking with lateral deflection by using breaker bars or rollers running

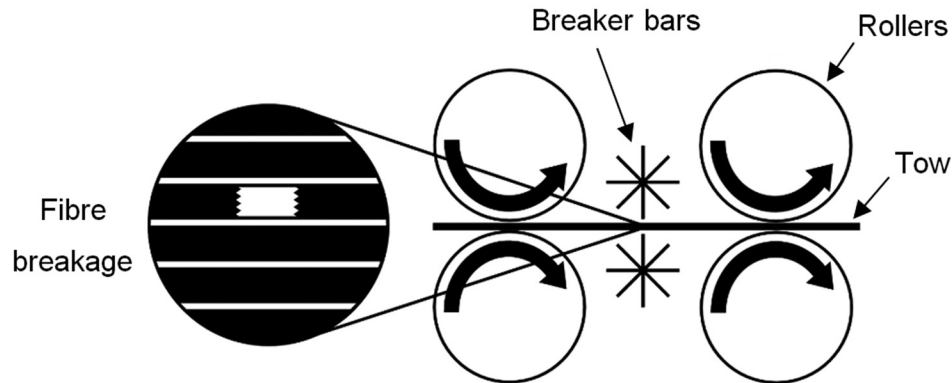


Figure 4. Stretch breaking overview.

at different speeds. In the late 1980's DuPont adapted the stretch breaking technology to produce discontinuous carbon fibres with random lengths between 25 and 150mm. Okine *et al.* [45–46] reported tensile stiffness and strength property retention of 100% for stretch broken AS4-carbon within an amorphous polyamide copolymer matrix. If the process did produce formable thermoplastics with 100% property retention then it is surprising that this did not translate to widespread use, and begs the question of which other factors of importance should be reported and discussed within literature. Elsewhere, Chang and Pratte [47] reported property retention of 96% for stretch broken AS4-carbon within a polyetherketoneketone (PEKK) matrix, and used the system to prepare a demonstrator wing rib for a Bell Helicopter V-22. With process development, the LDF (Long Discontinuous Fiber) Thermoplastic Composite Technology was sold by DuPont but never really gained a foothold in the market, due to difficulties with processing relating to high peak and yield stresses, and the materials were withdrawn in 1993 [26]. Perhaps a renewed interest will appear with stretch broken thermoplastic forms, as thermoplastic composites should be expected to become used more widely in high volume manufacturing.

A similar process has been under development by Hexcel in the US since the late 1990's to create SBCF (Stretch Broken Carbon Fiber) with support from a number of industrial partners including Boeing Integrated Defense Systems, Northrop Grumman, and the Applied Research Laboratory. The development of SBCF has been widely reported within a very short timeframe in SAMPE conferences, including efforts to generate material characterisation data alongside application examples [48]. In 2002, initial development led to an average broken filament length of 100 mm which proved beneficial with respect to continuous fibres for forming. In an effort to attain greater formability, a second generation of SBCF was developed with an average filament length of 70mm; and further size reductions lead to a 50 mm average [49]. The focus in recent years has been to develop a system utilising IM7/8552 to find applications in US Navy aircraft

programs [50]. Jacobsen [51–52] has reported on properties when stretched at the prepreg level, to retain high properties and alignment.

Dillon and Barsoum [53] reported on the developments for automated forming of SBCF materials, by understanding the uniaxial and biaxial response with varying temperature and pressure; and related works on forming a demonstrator fairing [54]. The work touched upon the difficulty of processing IM7 fibres, in respect to AS4, due to the lower strain response. Renieri *et al.* [55] echoes a similar point while investigating forming of hemi-ellipsoids—that the SBCF AS4 fibre is much more readily formable, and a material with a shorter broken fibre length is more useful. Munro *et al.* [56] investigated the formability of SBCF in order to understand time and rate dependence of the material, both analytically and experimentally. At high extension rates substantial deformation is accompanied by visual damage. Work undertaken in conjunction with Albany Engineered Composites has created the pi preform woven SBCF which can be used to preform complex geometry components and frames [57–58]. Current comparisons between SBCF and continuous materials rely on a range of test geometries, but fail to quantify laminate wrinkling or the resulting property reduction [59]. The material is thought to have a promising future, at least within literature, but it is unclear exactly if it has transferred into use for the US DoD systems for which it was identified [60].

Other stretch broken techniques have been developed by competitors, but appear to be much less widely reported. These include the Courtaulds Heltra process, with products marketed under the trade names Graftix and Filmix (0.1K tow spun cut-staple carbon fibres is co-spun with Polyether ether ketone, PEEK, to produce a highly formable yarn) [61]. A similar process developed in recent years is the spun carbon tow by Pharr Yarns, a ~1K tow spun from a stretch-broken 50K tow [62], with the possibility of being spun into a hybrid material. It has seen use in consumer goods including hockey sticks and bicycles. TPFL developed by Schappe is a stretch broken commingled carbon fibre/PEEK yarn

[63], stretch broken from 12K or 24K tow, and spun to yarns of 1K, 3K, or 6K tow. The material has found use in the consumer market within the Mantis HE electric golf caddy. Other forms of Schappe material are known to be available, such as slivers and stitching yarns, but they do not appear to be reported on in the literature. As identified by Creasy [64], in order to avoid high stresses when forming, the broken fibre length needs to be as small as possible but with widely distributed breaks (possibly done by a prior crimping process) to influence breaking zones and broken fibre length. There needs to be tighter control over the fibre domain to reduce drawing stresses.

Pepin Associates Inc. [65–66] has developed DiscoTex over a number of years, which is a discontinuous composite reinforcement offering enhanced formability. The fabric is created by assembling discrete lengths of tows with a soluble binder; has entered into Boeing's Material Specification Database, and can be used in a range of complex components that Boeing uses. Due to its entry into this database it has undergone a strict regime of testing for verification. The system has also been evaluated for use in composite patch preform repair [67] where it is well suited due to its high formability characteristics. Another recent product by Pepin Associates is DiscoTape, which is an aligned discontinuous unidirectional tape with a “brick-like pattern” [68]. Despite being investigated to form radomes, little other open literature appears available on it.

Recent work undertaken by Li *et al.* [69] introduced angled slits into prepreg in order to create Unidirectionally Arrayed Chopped Strand (UACS) laminates. This is a continuation of work undertaken by Taketa *et al.* [70–72]. The slit pattern used has an effect on the elastic properties as well as the material's flowability (and potentially local quality impacts for characteristics such as compaction behaviour). These methods, by which discontinuities are introduced into virgin prepreg, allow for good retention of stiffness, but suffer from a large reduction in strength and remove much of the value from the material in order to ease the draping process. DForm [73] developed by Cytec is similarly a slit prepreg for increased formability, but owing to the large strength reduction noticed from the slit process it is used and marketed as a material for complex geometry moulds. Although slit methods offer a high control of alignment and volume fraction, the slits introduce a much larger knockdown. Further process refinement may help reduce this to more desirable levels.

The PERFORM process [26,74] developed by IMT involves micro-perforation of a UD prepreg by laser drilling an array of holes 0.05 to 0.25 mm in diameter. This has the effect of controlled fibre length, alignment, and volume fraction. Some stretch broken processes by contrast can suffer losses on all accounts during impregnation, as there are control problems associated with impregnating a discontinuous tow dependent on the process, although these processes can

also occur at the prepreg level. Also highlighted is the ability to target regions where formability is required and laser drilling only those sections. Matthams and Clyne [75–76] investigated the properties of such a material. Stiffness had no discernible reduction which is in keeping with theory, however, tensile strength was reduced due to these inclusions. When compared with stretch broken systems there is a reduction in the stress needed to form parts, though direct comparisons are difficult through the literature as experimental procedures vary. PERFORM unfortunately represents another promising technology which has ceased to be reported in recent years, perhaps owing to lack of direct support from a major manufacturer for lengthy and costly certification processes. That said laser processing of composites for areas such as surface preparation for bonding do seem to continue to advance beyond other methods, and so it is likely the processing technique will remain in some form.

For induced discontinuity material, it is clear that the stretch broken materials are relatively successful, being that they are commercially available, but most seem to target or incorporate thermoplastic matrices by choice. Thermoset materials are in research; however most concentrate on the modification of continuous products. There are risks of knock downs in mechanical properties depending on the process used. The commercially available materials appear to be dominated by one or two suppliers and forms. This could change in the near future with the advent of recycled materials such as [77–78] becoming increasingly established, and it is suggested they could challenge the present scenario. Though not induced discontinuity forms per se, reforming virgin fibre selvage trim into spun tows and then into fabrics does show similarity to some of the techniques previously described. In terms of multifunctionality, as incorporated into the material, it is difficult to see how this is possible in these forms, and so should they be targeted for development further modifications will be required. This risks increasing costs and decreasing properties. That said, these forms will allow for multifunctionality to be incorporated as part of the lay-up process, although whether the combination will be better than a continuous material or offer significant advantages is debatable.

3. DISCUSSION

The literature surrounding the development of aligned short fibre materials spans several decades which can make direct comparisons between processes difficult, due to the methods by which data is presented, and the changes in properties of reinforcing fibres over that period. For example, over this period sporadic work appears to have been done in areas such as exploring and predicting elastic constant sensitivity to critical features [79–83], and failure methods [84–85]; however little to no work in comparing the various materials. The main issue appears to have been the existence

of a number of experimental obstacles to producing highly aligned discontinuous composites that could be accurately modelled. White and Abdin [86] and Papathanasiou *et al.* [87] are perhaps examples of this. It should be noted that predictive works for random fibre distributions have simultaneously continued [88–89] over the same timeframe. It could be argued that the difficulty in commercialising the products, along with the general shift to continuous product, negatively impacted on the materials keeping pace with general technology and fibre property developments.

As a result of this lack of clarity a chronological order of historic processes is proposed (though likely to be incomplete), and available in Figure 5, to begin to enable qualitative comparison between techniques with associated material data, as available, and shown in Table 1. Many historic processes reportedly offer better alignment though utilise a poorer quality fibre and so report reduced properties. For this reason effort has been made to compare property retention,

in strength and stiffness, to allow for variations in fibres and matrices. It is clear that future literature investigating discontinuous materials should acknowledge property retention for a wider array of properties, alongside listing aspect ratio and fibre alignment. If such a review is to also include hybrid requirements, then examples such as [90] should also be considered.

From the process literature sources it is shown that the convergent fluid processes failed to properly commercialise due to processing difficulties, although offered property retention and fibre lengths that were very agreeable. Then witnessed is a shift in alignment processes to longer fibres with pneumatic processes, and aspect ratios with accompanying large strength reductions, for the sake of high volume manufacturing. Numerous other alignment processes have been reported in academic literature, but these are lacking with respect to alignment and property retention. Induced discontinuity processes are commercially available in some forms

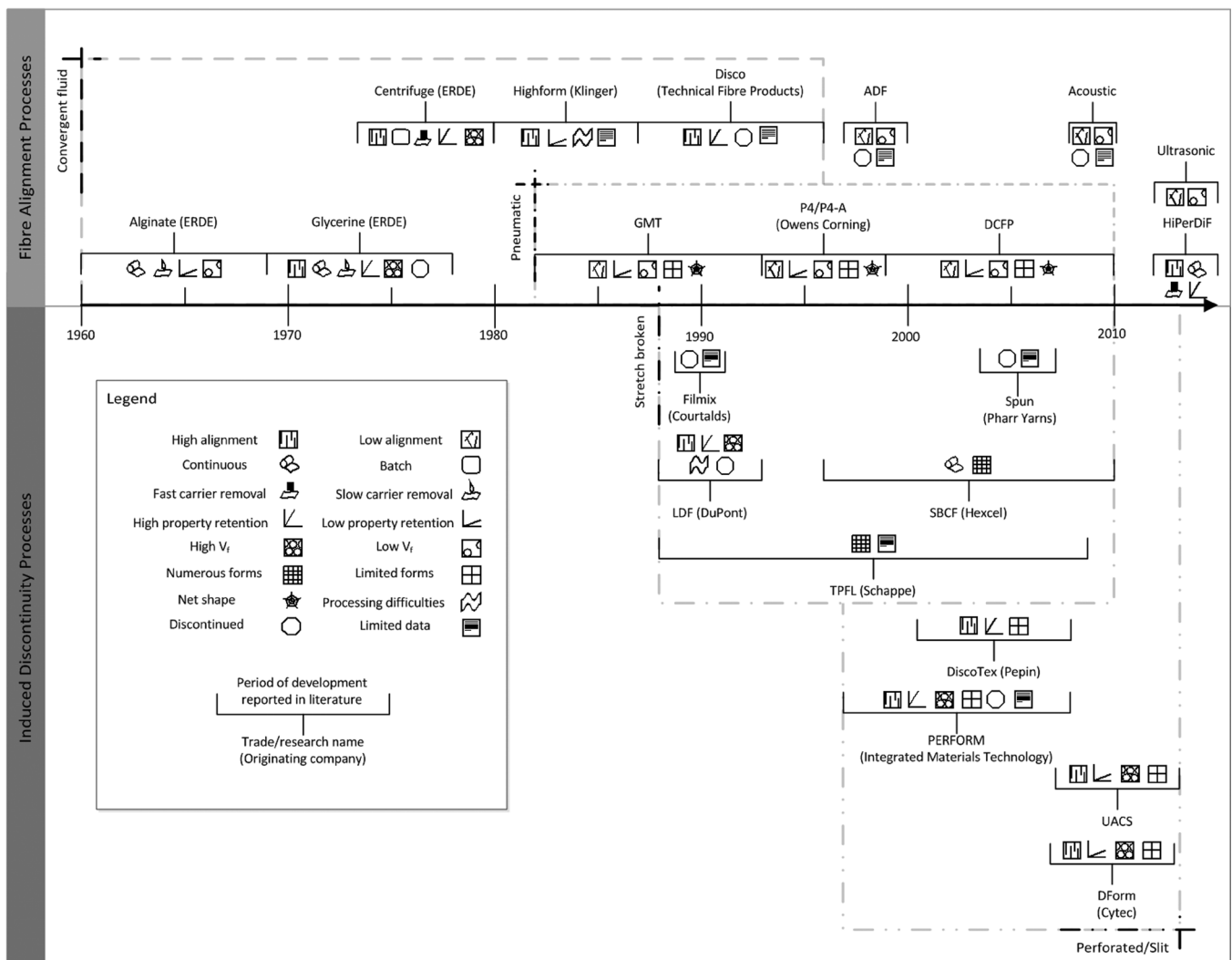


Figure 5. Timeline of aligned discontinuous material systems since 1960, qualitative comparisons with associated data in Table 1.

Table 1. Aligned Discontinuous Fiber Composite Material Comparisons to Those Processes Highlighted in Figure 5.

Method	Year	Matrix	Fibre	Type	Length (mm)	Alignment (°)	V _f (%)	E ₁ (GPa)	E _R (%)	σ ₁ (MPa)	σ _R (%)
LDF [45]	1987	PA	Carbon	Fiber	81.3	±5 (92%)	55	130	100	1696	100
SBCF [51]	2010	EP	Carbon	Prepreg	50		60	161	100	2625	94
DiscoTex [66]	2007	EP	Carbon	Tow	32			63	97	535	93
Centrifuge [22]	1980	EP	Carbon	Fiber	3		55	119	93	1211	85
Laser Drilled [75]	1999	PPS	Carbon	Prepreg	20–100		57	136	100	1500	82
Disco [28]	1996	PEI	Carbon	Fiber	3	±14 (100%)	50	100	94	1100	80
HiPerDiF [41]	2013	EP	Carbon	Fiber	3	±3 (80%)	55	115	91	1509	80
PERFORM [74]	2008	EP	Carbon	Prepreg	50			132	100	1546	78
UACS [69]	2013	EP	Carbon	Prepreg	25		60	49	97	500	68
Highform [45]	1987	PES	Carbon	Fiber	3.2	±5 (85%)	49	99	79	1000	60
Glycerine [15]	1978	EP	Glass	0.4K Tow	3.2–12.7	±15 (95%)	50	31	80	290	50
DForm [73]	2008	EP	Carbon	Prepreg	20–60			70	95	600	46
P4-A [30]	1999	EP	Carbon	3K-12K Tow	50.8–127		55	110	81	710	40
DCFP [34]	2008	EP	Carbon	6K, 24K Tow	28–115	±10 (21–94%)	35	55	85	293	31
Chopped [36]	2010	EP	Glass	Tow	7	±10 (78%)	48	27	62	300	25
Acoustic [24]	2010	EP	Glass	Tow	4.5	±10 (80%)	65	28	64	110	10
Vacuum Drum [24]	1980	EP	Carbon	Fiber	2–4		55	105		1200	
Vacuum Drum [25]	1985	PI/PES	Carbon	Fiber	3		55	91		955	
ADF [37]	1997	Nylon-12	Glass	0.2K, 0.4K Tow	3.2–25.4	±20 (70%)	40	17		225	
GMT [29]	1993	PE	Glass	Tow	25	±52 (100%)	15	3		38	
Ultrasonic [39]	2014	BisGMA/TEGDMA	Glass	Fiber	0.05		9	0.017		45	

Note: EP - epoxy, PA - polyamide, PI - polyimide, PES - polyethersulphone, PE - polyethylene, PEI - polyetherimide, PPS - poly-phenylene sulphide. Other fibre types and matrices are available for many of the methods. Length, alignment, fibre volume fraction, and elastic properties are supplied where reported. Data is ranked first by tensile strength retention (σ_R), then by stiffness retention (E_R), to account for different fibres and matrices.

but this has been through greater support in development from defence industry and government backing; owing to the fact they offered higher property retention although several products had noticeable processing difficulties. The effective aspect ratio of the reinforcement is critical for property retention, and formability within these induced discontinuity methods, as well as the random nature of stretch breaking processes, needs further refinement. The PERFORM process represents a system where the discontinuity can be targeted to increase formability in discrete regions, such as suggested in [91]. Above all else the key future technology is the development of a continuous process by which to produce highly aligned discontinuous carbon fibres with an aspect ratio and reinforcement volume fraction to allow for high processability and property retention. Multifunctionality should operate in collaboration with this top level need.

As in Figure 6, there exists a ‘sweet spot’ in which performance loss is acceptable for processability gains by using highly aligned short fibres. Unaligned short fibres can offer high processability in terms of volume and part complexity,

but lack performance, whereas continuous material forms do not utilise 100% of their properties when employed in complex geometries due to associated defect knockdowns, material variability, and design allowables. There are example processes that are perhaps beginning to explore such a relationship. A process recently developed by Toho Tenax entitled ‘Part via Preform’ involves creating a random strand sprayed preform and a placed preform of continuous fibre by automated fibre placement, which are brought together prior to resin transfer moulding [92]. Results are promising, but geometrical complexity is limited by the continuous tape placement. A modification of this process is being considered by the authors, which aims to use DCFP in conjunction with a highly novel tape placement process entitled ‘Continuous Tow Shearing’ [93–94] (that ultimately could be coupled up to the HiPerDiF process or enable hybrid materials use). Another process is Patch Preforming [95–96], whereby coupons of low areal weight or thermoplastic material are picked and placed to a tool according to a pre-programmed design for coupon architecture through the laminate. Al-

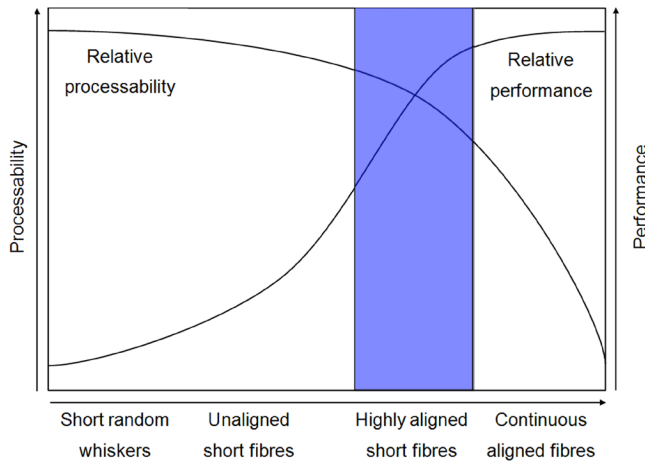


Figure 6. Performance and processability ‘sweet spot’ of highly aligned short fibres [44].

though such a process is not likely to be well suited to discontinuous materials such as SBCF it could offer opportunity for economic use of recycled material as scrap coupons, that though limited in its discontinuity could be made highly aligned, and work is known to be moving forward in this area [97]. Another interesting recent development of late is the deposition works of Voith Composites where rovings are deposited by an apparent modification of an Automated Fiber Placement head to form highly aligned and prepared preforms [98]. Such a process could offer significant benefits, and would certainly be an advance on examples such as Hexcel’s HexMC [99] which is limited to tooling materials (BMI resin) although some demonstrator parts as structures are known to have been trialled [100]. Finally, the advent of additive manufacturing could enable the ‘sweet spot’ design space to be fully realised. Examples of selective laser sintering with short carbon fibre have been reported [101] and though details are sparse at this time materials including random short fibre fibres are becoming increasingly available.

It is possible that the use of recycled CF (rCF) as short fibre, and applications towards the automotive sector [102–103], will begin to dominate this field. Most of the previous techniques certainly could be argued to be aiming towards this sector; and examples such as the 3-DEP™ process [104] and its use with rCF [105] (or DCFP as previous [35]) are perhaps evidence of this. Other examples in research on scrap material reuse as short fibre, such as [106–110], also show possible advances and requirements in this area of recycling. However many of these processes still employ unaligned/random forms that as [110] show can be significantly inhibited by the discontinuity nature and relative performance. The works of LeBlanc *et al.* [111] and also examples by Greene Tweed [112] suggest that this can be overcome, but these processes are still random by nature and dominated by thermoplastic matrices which may not be suitable for all

users. Many of these recent interests that could employ rCF use fibre lengths comparable to the induced discontinuity processes, yet these are orders of magnitude larger than the aligned discontinuous materials of interest.

Currently there exists no singular all-encompassing standard by which the productivity, formability, and flexibility of a material system can be judged. Examples such as Potter [113–114], and Tsuji *et al.* [115] are available, however there has not been a unified strategy whereby definitive characteristics can be reported. For example, Tsuji *et al.* [118] investigated the drapeability of aligned discontinuous fibre composites with particular attention paid to the contributions of fibre geometry, orientation, and volume fraction. Drapeability was defined as the tip deflection of a cantilevered beam. This somewhat neglects the various methods by which composite prepreg can deform during drape, and the required extension needed to form features with double curvature. The conclusions echoed previous works where discontinuous composites had improved drapeability, at the expense of reduced longitudinal modulus, but such formability impacts on mechanical properties needs further investigation. A greater body of work therefore needs to be undertaken in order to understand the forming of aligned short fibre architectures in comparison to other discontinuous products and continuous forms. Demonstrator parts in literature include a number of hemispheres, hemi-ellipsoids, and beaded panels [116–118]. A standardised component is required for direct comparison between material systems and effective property retention or degradation, with quantitative part quality measurements. In order to account for productivity, more research is required into the rate dependent properties of the materials during forming operations. Process and material flexibility is a somewhat more qualitative measurement, requiring the material to be used in numerous forms or processes.

In order to enable future development, and to ensure the current interest in discontinuous materials is maintained, it is suggested that a metric will need to be developed by which to judge various processes and materials. A wider array of data is needed within literature, and a more cohesive approach with regards to reported mechanical properties that at present can be extremely difficult to extract pertinent details from. For example, limited development of the pertinent areas of source books such as ASM v1 to v21 [119–120] has been evident and requires rectifying. Until such a time, it is difficult to envisage discontinuous material use in high value applications without bespoke development and use, or the widespread incorporation of multifunctionality to them.

4. CONCLUSIONS

An overview of the known published history of aligned short fibre composites has been presented, with a focus upon highly aligned advanced composites with properties near to that of continuous fibre composites. When continuous

carbon fibres were first developed there retained an interest to create aligned discontinuous fibre composites in order to form more complex components. This interest has reappeared in recent years with methods divided into those which align short fibres and those which introduce discontinuities into aligned fibres. Figure 5 and Table 1 together provide an overview of the history of those developments.

Alignment methods are dominated by convergent fluid and pneumatic processes. Convergent fluid processes use a viscous carrier fluid to induce alignment within short fibres, and pneumatic technology chops and sprays tows to create preforms. These methods generally suffer from lack of alignment and have an associated large property reduction with comparison to continuous forms. A recent fluid process which relies on momentum change of a low viscosity carrier (HiPerDiF) promises greater alignment and property retention.

Induced discontinuity methods involve stretch breaking, slit, and perforation methods. These methods usually have higher associated property retention. Stretch breaking is a process adapted from the textile industry in which a tow is stretched between rollers and randomly broken at intervals, the random nature of the breaks can introduce problems during forming. Perforations in prepreg, by laser drilling an array of holes, may represent a much smarter system where the discontinuity can be locally targeted to increase formability in discrete regions.

It is clear that discontinuous material systems have their uses and applications, but greater development is still required in order to better quantify and categorise the materials and their associated properties and processes. The immediate result of which should be the creation of a metric by which to standardise and compare the vast amount of historical data, and act as a guide for future developments.

5. ACKNOWLEDGEMENTS

This work was supported by the Engineering and Physical Sciences Research Council through the ACCIS Doctoral Training Centre [grant number EP/G036772/1], the EPSRC Centre for Innovative Manufacturing in Composites (CIM-Comp) [grant number EP/IO33513/1], and the G8-2012 Material Efficiency—A First Step Toward Sustainable Manufacture (grant number EP/K025023/1).

6. REFERENCES

- [1] ANON “Bigger, faster, cheaper” *JEC Composites Magazine*, 86, 23–24, 2014
- [2] P. Feraboli, E. Peitso, F. Deleo, T. Cleveland, and P. B. Stickler “Characterization of prepreg-based discontinuous carbon fibre/epoxy systems” *J Reinforced Plastics Composites*, 28(10) 1191–1214, 2009. <http://dx.doi.org/10.1177/0731684408088883>
- [3] H. Adam “Carbon fibre in automotive applications” *Mater. Des.* 18, 349–355, 1997. [http://dx.doi.org/10.1016/S0261-3069\(97\)00076-9](http://dx.doi.org/10.1016/S0261-3069(97)00076-9)
- [4] K. Potter, C. Langer, B. Hodgkiss, and S. Lamb “Sources of variability in uncured aerospace grade unidirectional carbon fibre epoxy prepreg” *Composites Part A*, 38(3), 905–916, 2007. <http://dx.doi.org/10.1016/j.compositesa.2006.07.010>
- [5] J. Sloan “Market outlook: surplus in carbon fibre’s future?” Cincinnati, OH, USA: High Performance Composites. Available: <http://www.compositesworld.com/articles/market-outlook-surplus-in-carbon-fibres-future> [14-08-2014]
- [6] F. Smith and P. Shakspeare “UK COMPOSITES 2013 A study into the status, opportunities and direction for the UK composites industry” Composites Leadership Forum (No report number). Also available: <http://www.compositesuk.co.uk/LinkClick.aspx?fileticket=opSQ1MrS8QY%3D&tabid=104&mid=532> [14-08-2014]
- [7] N. A. de Bruyne, “Plastic progress: Some Further Developments in the Manufacture and Use of Synthetic Materials for Aircraft Construction,” *Flight: The Aircraft Engineer*, 1939
- [8] P. McMullen “Fiber/resin composites for aircraft primary structures: a short history, 1936–1984” *Composites*, 15(3) 222–230, 1984 [http://dx.doi.org/10.1016/0010-4361\(84\)90279-9](http://dx.doi.org/10.1016/0010-4361(84)90279-9)
- [9] R. F. Gibson “A review of recent research on mechanics of multifunctional composite materials and structures” *Composite Structures* 92 2793–2810, 2010. <http://dx.doi.org/10.1016/j.compstruct.2010.05.003>
- [10] Y. Swolfs, L. Gorbatikh, and I. Verpoest, “Fiber hybridisation in polymer composites: A review,” *Compos. Part A Appl. Sci. Manuf.*, vol. 67, pp. 181–200, Sep. 2014. <http://dx.doi.org/10.1016/j.compositesa.2014.08.027>
- [11] G. E. G. Bagg, M. E. N. Evans, and A. W. H. Pryde “The glycerine process for the alignment of fibres and whiskers” *Composites*, 1(2) 97–100, 1969 [http://dx.doi.org/10.1016/0010-4361\(69\)90007-X](http://dx.doi.org/10.1016/0010-4361(69)90007-X)
- [12] N. J. Parratt “Whisker alignment by the alginate process” *Composites 1* (1) 25–27, 1969 [http://dx.doi.org/10.1016/S0010-4361\(69\)80008-X](http://dx.doi.org/10.1016/S0010-4361(69)80008-X)
- [13] G. E. G. Bagg, L. E. Dingle, R. H. Jones, and W. H. Pryde “Process for the manufacture of a composite material having aligned reinforcing fibres” United States Patent 3,617,437, 2 November 1971
- [14] A. K. Salariya and J. F. T. Pittman “Preparation of aligned discontinuous fibre pre-pregs by deposition from a suspension” *Polym. Eng. Sci.*, 20(12) 787–797, 1980 <http://dx.doi.org/10.1002/pen.760201205>
- [15] L. Kacir, M. Narkis, and O. Ishai “Aligned short glass fibre/epoxy composites” *Composites*, 9(2) 89–92, 1978. [http://dx.doi.org/10.1016/0010-4361\(78\)90585-2](http://dx.doi.org/10.1016/0010-4361(78)90585-2)
- [16] L. Kacir, M. Narkis, and O. Ishai “Oriented short glass-fibre composites. I. Preparation and statistical analysis of aligned fibre mats” *Polym. Eng. Sci.* 15 (7) 525–531, 1975 <http://dx.doi.org/10.1002/pen.760150708>
- [17] L. Kacir, M. Narkis, and O. Ishai “Oriented short glass-fibre composites. II. Analysis of parameters controlling the fibre/glycerine orientation process” *Polym. Eng. Sci.*, 15(7) 532–537, 1975 <http://dx.doi.org/10.1002/pen.760150709>
- [18] L. Kacir, M. Narkis, and O. Ishai “Oriented short glass fibre composites. III. Structure and mechanical properties of molded sheets” *Polym. Eng. Sci.*, 17(4) 234–241, 1977 <http://dx.doi.org/10.1002/pen.760170405>
- [19] L. Kacir, O. Ishai, and M. Narkis “Oriented short glass fibre composites. IV. Dependence of mechanical properties on the distribution of fibre orientations” *Polym. Eng. Sci.*, 18(1) 45–52, 1978 <http://dx.doi.org/10.1002/pen.760180110>
- [20] P. S. Allan, M. J. Bevis, J. R. Gibson, C. J. May, and I. E. Pinwill, “Shear Controlled Orientation Technology for the Management of Reinforcing Fibers in Moulded and Extruded Composite Materials,” *J. Mater. Process. Technol.*, vol. 56, pp. 272–281, 1996. [http://dx.doi.org/10.1016/0924-0136\(96\)85104-1](http://dx.doi.org/10.1016/0924-0136(96)85104-1)
- [21] P. S. Allan and M. J. Bevis, “Development and application of multiple live-feed moulding for the management of fibres in moulded parts,” *Compos. Manuf.*, vol. 1, no. 2, pp. 79–84, Jun. 1990. [http://dx.doi.org/10.1016/0956-7143\(90\)90240-W](http://dx.doi.org/10.1016/0956-7143(90)90240-W)
- [22] H. Edwards and N. P. Evans “A method for the production of high

- quality aligned short fibre mats and their composites" *In: Adv compos mater v1*. 26–29 Aug Paris, Fr. Oxford:Pergamon Press, 1620–1635, 1980
- [23] G. E. G. Bagg, J. Cook, L. E. Dingle, H. Edwards, and H. Ziebland "Manufacture of composite materials" United States Patent 4,016,031, 5 April 1977
- [24] H. Richter, "Single fibre and hybrid composites with aligned discontinuous fibres in polymer matrix" *In: Adv compos mater v1*. 26–29 Aug Paris, Fr. Oxford:Pergamon Press, 387–397, 1980
- [25] K. Friedrich, K. Schulte, G. Horstenkamp, and T. W. Chou "Fatigue behaviour of aligned short carbon-fibre reinforced polyimide and polyethersulphone composites" *J. Mater. Sci.* 20, 3353–3364, 1985 <http://dx.doi.org/10.1007/BF00545205>
- [26] R. Ford "Thermo-ductile composites: new materials for 21st Century manufacturing micro-perforated thermoplastic composites" *Mater. Des.* 22, 177–183, 2001 [http://dx.doi.org/10.1016/S0261-3069\(00\)00063-7](http://dx.doi.org/10.1016/S0261-3069(00)00063-7)
- [27] F. Pinto, A. White, and M. Meo "Characterisation of ductile prepregs" *Appl. Compos. Mater.*, 20(2) 195–211, 2012. <http://dx.doi.org/10.1007/s10443-012-9264-9>
- [28] T. Flemming, G. Kress, and M. Flemming "A new aligned short-carbon-fibre-reinforced thermoplastic prepreg" *Adv. Compos. Mater.*, 5(2) 151–159, 1996 <http://dx.doi.org/10.1163/156855196X00068>
- [29] M. L. Ericson and L. A. Berglund "Processing and mechanical properties of orientated preformed glass-mat-reinforced thermoplastics" *Compos. Sci. Technol.*, 49(2) 121–130, 1993 [http://dx.doi.org/10.1016/0266-3538\(93\)90051-H](http://dx.doi.org/10.1016/0266-3538(93)90051-H)
- [30] N. G. Chavka and J. S. Dahl "P4: Glass fibre preforming technology for automotive applications" *In: SAMPE 1999 23–27 May Long Beach CA, Covina, CA, USA: SAMPE*, 281–292, 1999
- [31] R. Rondeau, S. Reeve, and G. Bond "The effect of tows and filament groups on the properties of discontinuous fibre composites" *In: SAMPE 1999 23–27 May Long Beach CA, Covina, CA, USA: SAMPE*, 1999
- [32] S. Reeve, W. Robinson, T. Cordell, and R. Rondeau "Carbon fibre evaluation for directed fibre preforms" *In: SAMPE 2001 6–10 May Long Beach CA, Covina, CA, USA: SAMPE*, 790–803, 2001
- [33] S. Reeve, R. Rondeau, G. Bond, and F. Tervet "Mechanical property translation in oriented, discontinuous carbon fibre composites" *In: SAMPE 2000 21–25 May Long Beach, CA, Covina, CA, USA: SAMPE*, 2000
- [34] L. T. Harper, T. A. Turner, J. R. B. Martin, and N. A. Warrior "Fiber alignment in directed carbon fibre preforms—a feasibility study" *J. Compos. Mater.*, 43(1) 57–74, 2008 <http://dx.doi.org/10.1177/0021998308098151>
- [35] T. A. Turner, N. A. Warrior, and S. J. Pickering "Development of high value moulding compounds from recycled carbon fibres" *Plastics, Rubber and Composites*, 39(3–5) 151–156, 2010 <http://dx.doi.org/10.1179/174328910X12647080902295>
- [36] N. E. H. Shotton-gale, M. A. Paget, C. A. Smith, N. L. Jameson, L. Wang, S. A. Malik, J. M. Burns, F. Biddlestone, A. Prasad, D. E. E. Harris, R. Venkata, R. S. Mahendran, and G. F. Fernando "An investigation into techniques to fabricate highly aligned short-fibre prepregs" *In: SAMPE SEICO 10*, 12–14 April Paris, Fr. Covina, CA: SAMPE, 482–487, 2010
- [37] M. N. Vyakarnam and L. T. Drzal "A new process for aligning chopped fibres in composites" *Plast. Eng.*, 53(1) 2–6, 1997
- [38] M. N. Vyakarnam and L. T. Drzal "Composite material of aligned discontinuous fibres" United States Patent 6,025,285, 15 February 2000
- [39] M.-S. Scholz, B. W. Drinkwater, and R. S. Trask "Ultrasonic assembly of anisotropic short fibre reinforced composites" *Ultrasonics*, 54(4) 1015–1019, 2014 <http://dx.doi.org/10.1016/j.ultras.2013.12.001>
- [40] H. Yu, Personal communication, 2014
- [41] H. Yu, K. D. Potter, and M. R. Wisnom "A novel manufacturing method for aligned discontinuous fibre composites (High Performance-Discontinuous Fiber method)" *Composites Part A* 65, 175–185, 2014 <http://dx.doi.org/10.1016/j.compositesa.2014.06.005>
- [42] H. Yu, K. D. Potter, and M. R. Wisnom, "A novel manufacturing method for aligned short fibre composite" *In: ECCM 15 24–28 June, Venice, It. Venice: European Society of Composite Materials (ESCM)*, 2012
- [43] T. Harbers "Wetlaid nonwovens—a resource-efficient manufactured semi-finished product for composite structures made from recycled carbon fibres" *In: LCC-Symposium 2014 11–12 September Garching DE. Munich, DE: TUM*, 2014
- [44] T. E. Armiger, D. H. Edison, H. G. Lauterbach, J. R. Layton, and R. K. Okine "Composites of stretch broken aligned fibres of carbon and glass reinforced resin" European Patent 0,272,088, 9 March 1994
- [45] R. K. Okine, D. H. Edison, and N. K. Little "Properties and formability of a novel advanced thermoplastic" *In: Proc 32nd Int SAMPE Symp & Exhib 6–9 April Anaheim, CA, Covina, CA, USA: SAMPE*, 1413–1419, 1987
- [46] R. K. Okine, D. H. Edison, and N. K. Little "Properties and formability of an aligned discontinuous fibre thermoplastic composite sheet" *J. Reinf. Plast. Compos.*, 9(1) 70–90, 1990 <http://dx.doi.org/10.1177/073168449000900105>
- [47] I. Y. Chang and J. F. Pratte "LDF thermoplastic composites technology" *J. Thermoplast. Compos. Mater.*, 4(3) 227–252, 1991 <http://dx.doi.org/10.1177/089270579100400302>
- [48] N. W. Hansen, M. Abdallah, and G. Jacobsen "Development of stretch broken carbon fibres" *In: SAMPE 2005 1–5 May Long Beach, CA, USA. Covina, CA: SAMPE*, 2005
- [49] G. Jacobsen and W. Schimpf "Process development and characterization of stretch broken carbon fibre materials" *In: SAMPE 2009 18–21 May Baltimore, MD, USA. Covina, CA: SAMPE*, 2009
- [50] G. Jacobsen "Mechanical performance characterization of stretch broken carbon fibre materials" *In: SAMPE 2009 18–21 May Baltimore, MD, USA. Covina, CA: SAMPE*, 2009
- [51] G. Jacobsen "Mechanical characterization of stretch broken carbon fibre materials—IM7 fibre in 8552 Resin" *In: SAMPE 2010 17–20 May Seattle, WA, USA. Covina, CA: SAMPE*, 2010
- [52] G. Jacobsen and D. Maass "Characterization of stretch broken carbon fibre composites—IM7 fibre in 8552 Resin—stretched at prepreg level" *In: SAMPE 2011 23–26 May Long Beach, CA, USA. Covina, CA: SAMPE*, 2011
- [53] G. Dillon and M. Barsoum, "Characterization of stretch broken carbon fibre materials for automated forming processes" *In: SAMPE 2005 1–5 May Long Beach, CA, USA. Covina, CA: SAMPE*, 2005
- [54] M. Barsoum and J. Kirk, "Mechanized Forming With Stretch Broken Fibers", *In: SAMPE 2005 1–5 May Long Beach, CA, USA. Covina, CA: SAMPE*, 2005
- [55] G. D. Renieri, M. G. Mohamed, and N. W. Hansen "Composites forming investigations of stretch broken carbon fibre based prepreg forms" *In: SAMPE 2005 1–5 May Long Beach, CA, USA. Covina, CA: SAMPE*, 2005
- [56] C. B. Munro, D. Walczyk, Y. Bahei-El-Din, and G. Dvorak "Forming of stretch broken carbon fibre (SBCF) prepreg material over fixed shapes—material characterization & modeling" *In: SAMPE 2005 1–5 May Long Beach, CA, USA. Covina, CA: SAMPE*, 2005
- [57] M. McClain, J. Goering, and C. Rowles "Web stiffened stretch broken carbon fibre frame fabrication" *In: SAMPE 2009 18–21 May Baltimore, MD, USA. Covina, CA: SAMPE*, 2009
- [58] M. McLain PE, J. Goering, and C. Rowles "Preforming with stretch broken carbon fibre: an overview" *In: 42nd ISTC 11–14 October Salt Lake City, UT, USA. Covina, CA: SAMPE*, 2010
- [59] G. P. Dillon and D. Walczyk "Comparison of continuous fibre and stretch broken carbon fibre (SBCF) materials in forming processes" *In: SAMPE 2005 1–5 May Long Beach, CA, USA. Covina, CA: SAMPE*, 2005
- [60] S. Ng, R. Meilunas, and M. G. Abdallah "Stretched broken carbon fibre (SBCF) for forming complex curved composite structures" *In: SAMPE 2006 30 April–4 May Long Beach, CA, USA. Covina, CA: SAMPE*, 2006

- [61] S. Benson, T. Cook, E. Trewin, and R. M. Turner “Materials and processing—move into the 90’s” *Mater. Manuf. Process.*, 6(4) 753–757, 1991 <http://dx.doi.org/10.1080/10426919108934807>
- [62] J. E. Hendrix “Spun carbon composite reinforcements” In: SAMPE 2008 18–22 May Long Beach, CA, USA. Covina, CA: SAMPE, 2008
- [63] J. Guevel, M. François, G. Bontemps “Hybrid yarn for composite materials made from thermoplastic matrix and method for producing the same” European Patent 0,354,139, 30 December 1992
- [64] T. S. Creasy “Forming discontinuous fibre arrays by fracture of lubricated carbon-filament tows” *J. Mater. Sci.* 35 4431–4438, 2000 <http://dx.doi.org/10.1023/A:1004825511841>
- [65] A. Simmons “An analysis of the properties of carbon fibre aligned discontinuous prepreg tape” In: SAMPE 2012 21–24 May Baltimore, MD, USA. Covina, CA: SAMPE, 2012
- [66] A. E. Moody, A. L. Neal, R. Engelbart, A. Chute, J. Townsley “DiscoTex: highly formable carbon fibre fabric.” In: SAMPE 2007 3-7 June Baltimore, MD, USA. Covina, CA: SAMPE, 2007
- [67] E. Harris and Z. Olsenske “Evaluation of Aligned Discontinuous Fiber Based Formable Textiles” In: SAMPE 2009 18–21 May Baltimore, MD, USA. Covina, CA: SAMPE, 2009
- [68] E. Thompson “Manufacturability and transmissivity of radomes formed with aligned discontinuous composite reinforcement tape” In: SAMPE 2012 21–24 May Baltimore, MD, USA. Covina, CA: SAMPE, 2012
- [69] H. Li, W.-X. Wang, Y. Takao, and T. Matsubara “New designs of unidirectionally arrayed chopped strands by introducing discontinuous angled slits into prepreg” *Composites Part A* 45, 127–133, 2013 <http://dx.doi.org/10.1016/j.compositesa.2012.09.009>
- [70] I. Taketa, T. Okabe, and A. Kitano “Strength improvement in unidirectional arrayed chopped strands with interlaminar toughening” *Composites Part A*, 40(8) 1174–1178, 2009 <http://dx.doi.org/10.1016/j.compositesa.2009.05.006>
- [71] I. Taketa, T. Okabe, and A. Kitano “A new compression-molding approach using unidirectionally arrayed chopped strands” *Composites Part A*, 39(12) 1884–1890, 2008 <http://dx.doi.org/10.1016/j.compositesa.2008.09.012>
- [72] I. Taketa, N. Sato, A. Kitano, M. Nishikawa, and T. Okabe “Enhancement of strength and uniformity in unidirectionally arrayed chopped strands with angled slits” *Composites Part A*, 41(11) 1639–1646, 2010 <http://dx.doi.org/10.1016/j.compositesa.2010.07.010>
- [73] J. Nixon “The best of both worlds,” *Reinf. Plast.* 52(4) 36–38, 39, 2008
- [74] R. Ford and B. Griffiths “The creation of ductile, composite prepreps, with close to UD properties” In: 40th ISTC 8-11 September Memphis, TN, USA. Covina, CA: SAMPE, 2008
- [75] T. Matthams and T. Clyne “Mechanical properties of long-fibre thermoplastic composites with laser drilled microperforations: 1. Effect of perforations in consolidated material” *Compos. Sci. Technol.*, 59(8) 1169–1180, 1999 [http://dx.doi.org/10.1016/S0266-3538\(98\)00156-0](http://dx.doi.org/10.1016/S0266-3538(98)00156-0)
- [76] T. Matthams and T. Clyne “Mechanical properties of long-fibre thermoplastic composites with laser drilled microperforations: 2. Effect of prior plastic strain” *Compos. Sci. Technol.*, 59(8) 1181–1187, 1999 [http://dx.doi.org/10.1016/S0266-3538\(98\)00157-2](http://dx.doi.org/10.1016/S0266-3538(98)00157-2)
- [77] ANON “Formax presents next generation of reinforcements at composites engineering 2013” Leicester, UK: Formax. Available: http://www.formax.co.uk/composite_article.php?s=49&np=12013 [07-08-2014]
- [78] ANON “Sigmatex Recycled Fabrics” Runcorn, UK: Sigmatex. Available: http://www.sigmatex.com/Solution/Recycled_Fabrics2014 [07-08-2014]
- [79] J. L. Kardos “Critical issues in achieving desirable mechanical properties for short fibre composites” *Pure Applied Chemistry*, 57 (11) 1651–1657, 1985 <http://dx.doi.org/10.1351/pac19857111651>
- [80] J. C. Halpin “Stiffness and expansion estimates for orientated short fibre composites” *J Compos. Mater.*, 3, 732–734, 1969
- [81] H. Fukuda and T.-W. Chou “A probabilistic theory of the strength of short-fibre composites with variable fibre length and orientation” *J Materials Sci.*, 17(4) 1003–1011, 1982 <http://dx.doi.org/10.1007/BF00543519>
- [82] R. Mao “Complex moduli of aligned-short-fibre reinforced composites” *Compos. Sci. Technol.*, 36(3) 211–225, 1989 [http://dx.doi.org/10.1016/0266-3538\(89\)90021-3](http://dx.doi.org/10.1016/0266-3538(89)90021-3)
- [83] C. L. Tucker III and E. Liang “Stiffness predictions for unidirectional short-fibre composites: review and evaluation” *Compos. Sci. Technol.*, 59(5) 655–671, 1999 [http://dx.doi.org/10.1016/S0266-3538\(98\)00120-1](http://dx.doi.org/10.1016/S0266-3538(98)00120-1)
- [84] M. R. Piggott, M. Ko, and H. Y. Chuang “Aligned short-fibre reinforced thermosets: experiments and analysis lend little support for established theory” *Compos. Sci. Technol.*, 48(1-4) 291–299, 1993 [http://dx.doi.org/10.1016/0266-3538\(93\)90146-8](http://dx.doi.org/10.1016/0266-3538(93)90146-8)
- [85] I. Scheider, Y. Chen, A. Hinz, N. Huber, and J. Mosler “Size effects in short fibre reinforced composites” *Engineering Fracture Mechanics*, 100, 17–27, 2013 <http://dx.doi.org/10.1016/j.engfrac-mech.2012.05.005>
- [86] R. G. White and E. M. Y. Abdin “Dynamic properties of aligned short carbon fibre-reinforced plastics in flexure and torsion” *Composites* 16 (4) 293–306, 1985 [http://dx.doi.org/10.1016/0010-4361\(85\)90282-4](http://dx.doi.org/10.1016/0010-4361(85)90282-4)
- [87] T. D. Papathanasiou, M. S. Ingber, and D. C. Guell “Stiffness enhancement in aligned, short-fibre composites: A computational and experimental investigation” *Compos. Sci. Technol.* 54(1) 1–9, 1995 [http://dx.doi.org/10.1016/0266-3538\(95\)00025-9](http://dx.doi.org/10.1016/0266-3538(95)00025-9)
- [88] W. C. Jackson, S. G. Advani, and C. L. Tucker “Predicting the orientation of short fibres in thin compression moldings” *J Composite Materials*, 20, 539–557, 1986 <http://dx.doi.org/10.1016/002199838602000603>
- [89] S. Ranganathan, and S. G. Advani “Characterization of orientation clustering in short-fibre composites” *J Polymer Sci. Part B*, 28, 2651–2672, 1990 <http://dx.doi.org/10.1002/polb.1990.090281312>
- [90] J. Summerscales and D. Short “Carbon fibre and glass fibre hybrid reinforced plastics” *Composites* 9(3) 157–166, 1978 [http://dx.doi.org/10.1016/0010-4361\(78\)90341-5](http://dx.doi.org/10.1016/0010-4361(78)90341-5)
- [91] C. Ward, K. Hazra, and K. Potter “Development of the manufacture of complex composite panels” *Int. J. Materials and Product Technology*, 42(3/4) 131–155, 2011 <http://dx.doi.org/10.1504/IJMP.2011.045460>
- [92] ANON “Tenax® Part via Preform” Cologne, DE: Toho Tenax GmbH. Available: <http://www.tohotenax-eu.com/en/products/tenax-part-via-preform.html> [15-08-2014]
- [93] B. C. Kim, K. Potter, and P. M. Weaver “Continuous tow shearing for manufacturing variable angle tow composites” *Composites Part A*, 43(8) 1347–1356, 2012 <http://dx.doi.org/10.1016/j.compositesa.2012.02.024>
- [94] B. C. Kim, K. Potter, and P. M. Weaver “Manufacturing characteristics of the continuous tow shearing method for manufacturing of variable angle tow composites” *Composites Part A*, 61, 141–151, 2014 <http://dx.doi.org/10.1016/j.compositesa.2014.02.019>
- [95] O. Meyer “Fiber patch preforming technology” In: Erath, M.A., ed. SAMPE SETEC 02/-07 6-7 Sept Madrid, Sp. Covina, CA: SAMPE, 238–252, 2007.
- [96] B. Horn “Fiber patch placement—interaction of lay-up pattern and mechanical performance of the composite” In: LCC-Symposium 2014 11–12 September Garching DE. Munich, DE: TUM, 2014 .
- [97] T. Harbers, and B. Horn, Personal communication, 2014.
- [98] J. Ufer, M. Göttinger, and L. Herbeckfpp “Preform Technology for High Volume Manufacturing of Long Fiber Reinforced Structures” In: LCC-Symposium 2014 11–12 September Garching DE. Munich, DE: TUM, 2014.
- [99] ANON “HexMC User Guide” Stamford, Connecticut, USA: Hexcel Corporation, Publication No. HTI 303, 2014.
- [100] A. Mills, Personal communication, 2014.

- [101] B. I. Lyons and C. S. Huskamp "Method of reinforcement for additive manufacturing" United States Patent 2014/0050921, Feb 20 2014
- [102] P. Horrell "First drive: the BMW i8." London, UK: BBC Worldwide. Available: <http://www.topgear.com/uk/photos/bmw-i8-first-drive-car-review-2014-04-26> [13-08-2014]
- [103] Y. Yanga, R. Booma, B. Irionb, D-J van Heerdenb, P. Kuiper, and H. de Wita "Recycling of Composite Materials" *Chemical Engineering and Processing* 51, 53–68, 2012 <http://dx.doi.org/10.1016/j.cep.2011.09.007>
- [104] M. A. Janney "Making composites using the three dimensional engineered preform (3-dep) process" AATCC Symposium Papers pt 1, 59785561, 2008
- [105] G. Gardiner "Recycled carbon fibre update: Closing the CFRP life-cycle loop" *Composites Technology*, 20(6) 28–33, 2014
- [106] G. Nilakantan, R. Olliges, R. Su, and S. Nutt "Reuse strategies for carbon fibre-epoxy prepreg scrap" In: CAMX 2014 13–16 October Orlando, FL, USA, Covina, CA, USA: SAMPE, 2014
- [107] S. R. Nutt, T. Centea "Sustainable manufacturing using out-of-autoclave prepreps" In: AMX 2014 13–16 October Orlando, FL, USA, Covina, CA, USA: SAMPE, 2014
- [108] M.-S. Wu, T. Centea, S. R. Nutt "Process optimization for compression molding of reused prepreg scrap" In: Proc 29th Tech Conf ASC 8-11 September San Diego, CA, USA, Dayton, OH, USA: ASC Composites, 2014
- [109] S. Pimenta and S. T. Pinho "Recycling carbon fibre reinforced polymers for structural applications: Technology review and market outlook" *Waste Management* 31(2), 378–392, 2011. <http://dx.doi.org/10.1016/j.wasman.2010.09.019>
- [110] S. Pimenta and S. T. Pinho "The effect of recycling on the mechanical response of carbon fibres and their composites" *Composite Structures* 94, 3669–3684, 2012 <http://dx.doi.org/10.1016/j.compstruct.2012.05.024>
- [111] D. LeBlanc, B. Landry, A. Levy, P. Hubert, S. Roy, and A. Yousefpour "Compression moulding of complex parts using randomly-oriented strands thermoplastic composites." In: SAMPE Tech. Conf. 2–4 June Seattle, USA, Covina, CA: SAMPE, 2014
- [112] ANON "XYCOMP® composite material" Kulpsville, PA, USA: Greene Tweed. Available: <http://www.gtweed.com/markets/semi-solar/products/thermoplastic-composites/materials/xycomp-thermoplastic-composite-material/> [Accessed 13-08-2014]
- [113] K. D. Potter "The influence of accurate stretch data for reinforcements on the production of complex structural moulding Part 1. Deformation of aligned sheets and fabrics" *Composites* 10(3) 161–167, 1979 [http://dx.doi.org/10.1016/0010-4361\(79\)90291-X](http://dx.doi.org/10.1016/0010-4361(79)90291-X)
- [114] K. D. Potter "The influence of accurate stretch data for reinforcements on the production of complex structural moulding Part 2. Deformation of random mats" *Composites* 10(3) 168–173, 1979 [http://dx.doi.org/10.1016/0010-4361\(79\)90292-1](http://dx.doi.org/10.1016/0010-4361(79)90292-1)
- [115] N. Tsuji, G. S. Springer, and I. Hegedus "The drapeability of aligned discontinuous fibre composites," *J Composite Materials*, 31(5) 428–465, 1997 <http://dx.doi.org/10.1177/002199839703100501>
- [116] G. P. Dillon and D. H. Stiver III "Application of stretch broken carbon fibre materials to rotorcraft structures" In: SAMPE 2006 30 April - 4 May Long Beach, CA, USA. Covina CA: SAMPE, 2006
- [117] D. Cox and A. Nadel "Design, analysis and manufacturing transition for stretch broken carbon fibre materials" In: SAMPE 2009 18-21 May Baltimore, MD, USA. Covina, CA: SAMPE, 2009
- [118] G. P. Dillon and D. H. Stiver III "Development of enabling automated forming technology for stretch broken carbon fibre (SBCF) materials" In: SAMPE 2009 18–21 May Baltimore, MD, USA. Covina, CA: SAMPE, 2009
- [119] ANON "ASM Handbook v1, Composites" Metals Park Ohio: ASM Intl v1 xiv
- [120] ANON "ASM Handbook v21, Composites" Materials Park Ohio: ASM Intl v21 xx

GUIDE TO AUTHORS

SUBMISSION CHECKLIST FOR AN ORIGINAL SUBMISSION

Please ensure your final submission contains the following items:

Cover Letter: All submissions must be accompanied by a cover letter addressed to the Editor. The cover letter should start at the first page of the submission. The cover letter pages should not be numbered. Include the complete contact information for the corresponding author (name, affiliation, email, phone, fax, address); Provide a list of potential reviewers for the manuscript. Include the name, email, and institution. A minimum of four and maximum of six names should be provided. Of these at least two names must be from the US. If desired, you can also provide a list of individuals or institutions that you DO NOT want to review the manuscript; The cover letter must also include a declaration from the corresponding author, on behalf of all authors, that the work is original and has not previously been submitted to another journal for publication. If the results contained in the article have previously appeared in a magazine, conference proceedings, or a thesis/dissertation, this should be clearly stated; If any copyrighted material has been used in the manuscript, mention it in the cover letter and include proof of permission to re-use the copyrighted material; Disclose any conflict of interest with any persons or organizations that may be personal or financial in nature and that may affect or influence either your work or their work.

Types of Articles: Full length articles, review articles, and short letters will be accepted for publication. Authors interested in writing review articles should first contact the Editor.

Manuscript: Abstract, Keywords, Main Text, Figures, Tables, Acknowledgements, References

In addition, please note the following: Name your submission using the last name of the corresponding author, for e.g. Wang.pdf; Make sure the main text is in a single column format and checked for both spelling and grammar. All pages must be consecutively numbered; Make sure all symbols and equations appear properly in the final PDF document; If copyrighted material is used in the manuscript, please make sure permission has been previously obtained from the copyright holder. Proof of permission will need to be sent to the journal along with the submission; Color figures will appear in color in the online version of the article and in grayscale in the print version of the article.

Word-processing Software: Articles can be prepared using any word-processing software. However submissions must only be in the form of a single PDF document.

Article Structure and Hierarchy: The structure of the article should closely follow this order: Title, Authors, Affiliations, Abstract, Keywords, Corresponding author contact information, Main text (e.g. Introduction, Setup/Methodology, Results, Discussion, Conclusions), Acknowledgements, References, Figures, Tables, Appendix.

Title: The title must clearly distinguish between work that is experimental and numerical in nature. For e.g., “An Experimental Investigation of . . .” or “Numerical Modeling of . . .”. Use sentence case for the title, i.e. do not capitalize all letters. Avoid the use of abbreviations and refrain from using commercial names. For e.g., use Finite Element Analysis instead of FEA.

Author Names and Affiliations: Provide the author’s entire first and last name. Middle names, if any, can be included as an initial. Below the list of author names, provide the entire postal address for each affiliation that includes the department, organization, street address, zip or postal code, and country. Use lower case alphabetical superscripts to relate each author to each affiliation. These superscripts should appear after each author’s name and before each affiliation listing. The corresponding author should be identified by a * superscript that appears after the alphabetical superscripts, for e.g., John Wu a,b,*. If any of the authors have changed their affiliation, then provide as a footnote on the title page the new affiliation for the author. The affiliation must correspond to the place where majority of the work was performed.

Main Text: There is no page or word limit. The text should be in a single column with one-and-a-half or double line spacing and a minimum font size of 10 pt. Use of Times New Roman, Arial, or Calibri fonts are preferred. Each new paragraph must be clearly identified using either a tab indent or a blank line. Figures and tables, including their captions, should appear on separate pages at the end of the manuscript, and should not be inserted within the text. Number all pages consecutively in the manuscript and place the page number at the top right of each page.

Abstract: The abstract is meant to serve as a stand-alone version of the manuscript. It should be kept as brief as possible and concisely state the objective of the research, the principal results, and major conclusions.

Keywords: Select a minimum of three and a maximum of five keywords. Keywords should preferably be between one to three words. Do not include phrases or commercial names.

Corresponding Author Contact Information: Provide the official email address, phone number, and fax number of the corresponding author below the list of keywords or as a footnote in the title page. One corresponding author must be clearly identified for each manuscript and will be sole point of contact between the Editor/Journal and the authors.

Headings and Subheadings: Heading and subheadings in the article should be identified using a decimal system. Main headings appear as (1, 2, 3, . . .), sub-headings as (1.1, 1.2, 2.1, . . .), and sub-sub-headings as (1.1.1, 1.1.2, 2.1.1, . . .). Avoid any further division of sub-headings. The abstract is not numbered. All headings and sub-headings must appear in bold font in the text. The font size of the main headings must be 2 pt higher than the main text, for example if the main text has a 10 pt font size then the main headings must have a 12 pt font size. The font size of all lower-level headings must be the same as the main text.

Figures: Figures must appear on separate pages at the end of the manuscript and before the tables. Do not include more than two figures on each page. A descriptive figure caption, consecutively numbered, must accompany each figure and be placed below the figure. If symbols or abbreviations are used in the figure, explain them in the caption. If text is used inside a figure, use regular fonts and a large enough font size so that the text appears legible even if the figure is reduced in size for the final proof. Refer to each figure in the main text as Figure (1) or Figure (1.1). After the article is accepted for publication, if some of the figures embedded in the Word or PDF submissions are not of high enough quality, the journal manager will ask the corresponding author to provide high-resolution figures, for which separate instructions will be sent. All color figures will be converted to grayscale for the print version, but will appear in color in the online version. If a figure contains solid plot lines of different colors, make sure each plot line is clearly labeled so that it can be properly interpreted in the grayscale version.

Tables: Tables must appear on separate pages at the end of the manuscript and after the figures. Each table must appear on a separate page. Include a table heading above each table and number them consecutively using Roman numerals. Refer to each table in the main text as Table (I), Table (II), and so forth. Do not duplicate data between the figures and tables unless absolutely required. Tables comprising non-essential or large data sets should be placed in the Appendix if possible and appear as Table (A.I), Table (A.II), Table (B.I), and so forth.

Equations: Equations should appear within the main text, but must be separated from the text with a blank line both above and below the equation. Each equation should be followed by an equation number that is enclosed in rounded brackets and situated at the right hand margin of the page. Refer to each equation in the main text as Equation (1) or Equation (1.1). Describe the list of symbols used in each equation either in the text immediately following the equation or collectively in a separate table just after the abstract and just before the main text. This table does not need to be numbered. Its title should be ‘List of Symbols’.

Units: Use the international system of units (SI) and follow internationally accepted nomenclature and conventions. If any other system of units is used, which is strongly discouraged, then provide the SI equivalent of the quantity in rounded brackets, i.e. ()

Permission to Re-Use Copyrighted Material: The author(s) of the article are solely responsible for obtaining permission from copyright holders to re-use verbatim and without significant change images, tables, graphs, and text excerpts in excess of 200 words. Forms for obtaining such permission can be obtained from the journal’s Editor or Publisher. All required permissions must be submitted to the journal at the time of manuscript submission. Further the use of such copyrighted material must be clearly indicated in the cover letter.

Copyright Transfer: Once the Editor determines the article has been accepted for publication, a copyright form will be sent to the Corresponding Author requesting release of the copyright to the Publisher, DEStech Publications, Inc. It is assumed that the Corresponding Author will sign the copyright form on behalf of all other authors. Corresponding Authors are asked to return this form promptly, within 48 hours, since the article cannot be published until it is received. All accepted articles will be copyrighted in the name of the Publisher. After transfer of copyright the author retains certain rights to use the article for non-commercial and instructional purposes as well as personal presentations within the author’s research group.

Open Access and Supplementary Data: At this time we do not offer the possibility of open access and the inclusion of supplementary data. However since the articles do not have any word or page limit, supplementary data can either be included within the main set of figures and tables or within the appendix.

Acknowledgements: Acknowledgements appear before the list of references. Please acknowledge the funding source for your work. If you received no funding for your work, mention so in the cover letter. You can also acknowledge the role of any individuals or organizations that contributed to your work.

References: All references in the text should be consecutively numbered and appear within square brackets (e.g. [1] or Last Name et al. [1]). Ensure that all cited references in the text appear in the list of references at the end of the manuscript and vice-versa. The use of reference management software such as *EndNote* or *RefWorks* is encouraged. The format of the reference in the list of references is left to the author, since it will later be converted to the required format by the journal. However each reference in the list must contain all author names (either as the full name, or the last name and first initial of the first name), article title, full journal name (do not abbreviate), volume number, issue number, start and end page numbers, and year of publication. If complete bibliographic details are not available, the DOI number or the words ‘In Press’ can be used which imply the article has been accepted for publication. The use of unpublished works and personal communications as a reference is prohibited. The uses of web references is discouraged, but when necessary include the entire URL, date the webpage was last accessed, and any other pertinent information.

Note: The article may be rejected if it is determined that the author has not conducted a thorough literature review of previous works, or has simply cited old references instead of citing current and/or recent works.

Appendix: All text, figures, and tables belonging to the appendix must collectively appear in the appendix and should not be included within the main text and along with the main figures and tables. Identify each appendix as A, B, C, and so forth. Each figure in the appendix should be numbered as (A.1), (A.2), (B.1), and so forth while each table should be numbered as (A.I), (A.II), (B.I), and so forth. Once again, follow this order for each appendix: appendix main text, appendix figures, and appendix tables.

Author Inquiries and Contact Information: All inquiries related to the submission of the article should be directed to the Editor, Gaurav Nilakantan (Nilakantan@destechpub.com or gaurav.nilakantan@usc.edu); all inquiries related to processing of the article should be directed to the Journal Manager, Steve Spangler (sspangler@destechpub.com).